T H E　U N I V E R S I T Y　O F　M I C H I G A N

COLLEGE OF LITERATURE, SCIENCE, AND THE ARTS
Department of Physics

Technical Report

AN EXPERIMENTAL DETERMINATION OF THE K_S^0 CHARGED TO
NEUTRAL BRANCHING RATIO AND $|\Delta I| > 1/2$ TRANSITIONS

Jorge Guillermo Morfín

ORA Project 04938

under contract with:

administered through:

OFFICE OF RESEARCH ADMINISTRATION　ANN ARBOR

May 1970

This report was also a dissertation submitted in partial fulfillment of the requirements for the degree of Doctor of Philosophy in The University of Michigan, 1970.

TABLE OF CONTENTS

TABLE OF CONTENTS (Continued)

Page

TABLE OF CONTENTS (Continued)

Page

TABLE OF CONTENTS (Concluded)

Page

ACKNOWLEDGMENTS

I want to sincerely thank the following individuals for their assistance in this experiment and subsequent analysis.

Prof. Daniel Sinclair for serving as chairman of my committee and making this thesis not only an educational but a truly enjoyable experience as well,

Profs. John C. Vander Velde, Oliver Overseth, Robert Lewis, and Richard Teske for serving on my committee and willingly confronting the many questions that arose,

Assoc. Prof. C. Thornton Murphy for giving me encouragement when I needed it most,

Prof. Byron P. Roe and Dr. Jeremy Lys for their many helpful points and clarifications of the theory involved,

Mr. Kenneth Bartley for his time and effort spent in the editing stages of the experiment,

My fellow graduate students, both past and present, for their helpful discussions, in particular Charles L. Arnold, T. Michael Church, John Davidson, Anthony Fisher, Walter Gibbs, Robert Green, Hsien-Chih Hsiung, Richard Kiang, John Koschik, Lawrence Lovell, and Harvey Ring,

The scanning and measuring personnel for processing the film through the earliest and most tedious stages of analysis. My special thanks to "the girls", Vivian French, Marianne Rauer, and Marietta Ross for not only helping in the scanning but also assisting in the necessary bookwork. Thanks also to the many part-time scanners and measurers, particularly

LIST OF TABLES

LIST OF FIGURES

ABSTRACT

AN EXPERIMENTAL DETERMINATION OF THE K_s^0 CHARGED TO NEUTRAL BRANCHING RATIO AND $|\Delta I| > 1/2$ TRANSITIONS

by

Jorge Guillermo Morfín

Chairman: Daniel Sinclair

We have exposed the Michigan-ANL 40-inch heavy liquid bubble chamber filled with heavy Freon, CF_3Br, to a separated K^+ beam at the ZGS complex of Argonne National Laboratory. Approximately 150,000 pictures were taken at a transport momentum of 825 MeV/c. An auxiliary exposure of $\sim$ 20,000 pictures using a π^+ beam of the same transport momentum was also obtained for determination of π^+ contamination of the K^+ beam.

The resulting K^+ sample was scanned for the charge exchange reaction $K^+ + n \rightarrow K^0 + p$. Through subsequent edits those K^0's produced by the above reaction and decaying via the short-lived mode, K_s^0, were categorized as to whether their decay products were two charged pions $(\pi^+ + \pi^-)$ or two neutral pions $(\pi^\circ + \pi^\circ)$. The raw sample of 7500 $K_s^0 \rightarrow \pi^+ + \pi^-$ decays was then subjected to four corrections while the raw sample of 4280 $K_s^0 \rightarrow \pi^\circ + \pi^\circ$ decays underwent six corrections. The corrected charged and neutral samples contained 7736 ±99 and 3654 ±100 events, respectively.

With the resulting K_s^0 charged to neutral branching ratio

of 2.117 ±0.064 we have investigated the difference in $\pi\pi$

phase shifts $|\delta_o^2 - \delta_o^o|$ where δ_o^2 and δ_o^o are the s-wave isotensor

and isoscalar phase shifts, respectively. Assuming no

$\Delta I = 5/2$ transitions we find $|\delta_2 - \delta_o| = (72 \, {}^{+10}_{-11})°$. We have

also investigated the relative magnitudes of $I = 2$ and $I = 0$

states in the composition of the 2π final state and find

$Re(A_2/A_o) = 0.022 \pm 0.014$. Using the results of this last

investigation we have examined the relative magnitudes of

$\Delta I = 5/2$ and $\Delta I = 3/2$ transitions in the $K_S^o \to 2\pi$ decay. We

find this ratio to be $\alpha_{5/2}/\alpha_{3/2} = -0.391 \pm 0.510$ or -2.18 ± 2.85.

As a check on our experimental method, a careful tabula-

tion of all K_L^o production was kept. After five corrections

were applied to the raw sample the total K_L^o production was

compared to the total K_S^o production and an estimate of the

phase of the amplitude for coherent regeneration in Freon,

$(-40 \pm 25)°$, has been obtained.

In the appendices we examine the phenomenology of $K_S^o \to 2\pi$

decays including regeneration and interference phenomena. We

also give a resume of the status regarding $\pi\pi$ phase shifts.

CHAPTER I

PHYSICS OF THE K_S^0 BRANCHING RATIO

1. PHYSICAL INTEREST IN THE K_S^0 BRANCHING RATIO

The function of the $|\Delta I| = 1/2$ selection rule in non-leptonic weak interactions has been of great interest to experimentalists within the field since its formal introduction by Gell-Mann and Pais[1] in 1954. On the other hand, the theorists' response has been justifiably non-commital since the validity or non-validity of this selection rule would not alter present weak interaction theory to any great extent as long as any violation occurred in a prescribed[2] manner.

There are many predictions of the $|\Delta I| = 1/2$ rule that have been repeatedly checked through experimentation. Table I summarizes predictions of the $|\Delta I| = 1/2$ rule along with the current experimental results; phase space corrections are included where significant.

The decay of the Σ hyperon has not been included since the usual test of the $|\Delta I| = 1/2$ rule for the Σ family is the closure of a triangle plotted on the s-wave and p-wave axis. By defining the amplitudes

$$\Sigma_+^+ \equiv \Sigma^+ \rightarrow n\pi^+$$

$$\Sigma_o^+ \equiv \Sigma^+ \rightarrow p\pi^o$$

$$\Sigma_-^- \equiv \Sigma^- \rightarrow n\pi^- \quad ,$$

TABLE I

STATUS OF THE $\Delta I = 1/2$ RULE

Ratio	$\Delta I = 1/2$ Prediction	Experimental Value[*]
Kaons		
$\dfrac{\Gamma(K^+ \to \pi^+\pi^\circ)}{\Gamma(K_S^\circ \to 2\pi)}$	0.0	$(1.47 \pm .03) \times 10^{-3}$
$\dfrac{\Gamma(K_S^\circ \to \pi^+\pi^-)}{\Gamma(K_S^\circ \to \pi^\circ\pi^\circ)}$	2.0	See Chapter II
$K \to 3\pi$	See Table II	See Table II
Hyperons		
$\dfrac{\Gamma(\Lambda \to p\pi^-)}{\Gamma(\Lambda \to p\pi^-) + \Gamma(\Lambda \to n\pi^\circ)}$	.66	.644 $\pm$ .008
$\dfrac{\Gamma(\Xi^\circ \to all)}{\Gamma(\Xi^- \to all)}$	.50	.55 $\pm$ .04
$\dfrac{\Gamma(\Omega^- \to \Xi^\circ\pi^-)}{\Gamma(\Omega^- \to \Xi^-\pi^\circ)}$	2.0	$\dfrac{8 \text{ events}}{3 \text{ events}}$

[*]All experimental values in this table are taken from Reference 7.

the $|\Delta I| = 1/2$ prediction is

$$\sqrt{2}\, \Sigma_{o}^{+} + \Sigma_{+}^{+} - \Sigma_{-}^{-} = 0 \quad .$$

The amplitudes Σ_{+}^{+} and Σ_{-}^{-} are fairly well known, and the orientation of Σ_{+}^{+} and Σ_{-}^{-} with respect to the s and p axis is also well known, being determined from the asymmetry parameters α, β, and γ. However, the parameters of the decay $\Sigma^{+} \to p\pi^{\circ}$ have, at present, an inherent uncertainty reflected by the fact that α_{o}^{+} has been measured three times with results

$$\alpha_{o}^{+} = -0.80 \pm 0.16^{3}$$
$$= -0.986 \pm 0.07^{4}$$
$$= -0.88 \pm 0.05^{5} \quad .$$

Also, the sign of γ_{o}^{+} is still uncertain necessitating two solutions, both of which are shown in Figure 1. Note that closure of the triangle is a necessary but not sufficient condition for the assumption of $\Delta I = 1/2$ dominance in Σ decay[6].

The $|\Delta I_{3}| = 1/2$ rule is equivalent to the $\Delta S = 1$ rule since in the relation

$$2(Q - I_{3}) = S + B \qquad (1.1)$$

both baryon number (B) and electric charge (Q) are strictly
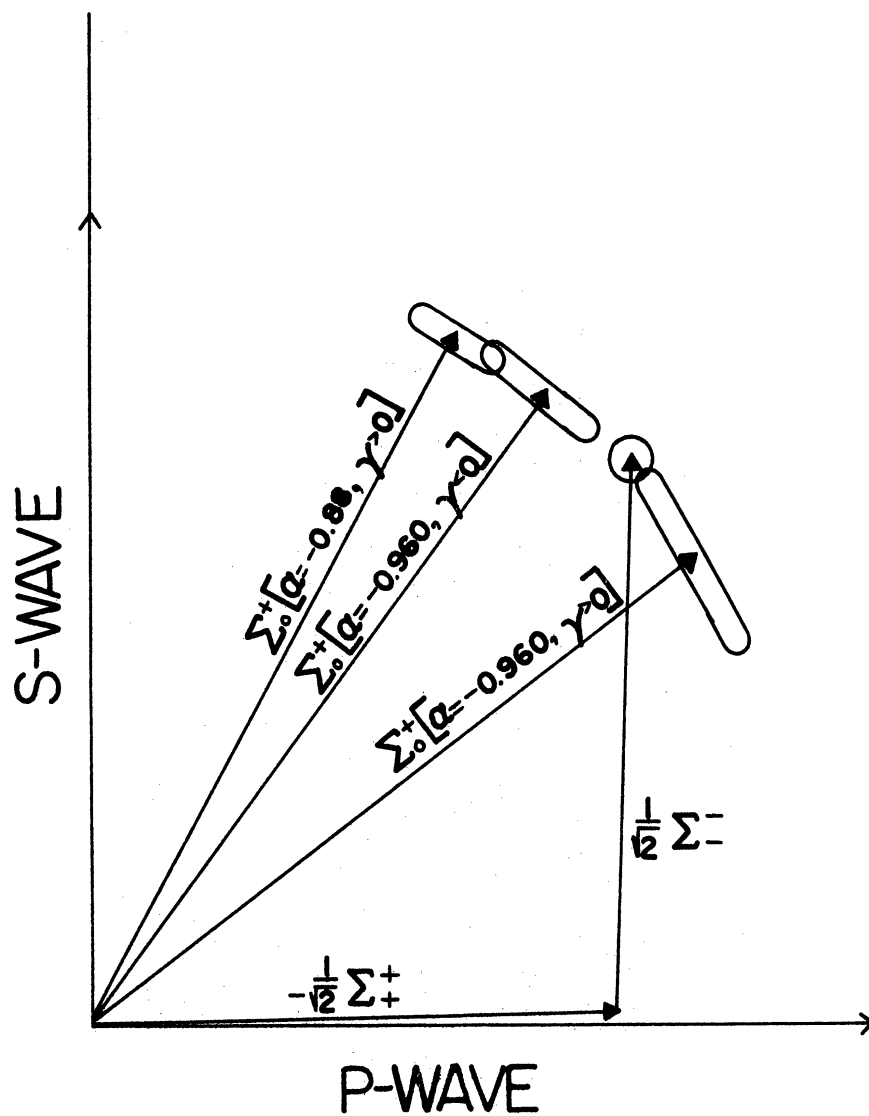
Figure 1. Graphical representation of the triangular relations for the Σ decay. If ΔI = 1/2 rule holds, the triangle should close.

conserved. The simplest way to insure $|\Delta I_3| = 1/2$ in relation (1.1) is to assume $|\Delta I| = 1/2$. The observation that the $|\Delta I| = 1/2$ rule is most likely only an approximate selection rule has been hypothesized, based on the presence of the decay mode $K^+ \to \pi^+\pi^\circ$. As will be demonstrated shortly, this weak decay requires a $|\Delta I| > 1/2$ transition. Simplistic arguments lead to the result that if purely electromagnetic corrections allowed $K^+ \to \pi^+\pi^\circ$ then the ratio of $K^+ \to \pi^+\pi^\circ$ to $K_s^\circ \to 2\pi$ would be

$$R\binom{+}{\circ} = \frac{\Gamma(K^+ \to \pi^+\pi^\circ)}{\Gamma(K_s^\circ \to 2\pi)} \approx \frac{1}{(137)^2} \approx 5 \times 10^{-5} \quad .$$

Experimentally we find[7]

$$R\binom{+}{\circ} = \frac{1.7 \times 10^7}{1.2 \times 10^{10}} \approx 1.4 \times 10^{-3}$$

so that electromagnetic corrections fail by about two orders of magnitude to explain the abundance of $K^+ \to \pi^+\pi^\circ$. Thus the question before the experimentalist is not one of the validity of the $|\Delta I| = 1/2$ rule but rather by how much is the $|\Delta I| = 1/2$ rule violated and what is the composition of the $|\Delta I| > 1/2$ component of the weak decay Hamiltonian (i.e., is there also a $\Delta I = 5/2$ as well as a $\Delta I = 3/2$ component).

There are several ways to experimentally answer these questions, and among the most direct methods of determination

are the $K \to 2\pi$ and $K \to 3\pi$ decays. By comparing the

$K \to 3\pi$ decay rates, the existence of $|\Delta I| = 3/2$ and $|\Delta I| =$

5/2 amplitudes of the decay can be separately determined.

However, due to the unreliability of necessary phase space

calculations, there is no confidence in tests of $|\Delta I| = 1/2$

rule for $K \to 3\pi$ decay to much better than 10%. The 3π

decays of the K meson have been recently summarized by Aubert[8]

and Overseth[9] and Table II summarizes these decays. In Over-

seth's notation

$$\gamma(+-_o) = \frac{\Gamma(K \to \pi^+\pi^-\pi^o)}{\varphi}$$

where φ is the phase space factor due either to Trilling[10]

or Devlin[11] as indicated. The results are divided into those

ratios which indicate $\Delta I = 3/2$ transitions or $\Delta I \geq 5/2$ tran-

sitions. The table shows no clear evidence for any $|\Delta I| > 5/2$

amplitude but evidence consistent with a $|\Delta I| = 3/2$ amplitude

is indicated.

The overall 10% uncertainty in any $|\Delta I| = 1/2$ test from

$K \to 3\pi$ decay can be cut by more than half if one looks at

the $K \to 2\pi$ decay. Unfortunately, the only thing that can

be determined <u>directly</u> from $K \to 2\pi$ decay is the existence

of $|\Delta I| \geq 3/2$ amplitude and any measurement of the relative

amount of $|\Delta I| = 3/2$ and $|\Delta I| = 5/2$ transitions must be based

on knowledge of $\pi\pi$ phase shift. However, it was our opinion

that improved accuracy in the measurement of $\pi\pi$ phase shifts

would soon be available, and for this reason we proposed to
determine the branching ratio

$$R = \frac{\Gamma(K_S^o \to \pi^+\pi^-)}{\Gamma(K_S^o \to \pi^o\pi^o)} \qquad (1.2)$$

in order to directly determine the $|\Delta I| \geq 3/2$ amplitude, and
ultimately the ratio of $|\Delta I| = 3/2$ to $|\Delta I| = 5/2$ amplitudes
of the weak interaction transition matrix which governs the
$K_S^o \to 2\pi$ decay.

TABLE II

$\Delta I = 1/2$ RULE FOR $K \to 3\pi$ DECAY

Ratio	Prediction	Experimental Value	
		φTrilling	φDevlin
$\dfrac{\gamma(ooo)}{3/2\ \gamma(+-o)}$	1.0 if no $\Delta I \geq 5/2$ transitions	0.935 ±0.06	1.00 ±0.06
$\dfrac{\gamma(++-)}{4\gamma(+oo)}$	1.0 if no $\Delta I \geq 5/2$ transitions	1.03 ±0.03	1.00 ±0.03
$\dfrac{\gamma(+-o)}{2\gamma(+oo)}$	1.0 if no $\Delta I = 3/2$ transitions	0.875 ±0.044	0.80 ±0.044
$\dfrac{\gamma(ooo)}{\gamma(++-)\ -\ \gamma(+oo)}$	1.0 if no $\Delta I = 3/2$ transitions	0.79 ±0.04	0.79 ±0.04

2. ISOSPIN ANALYSIS OF $K \to 2\pi$ DECAYS

The concept of isotopic spin was first introduced[12] in low-energy nuclear physics to describe, phenomenologically, the similarity in nuclear force between any two nucleons. Thus the concept of charge was superfluous when discussing nuclear type forces, though electromagnetic corrections keep this statement from being totally valid. If we now go to isospin space (sometimes called SU(2) space) the π meson multiplet with its three charge states is represented by a single isovector ($I = 1$) with three projections on the I_3 axis. These states are ($|I, I_3\rangle$), as follows:

$$|1, +1\rangle = \pi^+ \tag{1.3a}$$

$$|1, 0\rangle = \pi^\circ \tag{1.3b}$$

$$|1, -1\rangle = \pi^- \;. \tag{1.3c}$$

A similar analysis of the kaon family shows that the four members are divided into two doublets with isospin 1/2. The first doublet is

$$|1/2, 1/2\rangle = K^+ \tag{1.4a}$$

$$|1/2, -1/2\rangle = K^\circ \tag{1.4b}$$

while the second doublet is

$$|1/2, 1/2\rangle = \overline{K^\circ} \tag{1.5a}$$

$$|1/2, -1/2\rangle = K^- \;. \tag{1.5b}$$

In this experiment we are primarily interested in the 2π final states of the K_S^0 decay, namely $|\pi^+\pi^-\rangle$ and $|\pi^\circ\pi^\circ\rangle$. Using Clebsch-Gordon coefficients[7] we can construct these isospin amplitudes to be

$$|I, I_3\rangle = |0, 0\rangle = \frac{1}{\sqrt{3}} [\,|\pi^+\pi^-\rangle + |\pi^-\pi^+\rangle - |\pi^\circ\pi^\circ\rangle\,] \quad (1.6)$$

$$|1, 0\rangle = \frac{1}{\sqrt{2}} [\,|\pi^+\pi^-\rangle - |\pi^-\pi^+\rangle\,] \quad (1.7)$$

$$|2, 0\rangle = \frac{1}{\sqrt{6}} [2\,|\pi^\circ\pi^\circ\rangle + |\pi^+\pi^-\rangle + |\pi^-\pi^+\rangle\,]. \quad (1.8)$$

Note that I_3 is always 0 since our final state has net charge 0, and that the $|0,0\rangle$ and $|2,0\rangle$ state vectors are symmetric while the $|1,0\rangle$ state vector is antisymmetric under the interchange of the isotopic spin coordinates of the two π mesons. Since the initial kaon state is that of a spinless boson, conservation of angular momentum restricts the final 2π spatial state to be of an s-wave nature and thus symmetric. Bose-Einstein statistics, which demand symmetry for the total 2π final state wave function, thus restricts the isospin wave function to be also symmetric. Thus the allowed final 2π isospin states are $|0,0\rangle$ and $|2,0\rangle$ while the initial isospin state is isospin 1/2. The $|\Delta I| = 1/2$ selection rule says simply that the change in isospin between initial and final states in a weak decay is 1/2. If the weak interaction Hamiltonian governing this decay adheres strictly to this selection

rule then only the $|0,0\rangle$ final state is allowed and the branching ratio is

$$R = \frac{\Gamma(K^\circ_S \rightarrow \pi^+\pi^-)}{\Gamma(K^\circ_S \rightarrow \pi^\circ\pi^\circ)} = \frac{2/3}{1/3} = 2.0 \quad . \qquad (1.9)$$

Of course this result will be modified by a phase space factor due to the very slight mass difference between the charged and neutral modes of the final state pions. This turns out to be given by[13]

$$\frac{\sqrt{m^2_{K^\circ} - 4m^2_{\pi^+}}}{\sqrt{m^2_{K^\circ} - 4m^2_{\pi^\circ}}} \approx 0.988 \qquad (1.10)$$

so that we may safely disregard this for now. A more dramatic effect will be observed if there is a part of the weak interaction Hamiltonian that allows $|\Delta I| = 3/2$ or even $|\Delta I| = 5/2$ transitions. In this case the final state will be a mixture of $|0,0\rangle$ and $|2,0\rangle$ isospin amplitudes such that

$$|2\pi\rangle = A_\circ |0,0\rangle + A_2 |2,0\rangle \quad . \qquad (1.11)$$

The relative amount of $|0,0\rangle$ and $|2,0\rangle$ amplitudes can be calculated with the aid of $K^+ \rightarrow 2\pi$ isospin analysis. In the decay $K^+ \rightarrow \pi^+\pi^\circ$ the third component of isospin in the

final state will be 1, i.e., a final state of charge +1, so

that the only allowed values of I are I = 2 and I = 1. Using

Clebsch-Gordon Coefficients we can construct these states as

$$|2,1\rangle = \frac{1}{\sqrt{2}} [|\pi^+\pi^\circ\rangle + |\pi^\circ\pi^+\rangle] \qquad (1.12)$$

and

$$|1,1\rangle = \frac{1}{\sqrt{2}} [|\pi^+\pi^\circ\rangle - |\pi^\circ\pi^+\rangle] \qquad (1.13)$$

where $|2,1\rangle$ is symmetric and $|1,1\rangle$ antisymmetric under the

interchange of pairs of pions. Using arguments similar to

those employed for the $K_S^\circ \rightarrow 2\pi$ decay, we find that the boson

nature of the final state again demands symmetry of the total

wave function and thus symmetry of the isospin wave function.

Thus the allowed final 2π state has isospin 2 while the ini-

tial K^+ state has isospin 1/2, so that in no way can a $\Delta I =$

1/2 amplitude contribute to this decay. Since this decay is

governed solely by $\Delta I \geq 3/2$, if charge independence of nuclear

forces is valid and ignoring any possible second order weak

interaction effects ($\Delta S = 2$ transition in $K^\circ\text{-}\overline{K}^\sigma$ complex) there

is most likely a similar violation of the $|\Delta I| = 1/2$ rule in

$K_S^\circ \rightarrow 2\pi$ decay.

We may now, simply with the use of Clebsch-Gordon coef-

ficients, derive the useful relation[*] first specified by

---

[*]This relation is rigorously derived in Appendix C starting
 with the modified Weisskopf_Wigner treatment of the time-
 dependent amplitudes K and K̄.

Abbud, Lee, and Yang[14]

$$R - 2 = 6\sqrt{2} \; Re\left(\frac{A_2}{A_o}\right) \cos\left(\delta_2 - \delta_o\right) + \left(\Delta_{em}\right) \qquad (1.14)$$

which starts with the 2π state constructed as

$$|2\pi\rangle = A_o |0,0\rangle + A_2 |2,0\rangle e^{i(\delta_2 - \delta_0)} \qquad (1.15)$$

where

$$A_I = \langle (2\pi)_I | H_{wk} | K^o\rangle \qquad .$$

$|(2\pi)_I\rangle$ is the stationary 2π eigenstate of H_{st} with total iso-spin I, while the δ_I are the respective s-wave phase shifts.

The branching ratio R becomes[*]

$$R = \frac{\frac{2}{3} A_o^2 + \frac{1}{3} A_2^2 + \frac{4}{\sqrt{18}} Re \, A_2 \, A_o \cos\left(\delta_2 - \delta_o\right)}{\frac{1}{3} A_o^2 + \frac{2}{3} A_2^2 - \frac{4}{\sqrt{18}} Re \, A_2 \, A_o \cos\left(\delta_2 - \delta_o\right)} \qquad .$$

Dividing through by A_o^2 we find

$$R = \frac{\frac{2}{3} + \frac{1}{3} \left|\frac{A_2}{A_o}\right|^2 + \frac{4}{\sqrt{18}} Re\left(\frac{A_2}{A_o}\right) \cos\left(\delta_2 - \delta_o\right)}{\frac{1}{3} + \frac{2}{3} \left|\frac{A_2}{A_o}\right|^2 - \frac{4}{\sqrt{18}} Re\left(\frac{A_2}{A_o}\right) \cos\left(\delta_2 - \delta_o\right)} \qquad .$$

---

[*] We ignore the $Im(A_2/A_o)$ since we show (page 15, expression 1.19) that it is of the order of 10 to the minus four while the real part is two orders of magnitude larger. Thus the relative phase between A_2 and A_0 is ≈ 0 or $n\pi$.

Ignoring second order terms

$$R = \frac{2 + \frac{4}{\sqrt{2}} \, \mathrm{Re}\left(\frac{A_2}{A_o}\right) \cos\left(\delta_2 - \delta_o\right)}{1 - \frac{4}{\sqrt{2}} \, \mathrm{Re}\left(\frac{A_2}{A_o}\right) \cos\left(\delta_2 - \delta_o\right)}$$

$$= 2 \left[1 + \frac{2}{\sqrt{2}} \, \mathrm{Re}\left(\frac{A_2}{A_o}\right) \cos\left(\delta_2 - \delta_o\right)\right]$$

$$\times \left[1 + \frac{4}{\sqrt{2}} \, \mathrm{Re}\left(\frac{A_2}{A_o}\right) \cos\left(\delta_2 - \delta_o\right)\right]$$

$$= 2 \left[1 + \frac{6}{\sqrt{2}} \, \mathrm{Re}\left(\frac{A_2}{A_o}\right) + 4\left(\mathrm{Re}\,\frac{A_2}{A_o}\right)^2\right] \qquad .$$

Again ignoring second order terms

$$R - 2 = 6\sqrt{2} \, \mathrm{Re}\left(\frac{A_2}{A_o}\right) \cos\left(\delta_2 - \delta_o\right) \qquad .$$

To determine the value of $\mathrm{Re}(A_2/A_o)$ we need only realize the relation between the standing wave amplitudes A_I and the $|\Delta I| = 1/2$, $3/2$, and $5/2$ transition amplitudes $\alpha_{1/2}$, $\alpha_{3/2}$, and $\alpha_{5/2}$, respectively. Assuming $\alpha_{3/2} \gg \alpha_{5/2}$ we find

$$A_o = \frac{\alpha_{1/2}}{\sqrt{2}} \qquad\qquad (1.16)$$

and

$$A_2^o = \frac{1}{\sqrt{2}} \alpha_{3/2} + \frac{1}{\sqrt{2}} \alpha_{5/2} * \qquad (1.17)$$

for the K^o decay. For the $K^+ \to \pi^+\pi^o$ decay we define

$$A_2^+ = \langle (\pi^+\pi^o)_2 | H_{wk} | K^+ \rangle$$

and in terms of $\alpha_{3/2}$ we find

$$A_2^+ = \frac{\sqrt{3}}{2} \alpha_{3/2} - \frac{1}{\sqrt{3}} \alpha_{5/2} . \qquad (1.18)$$

From the decay rate of $K^+ \to \pi^+\pi^o$ we can determine

$$\left| \frac{A_+}{A_o} \right| = .0544$$

and from expressions above we see

$$\frac{A_2^+}{A_2^o} = \sqrt{\frac{3}{2}}$$

---

*Neither the general Cabibbo theory nor any current-current form of the weak interaction based on octet x octet interactions can accommodate a $\Delta I = 5/2$ term. The usual current-current theory describes the $K_s^o \to 2\pi$ decays with products of currents of the form $J_\mu S_\mu^*$ where J_μ is the $\Delta S = 0$ current with $\Delta I = 1$ and S_μ is the $\Delta S = 1$ current with $\Delta I = 1/2$. Thus the product contains $\Delta I = 1/2$ and $\Delta I = 3/2$ but no $\Delta I = 5/2$ component.

so that

$$\left|\frac{A_2}{A_o}\right| = \sqrt{\frac{2}{3}} \ (.0544) = .044 \quad .$$

Since we are interested in the $\mathrm{Re}(A_2/A_o)$ we can subtract $|\mathrm{Im}(A_2/A_o)|$ by noting that[15]

$$\left|\mathrm{Im}(\frac{A_2}{A_o})\right| \leq \frac{\sqrt{2}}{3} \ (|\eta_{+-}| + |\eta_{oo}|) \tag{1.19}$$

where $|\eta_{+-}|$ and $|\eta_{oo}|$ are the CP violating parameters

$$|\eta_{+-}| = \frac{A(K_L^o \rightarrow \pi^{\binom{+}{o}}\pi^{\binom{-}{o}})}{A(K_S^o \rightarrow \pi^{\binom{+}{o}}\pi^{\binom{-}{o}})} \quad . \tag{1.20}$$

Thus the imaginary part of A_2 reflects the CP violation within the K^o-$\overline{K}^o$ system and is consequently on the order of 10^{-3}. Hence we may assume

$$\mathrm{Re}(\frac{A_2}{A_o}) \approx .043$$

so that again, without prior knowledge of the $\pi\pi$ s-wave phase shift, the limits on the branching ratio are given by expression (1.14) to be

$$1.64 < R < 2.36 \ ^* \quad .$$

We now consider the possibility of $\Delta I = 5/2$ transitions taking place so that in expressions (1.17) and (1.18) the $\alpha_{5/2}$ terms are not zero. There are two possibilities. If we assume that $\alpha_{5/2}$ and $\alpha_{3/2}$ are complex then we can merely set an upper limit on the ratio $\left| \dfrac{\alpha_{5/2}}{\alpha_{3/2}} \right|$. If, on the other hand, we assume that $\alpha_{5/2}$ and $\alpha_{3/2}$ are both real then a quadratic equation exists for $\left(\dfrac{\alpha_{5/2}}{\alpha_{3/2}} \right)$ and there are thus two solutions.

In the first case, $\alpha_{5/2}$ and $\alpha_{3/2}$ complex, we find

$$|\gamma| \equiv \left| \frac{A_2^+}{A_2} \right| = \frac{\left| \dfrac{A_2^+}{A_o} \right|}{\left| \dfrac{A_2}{A_o} \right|} = \left| \frac{0.462 \cos (\delta_2 - \delta_o)}{R - 2} \right| = \frac{\left| \dfrac{\sqrt{6}}{2} \alpha_{3/2} - \sqrt{\dfrac{2}{3}} \alpha_{5/2} \right|}{\left| \alpha_{3/2} + \alpha_{5/2} \right|}$$

$$(1.21)$$

Upon examining the relation between $|\gamma|$ and the relative phase between $\alpha_{5/2}$ and $\alpha_{3/2}$ we arrive at the inequality

$$\frac{\dfrac{\sqrt{6}}{2} - \sqrt{\dfrac{2}{3}} \left| \dfrac{\alpha_{5/2}}{\alpha_{3/2}} \right|}{1 + \left| \dfrac{\alpha_{5/2}}{\alpha_{3/2}} \right|} \leqslant |\gamma| \leqslant \frac{\dfrac{\sqrt{6}}{2} + \sqrt{\dfrac{2}{3}} \left| \dfrac{\alpha_{5/2}}{\alpha_{3/2}} \right|}{1 - \left| \dfrac{\alpha_{5/2}}{\alpha_{3/2}} \right|} \quad . \qquad (1.22)$$

---

*Current experimental values of $(\delta_2 - \delta_o)$ definitely indicate a first quadrant result so that we may possibly restrict the value of R to be $2.0 < R < 2.36$. See Appendix D.

With this we can set an upper limit of

$$\left| \frac{\alpha_{5/2}}{\alpha_{3/2}} \right| \leq \frac{|\gamma| + \frac{\sqrt{6}}{2}}{|\gamma| - \sqrt{\frac{2}{3}}} \quad . \tag{1.23}$$

On the other hand, assuming $\alpha_{5/2}$ and $\alpha_{3/2}$ are real, we find

$$\pm\gamma = \frac{\frac{\sqrt{6}}{2} - \sqrt{\frac{2}{3}}\left(\frac{\alpha_{5/2}}{\alpha_{3/2}}\right)}{1 + \left(\frac{\alpha_{5/2}}{\alpha_{3/2}}\right)} \quad . \tag{1.24}$$

The resulting solutions are

$$\frac{\alpha_{5/2}}{\alpha_{3/2}} = \frac{\frac{\sqrt{6}}{2} - \gamma}{\gamma + \sqrt{\frac{2}{3}}} \quad ; \quad \frac{\alpha_{5/2}}{\alpha_{3/2}} = \frac{\frac{\sqrt{6}}{2} + \gamma}{\sqrt{\frac{2}{3}} - \gamma} \quad . \tag{1.25}$$

3. ELECTROMAGNETIC CORRECTIONS* TO THE K_s^o BRANCHING RATIO

In expression (1.14) the last term within parentheses (Δ_{em}) corresponds to the sum of corrections due to electromagnetic effects. Wu and Yang[16] noted that these corrections lead to small changes in the ratio R. The explicit form of the electromagnetic correction contains five terms[17]

$$\Delta_{em} = 2\left[\frac{3\alpha}{\pi}\ell n \frac{\Lambda}{m_\pi} + a\ell n \frac{\omega}{m_\pi} - 0.015 + \frac{\pi a(1 + V^2)}{2V} + aC \right] \quad . \tag{1.26}$$

---

*These corrections include the previously mentioned phase space considerations.

The first term contains renormalization effects at the $K\pi\pi$ vertex and pion wave function renormalization and is logarithmically divergent at Λ the cutoff momentum. The second term describes soft photon emission[18] in $K^+ \to \pi^+\pi^-$ (i.e., $K^+ \to \pi^+\pi^-\gamma$) with γ energy less than ω. The constant a is defined as

$$a = \frac{2\alpha}{\pi}\left[\frac{1 + V^2}{2V}\ln\left(\frac{1 + V}{1 - V}\right) - 1\right] \qquad (1.27)$$

where V is the velocity of the π^+ in the K rest system. The third term is due to phase space differences and was calculated earlier. The fourth term is a correction factor from the Coulomb interaction. The fifth and last term is a result of strong-interaction corrections to the electromagnetic correction. In addition some of the finite contributions of the first two terms are contained in C.

There have been only four attempts at evaluating the term Δ_{em}. The first was only a partial estimation by Lee and Wu[19]. In 1967 Abbud, Lee, and Yang[14] attempted a complete evaluation of Δ_{em} and arrived at the estimate $\Delta_{em} = -.04 \pm.04$. However, they neglected to include the fourth term in equation (1.23), and Belavin and Narodetsky[17] recalculated Δ_{em} including this important Coulomb term. Their result was $\Delta_{em} = .006$ with no assigned error. Finally in early 1969 Nachtman and de Rafael[20] recalculated Δ_{em} with a revised estimate of the last term. Their result, the result we will use in this paper, is $\Delta_{em} = -.006$. As can be seen the correction is small and is more than absorbed by the current experimental errors in both R and $\delta_2 - \delta_o$, so that we feel justified in ignoring it in our rough quantitative calculations.

CHAPTER II

EXPERIMENTAL METHOD

1. PREVIOUS EXPERIMENTAL VALUES OF $R = \Gamma(K_S^o \rightarrow \pi^+\pi^-)/\Gamma(K_S^o \rightarrow \pi^o\pi^o)$

   Although the existence of the charged mode of the K_S^o was
experimentally confirmed[21] as early as 1947, it was not until
ten years later[*] that the state of the art, plus enhanced
theoretical understanding of the phenomena, enabled the exper-
imentalists to attempt an accurate measurement of R. Since
the experiment of Eisler[22] in 1957 there have been essentially
only nine experimental determinations of R including the pre-
sent experiment under discussion. These experiments can logi-
cally be grouped into two temporal categories which we will
call the "old" and the "recent" experiments. The first seven
of the nine experiments make up the "old" group. All seven
were performed between 1957 and 1963 and most quoted errors
on R of 10% or greater. Between 1964 and 1968 no experiments
were carried out, and the recent category did not begin until
the experiment of Gobbi et al.[23] in 1969. The experiment
which we present here is the only other recent attempt at
determining R. The last two "recent" experiments reflect
the improved experimental techniques in assigning errors of
2-3% on R.

---

[*]There were several early experiments on V^o particles between
1947 and 1957. However, they observed only the charged
mode, and this plus extremely limited statistics made their
results only approximate at best.

1.1 Eisler et al.

The experiment of Eisler et al. used a propane bubble chamber and was the first to observe the neutral decay $K_s^o \rightarrow \pi^o \pi^o$ by observing the subsequent conversion ($\gamma \rightarrow e^+ e^-$) of one or more of the resulting four γ's ($\pi^o \rightarrow \gamma\gamma$). The K^o's were produced in the associated reaction

$$\pi^- + p \rightarrow \Lambda^o + K^o \qquad (2.1)$$

which was the predominant method of K^o production for the old category of experiments.[*] The resulting statistics of 168 charged decays and only six <u>observed</u> neutral decays emphasized the very poor gamma detection efficiency in these early chambers. Based solely on the charged sample Eisler et al. found R to be 5.25 ±3.37, while based on both the charged and neutral decays R was found to be 6.0 ±2.68. The results were self-consistent, but somewhat inconsistent with any $\Delta I = 1/2$ prediction of 2.0 for R.

1.2 Crawford et al.

The experiment of Crawford et al.[24] used reaction (2.1) in a hydrogen bubble chamber to compile a total of 1091 recorded events. In 227 events both the Λ and K^o decayed

---

[*]A more detailed analysis of the general method used in these associative production experiments is given in the description of the Chretien et al. experiment (Section 1.7 of this chapter), the last of the "old" experiments.

within the fiducial volume via their charged modes, for 594 events only the Λ decayed via its charged mode, and for the remaining 270 events only the K° decayed via its charged mode. After correcting for fiducial volume characteristics and scanning efficiency (30% double scan), the LRL group arrived at a value for R, based solely on the charged mode, of 2.11 ±.29[*]. In addition, this experiment detected three events which were consistent with $K_S^\circ \to \pi^\circ \pi^\circ$. Corrections for the extremely poor conversion efficiency of hydrogen led to a value of R, based only on neutral decays, of 2.7 ±1.1. We quote this value of R for completeness only since we feel the assigned error is underestimated.

1.3 Baglin et al.

The experiment of Baglin et al.[25] used a mixture of propane and methyliodide with radiation length of about 10 cm in a small (3.4 x 2.4 x 2.0 radiation lengths) chamber to detect the K° decays. Contrary to previous experiments, Baglin looked primarily for the neutral K° decays. Again using reaction (2.1), only those events in which the associated Λ decayed via its charged mode <u>and</u> two of the four γ's converted within the fiducial volume were used. To the raw sample of 16 events, four major corrections were made. The first

---

[*]In most experiments the K_S° charged to neutral ratio is quoted as $\Gamma(K_S^\circ \to \pi^+\pi^-)/\Gamma(K_S^\circ \to \text{all})$. For such cases we re-expressed the result in the form $\Gamma(K_S^\circ \to \pi^+\pi^-)/\Gamma(K_S^\circ \to \pi^\circ\pi^\circ)$.

compensated for randomly scattered tracks simulating charged

Λ decays. The second correction considered the possibility

of alternate origins for the observed gammas. Thirdly, those

charged Λ decays with a short line of flight or a slow secon-

dary were accounted for. The last correction used Monte Carlo

techniques to determine the γ-ray detection efficiency. The

resulting value of R was 2.85 ±.66, within 1.5 S.D. of being

consistent with the $\Delta I = 1/2$ rule.

1.4 Brown et al. (1961)

J. L. Brown et al.[26] were the first experimentors to try

and obtain a value of R using accurate counts of both the

charged and neutral decays. The Michigan 21-liter bubble

chamber was filled with a mixture of 99.5% Xenon and .5%

ethylene with a resultant radiation length of 3.9 cm. Thus

the cylindrical chamber was approximately 7.7 radiation lengths

in diameter and 6.4 radiation lengths deep so that the average

γ detection efficiency was $\approx 70\%$. The source of K°'s again

was a π^- beam and the associated production $\pi^- p \rightarrow \Lambda^\circ K^\circ$.

As was customary in these associated production experiments,

only those K decays accompanied by an easily scanned $\Lambda^\circ \rightarrow$

$\pi^- p$ were counted. The charged K decays were easily scanned,

and the neutral decays were defined as the intersection of

2, 3, or 4 γ-ray pairs in association with the charged decay

mode of the Λ. The neutral decays of the K° were subjected

to additional checks in the form of

1. Comparison of decay length distributions. Average

decay length, $\bar{L}$, of the two modes should be the same; however, it was found that $\bar{L}(K_S \to \pi^+\pi^-) = 1.7 \pm .22$ while $\bar{L}(K_S \to \pi^\circ\pi^\circ) = 2.25 \pm .34$, a difference of two to three standard deviations.

2. <u>Subtractions of stray-γ events</u>. A check on the number of events incorrectly identified as neutral events, because of the intersection of background γ-ray pairs, is obtained by counting the number of times this happens in association with an event where <u>both</u> the Λ° and K° are observed to decay via their charged modes. In 120

$$\pi^- + p \to \Lambda^\circ + K^\circ$$
$$ \mathrel{\raisebox{-1ex}{$\llcorner$}}\!\!\to \pi^-\pi^+$$
$$ \mathrel{\raisebox{-1ex}{$\llcorner$}}\!\!\to \pi^- + p$$
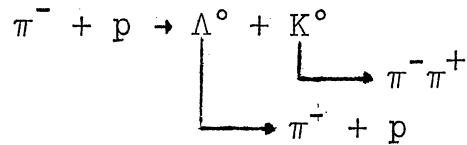
only one event had such a spurious γ pair association.

The resulting uncorrected statistics were 120 $K_S^\circ \to \pi^+\pi^-$ decays which, when corrected for decays outside of the fiducial volume or too close to the origin, became a sample of 130.2 charged events. The $K_S \to \pi^\circ\pi^\circ$ raw sample contained 49 events, and after similar corrections the final neutral sample was 56.5. The resulting branching ratio was R = 2.33 ±0.27.

1.5 Anderson et al.

During the 1962 CERN Conference on High Energy Physics a value of R attributed to Anderson et al.[27] was entered into the record with the only accompanying description being that it was carried out in the 72-inch hydrogen bubble chamber and only the charged mode was counted. Since there was never any follow-up publication, we give the Anderson et al. value of R = 2.85 ±.35 only for the sake of completeness.

1.6 Brown et al. (1963)

A Michigan-LRL collaboration[28], consisting of nearly the same physicists as the earlier Brown et al. experiment, rede-termined the branching ratio in 1962. The xenon chamber was again used to get maximum gamma conversion, but for the first time the K° production mechanism was the more efficient charge exchange reaction $K^{+} + n \rightarrow K^{\circ} + p$ rather than the associa-ted production reaction. A separated K^{+} beam of .8 GeV/c was used and charge exchanged approximately 5% of the time. If there is negligible π^{+} contamination in the beam a reliable signature of K° production is the charge exchange reaction itself which, in turn, is reliably identified by requiring all prongs from the interaction to stop in the chamber with-out decaying. Double scanning of the film resulted in ~ 12,000 charge exchanges of which 7,000 were within the fiducial volume. Hence around 3500 K_{s}°'s were in the initial sample, which is about a twenty-fold increase in statistics over the earlier Michigan experiment.

The charged sample underwent four major corrections which accounted for scanning efficiency, kinematic failures (mislabeling V°'s), extremely short pion secondaries and negligible line of flight. The final sample contained 2477 events. The neutral sample was corrected for scanning efficiency, γ conversion efficiency, and beam contamination and ultimately contained 1250 events. The resulting branching ratio stands alone in being the only result lower than the $\Delta I = 1/2$ prediction of 2.0. It was found that R = 1.98 ±.12.

1.7 Chretien et al.

The last of the experiments which fall into the "old" category was a four-institution collaboration henceforth referred to as Chretien et al.[29] This collaboration followed the methods previously established by branching ratio experiments prior to the Michigan-LRL experiment, described in the last section, in that they used a 1.144 GeV/c π^- beam to produce K°'s via the reaction $\pi^- + p \rightarrow \Lambda^° + K^°$. The chamber used was the 51.5-liter cylindrical chamber at the Cosmotron filled with a mixture of methyl iodide, propane, and ethane which resulted in a radiation length of 8.4 cm and an 82% probability of converting two of the four γ rays. Since the purpose of this experiment, as well as the other associative reaction experiments, was not only to measure the branching ratio of the K° but also the branching ratio R_Λ of the $\Lambda^°$

$$R_\Lambda = \frac{\Gamma(\Lambda^\circ \to p + \pi^-)}{\Gamma(\Lambda^\circ \to n + \pi^\circ)}$$

there were three types of events recorded.

1. The $\Lambda_c^\circ K_c^\circ$ sample,

$$\pi^- + p \to \Lambda_c^\circ + K_c^\circ$$

and

$$\Lambda_c^\circ \to p + \pi^- \quad , \quad K_c^\circ \to \pi^+ + \pi^- \quad .$$

2. The $\Lambda_c^\circ K_n^\circ$ sample

$$\pi^- + p \to \Lambda_c^\circ K_n^\circ$$

with Λ_c° as above and

$$K_n^\circ \to \pi^\circ + \pi^\circ \to 4\gamma$$
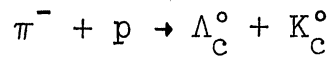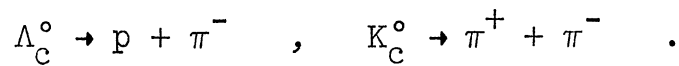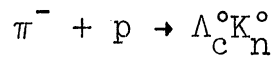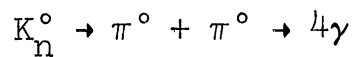
with at least two of the γ's converting.

3. The $K_c \Lambda_n$ sample

$$\pi^- + p \to K_c^\circ + \Lambda_n^\circ$$
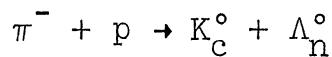
with K_c° as above and

$$\Lambda_n^\circ \to \pi^\circ + n$$
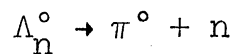
with the two γ's converting.

The K° branching ratio was determined using the $\Lambda_c K_c$ and $\Lambda_c K_n$ samples. The basis of the scanning was the search for all two prong V configurations associated with a π^- interaction and then a subsequent search for possible associated γ-rays. All charged V decays were then measured twice while neutral decays were measured as to projected line of flight of the converted gammas. A consistency check on the K° sample was provided by a Bartlett S function determination of the mean K_s° lifetime $\tau_{K_s^\circ} = (0.87 \pm 0.05) \times 10^{-10}$ compared to[7] $(.862 \pm .006) \times 10^{-10}$. Any possible bias toward the neutral $(\Lambda_c K_n)$ or charged $(\Lambda_c K_c)$ modes was determined by demanding similar properties of the charged Λ decay in both cases. The initial raw sample of charged events was 508 events while the initial neutral event count stood at 198.

Five corrections were made to the raw charged sample:

1. A 16.4% correction was made to compensate for those K_c° decays which occurred between 0 and .3 cm from the π^- interaction.

2. A 3.8% correction for K_c° decays with secondaries of .5 cm or less and/or K_c° decays with opening angles less than 15° or greater than 160°.

3. A 1.7% correction for K_c°'s having momentum less than 100 MeV/c. This correction is closely correlated to corrections 1 and 2 above and contains only the events not <u>already</u> corrected for in 1 and 2 above.

4. This correction compensates for those K_c°'s which

interact in flight before decaying and therefore fail, kinematically, the requirement for K_c decays. The correction amounted to .7%.

5. This was an overall correction for background simulation of a K_c^o event (fake V's) and possible errors in the analysis procedure and was estimated as 0 ±1%.

The final corrected number of charged decays was 628 ±35.9.

The neutral sample underwent six corrections before arriving at the final quoted number.

1. Monte Carlo techniques were used to correct for the conversion efficiency of two or more γ's from the K_n decay. A 22.1% correction resulted.

2. A 6.1% correction was made to compensate for associated γ conversions accidentally pointing to alternate origins.

3. This is the complementary correction to 2 above and accounts for background γ's accidentally simulating K_n decays. This negative (subtractive) correction amounted to 2%.

4. This 1.6% correction was made to compensate for the difference in scanning efficiency for those events labeled as K_n decays and those labeled K_c decays. As might be expected, the charged decays were "easier" to find.

5. A .9% negative correction was made to account for charge exchange events $(\pi^- + p \rightarrow n + \pi^o)$ in which the resulting neutron star simulated a V and both

γ's converted.

6. As in the charged sample, this last overall correction was for analysis uncertainties but, in addition, this correction compensated for charged V's which satisfied both the Λ_c and K_c events and thus amounted to .8%.

The final corrected neutral sample thus contained 255 ±21.2 events, which resulted in a final value of R = 2.47 ±.25.

1.8 Summary of Older Generation Experiments

With the exception of the Michigan-LRL collaboration, all of the old generation experiments used π^-p production techniques to obtain their sample of K_s^o's and were thus characterized by low statistics. In addition, these early experiments were most likely hindered by a general lack of refinement in the measuring and subsequent analysis of both the charged and neutral modes. This is especially important when one realizes that to guarantee a reasonable gamma conversion efficiency high-Z elements have to be used. These very same high-Z elements increase multiple scattering effects, thus making tracks which would be easily measured smooth curves in hydrogen or deuterium, a nightmare collection of partially connected kinks. Thus even the charged decays of the K_s^o, confirmed through measurement under these conditions, must be analyzed carefully, not to mention the much less massive (and thus more scattered) e^-e^+ conversion pairs. Even today with the much more sophisticated geometrical reconstruction

programs, relatively large uncertainties must be attached to tracks measured in heavy liquid chambers. The alternative to this measurement uncertainty is to use a hydrogen (or other low-Z) chamber and not count the neutral decays at all. This has a decided disadvantage in that a major quantity, the number of neutral decays, necessary for the branching ratio being determined is not seen but rather inferred by two other numbers and a constraint relation. Thus any error in the treatment of these two other charged samples is compounded when the number of neutral decays is inferred from these erroneous quantities. It is a well known observation of these branching ratio experiments that, due to less statistics and the necessity of greater corrections, the major portion of the final error attributed to the branching ratio comes from the neutral sample when it is directly measured. Thus the final error of those experiments which infer, rather than determine, the number of $K^\circ \rightarrow 2\pi^\circ$ decays might possibly be underestimated.

As can be seen from Figure 2 all of the results, with the exception of the preliminary Anderson et al. value and the 6% determination of Brown et al. (1963), are consistent within errors. It can also be noted that, within errors, the value of the branching ratio as determined by these old generation experiments ranges from 1.83 to 3.5 with a world average[7] of 2.165 ±0.08. Thus more refined experiments, in terms of beam, chamber, and analysis, were clearly needed. After a lapse of about five years, during which many of the
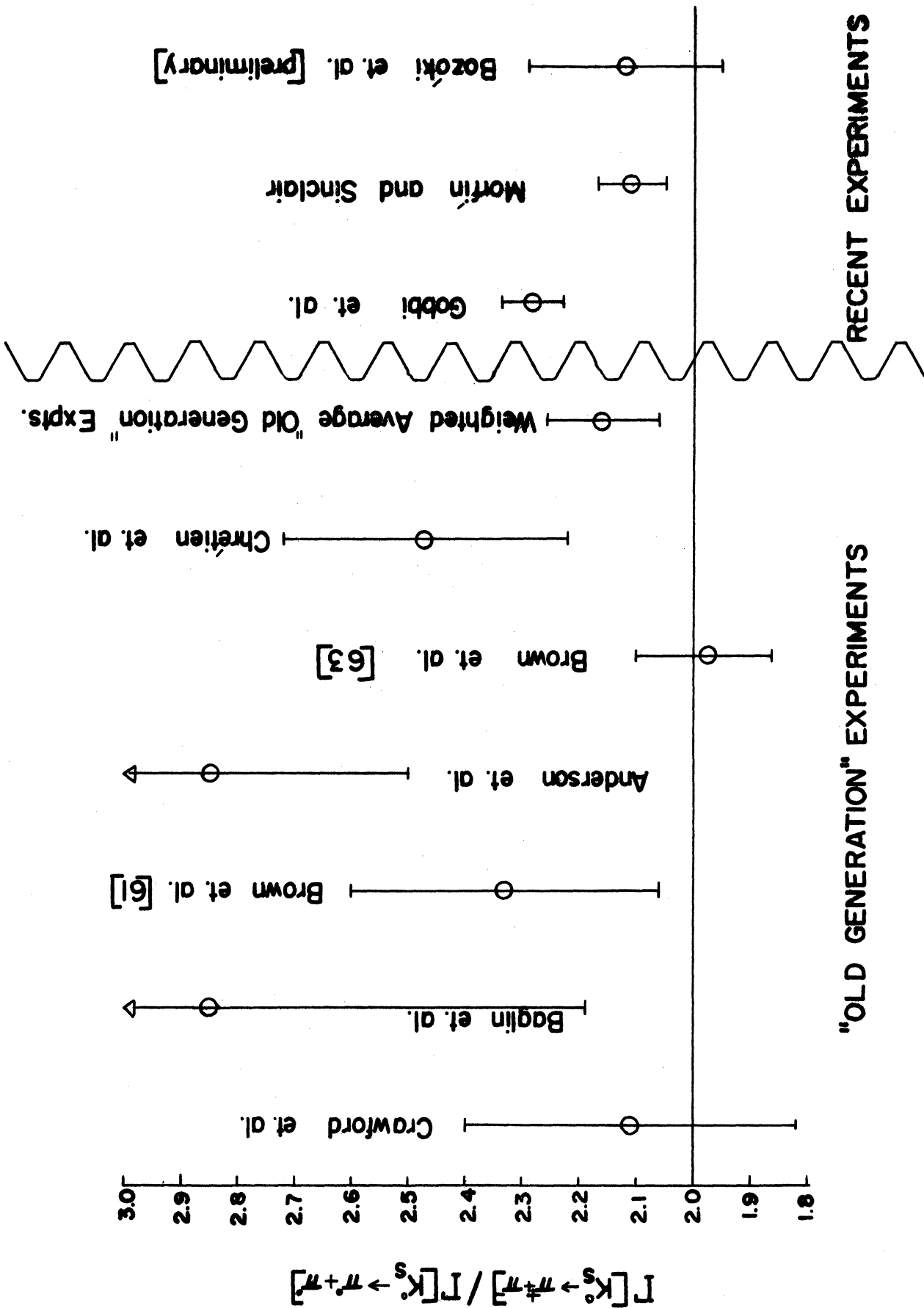
Figure 2. Graphical summary of all reported values for the K_S° charged to neutral branching ratio.

necessary refinements were realized, the experiment of Gobbi et al. began the second generation of experiments to determine R.

1.9   Gobbi et al.

The first experiment of the new generation of determinations was unique in that it was a spark chamber experiment. They used a 2 BeV/c unseparated K^+ beam coming down a beam line containing a counter telescope and differential Cerenkov counter set to reject π^+, p, and μ^+. As in the Brown et al. experiment of 1963, the charge exchange reaction, $K^+ + n \rightarrow K^\circ + p$, is used in this experiment. Detection equipment consisted of a 24-gap, aluminum-foil spark chamber for the charged decays and a 4-radiation length, 49-gap, steel spark chamber for the detection of the neutral decays. In addition to the above, a third spark chamber was used to register the K^+ point of entry into the target so that kinematical analysis of the charged decays could be performed. Due to the veto counters surrounding the target, front edge of the fiducial volumes for the charged and neutral modes were defined electonically and the effective front edge of the neutral fiducial volume is displaced upstream. The back edge of the fiducial volume is the last plate in the steel chamber while the sides are unbounded (detection efficiency quoted as constant and near 100% up to $\approx 45°$).

All pictures were double scanned and the raw sample of charged and neutral decays was 6608 and 3016 events,

respectively, leading to an uncorrected branching ratio of 2.191 ±.048. Seven corrections were made on this <u>raw branching ratio</u> (quoted as a percentage).

1. +3.8 ±.1 to compensate for neutral decays in the downstream veto counter that did not convert and thus were accepted, while charged decays in this veto counter were rejected.

2. +1.0 ±0.5 to account for background to two γ events such as $K^+n \rightarrow p\pi^\circ K^\circ$ and the charge exchange of beam contamination pions.

3. -0.5 for those events in which only one or no γ's converted and thus were not counted.

4. +0.3 for neutral decays which escape the target.

5. -0.1 for γ's with momentum back towards the target.

6. +0.1 for backgoing π interactions.

7. -0.3 for possible admixture of 3-body decays.

The net result of these corrections was to raise the branching ratio to 2.285 ±.055. Thus the first of the recent experiments showed a violation of the $\Delta I = 1/2$ rule of five standard deviations.

2. GENERAL METHOD OF THE PRESENT EXPERIMENT

As in the experiment of Brown et al. (1963) and Gobbi et al. (1969), the K°'s in this experiment were produced via the charge exchange reaction $K^+ + n \rightarrow K^\circ + p$. Unlike the Gobbi et al. experiment, this experiment used a heavy liquid bubble chamber to observe the decays.

The basis of our method was to use the charge exchange of a K^+ ($K^+ + n \to K^\circ + p$) as a signature for the creation of a K°. The vicinity of a charge exchange (Type I event) could then be examined for evidence of a charged decay of the K° (a V whose arms were consistent with $\pi^+\pi^-$) or a neutral decay (one or more electron pairs). The topological definition of a charge exchange was a beam track interaction whose visible products, if any, were protons, i.e., heavily ionizing positive tracks which stopped in the chamber without evidence of a subsequent decay.

There are two difficulties with the method as described so far. The first is that a π^+ contamination in the beam produces π°'s by charge exchange and such events are not easily distinguished from K^+ charge exchanges followed by a neutral decay of the K°. A second difficulty is that many of the K°'s decay so close to the charge exchange point that the separation between that point and the vertex of the V cannot be resolved by the scanner.

In order to overcome these difficulties we asked the scanners to look for any beam interactions which produced a negative track (a Type II event). By subsequent examination of the Type II events we were able to classify them as follows:

1. The negative track was a π^- and was accompanied by a π^+. Other tracks (if any) from the interaction vertex were protons. Since none of the events of this type were accompanied by V's we then deduced

that either they arose from a π^+ contamination in

the beam or they were charged decays of K°'s very

close to the charge exchange vertex.

2. The negative track was a π^- and all other tracks

(if any) from the vertex were protons. Since none

of the events of this type were accompanied by V's

we then deduced that they were due to the interaction

of a π^+ contamination in the beam.

3. The negative track was a π^- and was accompanied by

two π^+ tracks and no other tracks. Such events were

easily recognized as τ^+ decays in flight.

4. The negative track was an electron either from a

Dalitz pair or from the conversion of a γ-ray close

to the interaction vertex.

We used the "π^- only" events described in (2) above as

a measure of the π^+ contamination in the K$^+$ beam. The scan-

ners scanned 9400 π^+ pictures taken at precisely the same

momentum as the K$^+$ pictures. The scan rules for the π^+ film

were the same as those for the K$^+$ film.

The sample was then subjected to four separate edits to

further classify the events, a re-edit to check our editing

accuracy, and a partial measurement of the charged decays to

both confirm our classification of the $K_s^o \rightarrow \pi^+\pi^-$ events and

to give realistic input to our Monte Carlo program. The raw

sample of charged decays was then corrected for such things

as editing errors, and π^+ contamination of the beam, while

the raw sample of neutral decays was corrected for stray γ's,

editing errors, unobserved γ's, and π^+ contamination of the
beam. These corrections were based on both previous observa-
tions and Monte Carlo predictions. Our initial statistics
and relatively small corrections enabled us to keep the error
of the final branching ratio down to $\approx 3\%$.

CHAPTER III

THE EXPERIMENT AND REDUCTION OF THE DATA

1. THE BEAM AND THE CHAMBER

The beam used for this experiment was the low momentum, two-stage separated $28°$ beam at the ZGS installation of Argonne National Laboratory. The beam elements included seven quadrupoles, three bending magnets, and two electrostatic separators; in addition there were two preset mass slits and one set (horizontal and vertical) of remotely controlled collimators. The beam was designed to operate in two modes by reversing the polarities of the first doublet (Q_1 and Q_2). In Mode A the ratio of separation-to-image size is maximized at the first mass slit while in Mode B this ratio is ≈ 2.5 times less favorable but the solid angle of the beam is increased by $\approx 50\%$. For this experiment beam contamination (primarily π^+, p, and μ^+) was crucial so that Mode A, as in Figure 3, was employed.

Essentially*, the first two quadrupoles make the beam parallel in the vertical plane while focusing the beam horizontally at the first mass slit. The first bending magnet deflects the beam by $15°$ while providing momentum dispersion. The first spectrometer provides mass separation by deflection in the vertical plane. Following this spectrometer a

---

*For full details of the beam see M. Derrick and G. Keyes, Low Momentum Separated Beam, unpublished but obtainable from Argonne National Laboratory, Argonne, Illinois.
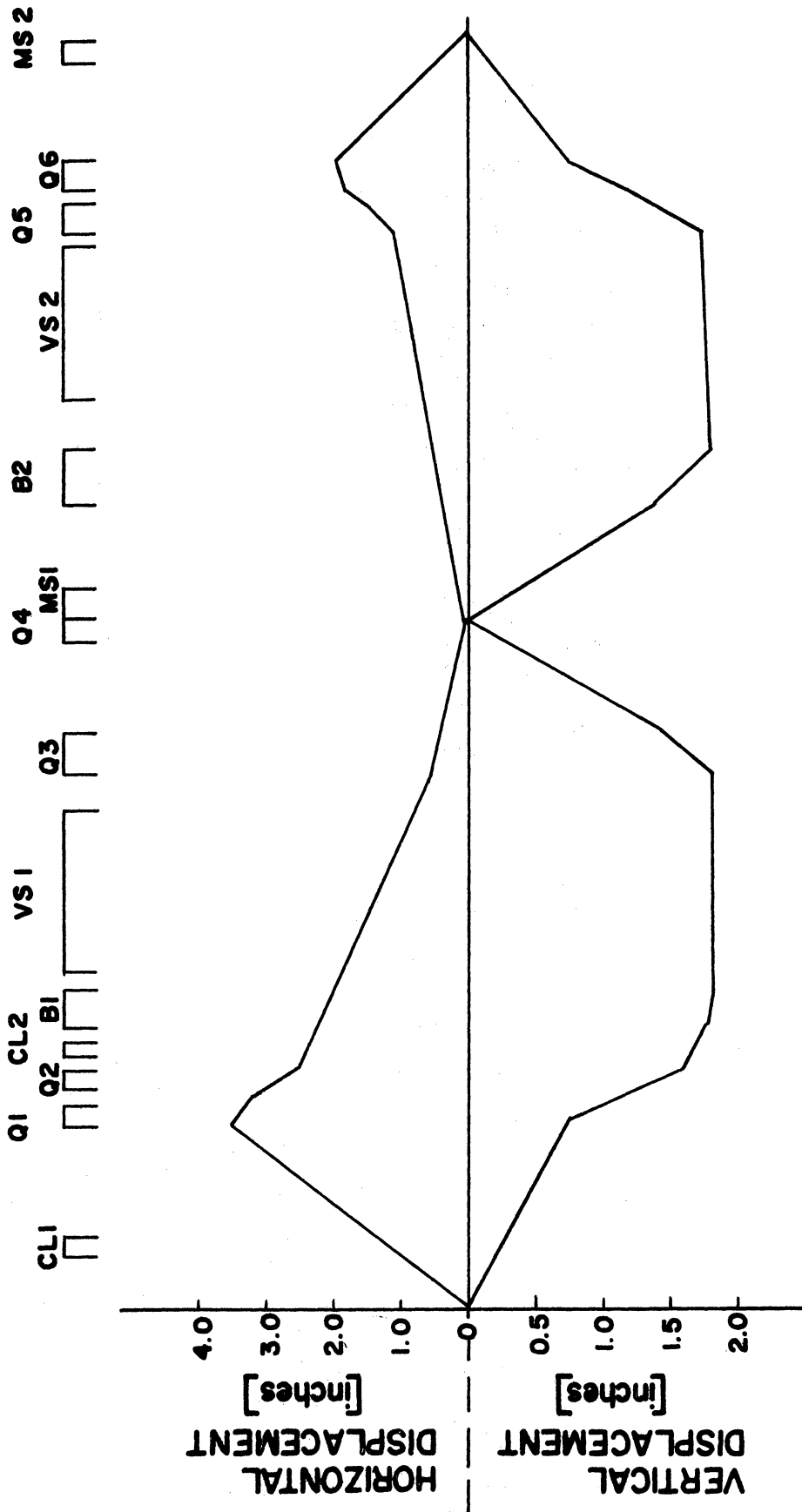
Figure 3. The vertical and horizontal effects of each component in the 28° beam line when operating in Mode A.

quadrupole is situated with a field gradient to give both horizontal and vertical focus at the first mass slit. Diverging particles at this point are made parallel in the vertical plane by the $40°$ second bending magnet. The second stage introduces another separator, and a final doublet of quadrupoles to provide focus on the last mass slit.

For monitoring the beam four cascade counters--though only three were used for this experiment--and one differential Cerenkov were available. The mass limit on the Cerenkov counter was set so that any particle of mass $m < m_{K^+}$ would not trigger the counter. Thus a coincidence circuit of Tl, T2, T3, and C would essentially count only K^+ and p, while a circuit containing Tl, T2, T3 in coincidence with the Cerenkov in anti-coincidence ($\bar{C}$) would essentially count only π^+ and μ^+. Naturally, a circuit which excluded the Cerenkov entirely would count <u>all</u> charged particles. An inhibit circuit was employed using Tl, T2, T3, and $\bar{C}$ such that when the number of $\pi^+ + \mu^+$ was greater than two no picture was taken.

The K^+ beam was transported at 825 MeV/c. After traversing the monitoring equipment and the beam window, the K^+ momentum was down to approximately 790 MeV/c upon entering the liquid, and was further reduced to ≈ 700 MeV/c in traveling ~ 23 cm to enter the fiducial volume. This momentum was chosen since it was high enough to overcome decay loss along the beam line, and low enough not to introduce $\pi°$ production from the interaction $K^+ + n \rightarrow K° + \pi° + p$ as shown in Figure 4.
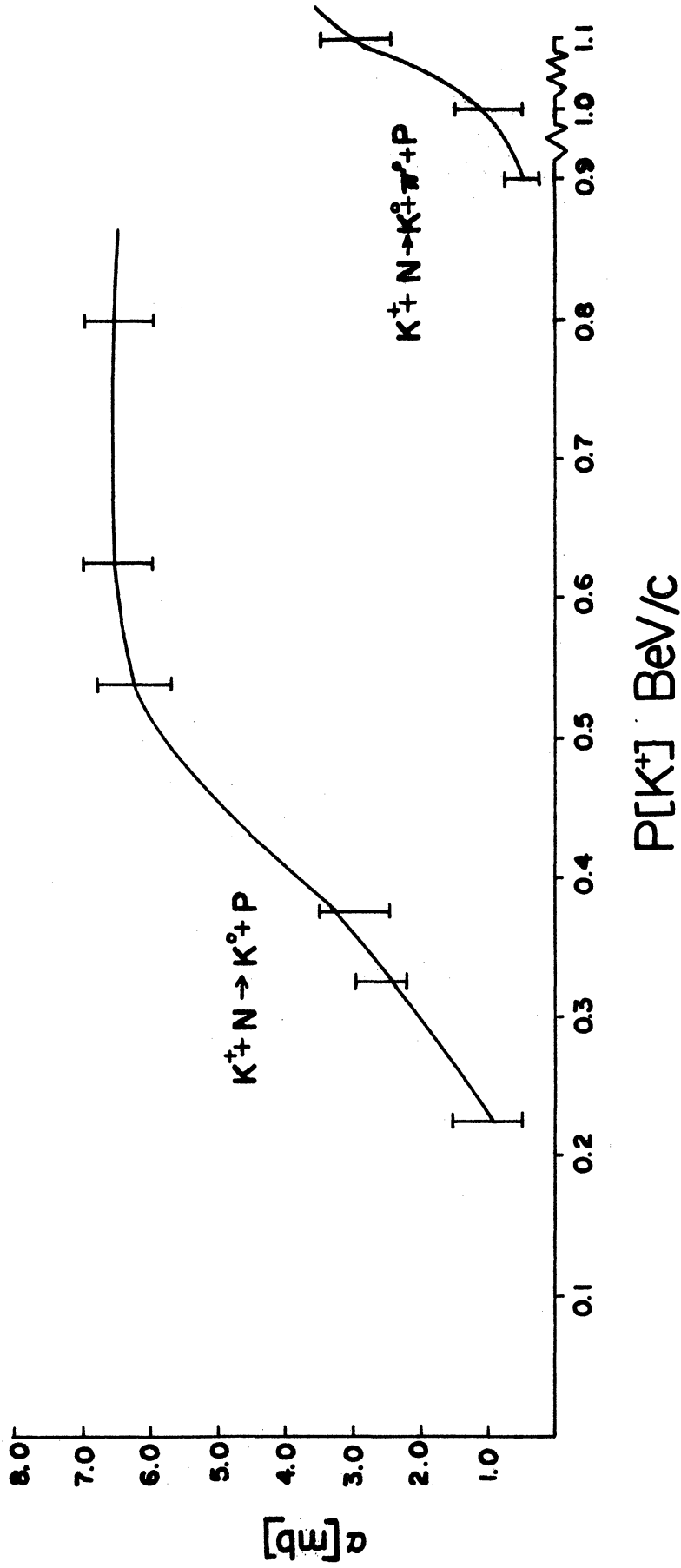
Figure 4. Comparison of the cross sections for $K^+ + n \rightarrow K^\circ + p$ --the primary interaction--and $K^+ + n \rightarrow K^\circ + \pi^\circ + p$, a possible source of false γ events.

The 40-inch heavy liquid Michigan-Argonne bubble chamber, filled with heavy freon (CF_3Br), served as both target and detector for the highly separated K^+ beam described above. Heavy freon, radiation length $\approx$ 11 cm, was chosen since we wished the γ conversion efficiency to be as high as possible in order to detect the neutral decay of $K_s^o \rightarrow 2\pi^o \rightarrow 4\gamma$. It was determined[30] that the conversion efficiency ($\gamma \rightarrow e^+e^-$ or $\gamma \rightarrow$ Compton e^-) of photons in the 40-inch HLBC filled with heavy freon is .862 ±.015. Using Monte Carlo techniques we also determined that 98.5% of the neutral decays have at least one gamma convert within a sphere of radius 20 cm centered on the charge exchange point. It was this observation which we incorporated into our edit rules.

A total of 150,000 frames, each with four stereo views, were taken in this chamber using the K^+ beam. In addition, 20,000 frames were taken of π^+ beam interactions for determination of π^+ contamination of the beam.

2. SCANNING

An initial beam survey was carried out to restrict the definition of a "good" beam track. The position of entry, rate-of-change of angle and dip were measured from a sample of K^+ beams and π^+ beams. It was found to be impossible to confidently eliminate any π^+ contamination using the results, but all off-momenta beams could be eliminated by constructing a two-piece template. The template consisted of a base whose upper portion was an arc of 58.4 cm radius of curvature, a

second piece whose bottom edge was an arc of 58.4 cm slid

along the base and was used to define the entrance angle of

a good beam within ±6°.

Since the purpose of this experiment was to determine a

branching ratio, scanning rules were of _utmost importance_.

For this experiment, the possibility of missing an event,

though unfortunate, was not disastrous as long as no bias

towards the charged or neutral decays was involved. The

scanning rules were designed with this in mind and because

of their importance they have been reproduced, as used, in

Appendix A of this paper.

The most important requirement of our scan rules is the

necessity of along-the-track scanning. If the scanner will

consistently follow the beam track from the point it enters

the fiducial volume to the point where it either interacts

or leaves the fiducial volume there will be _no_ bias toward

one decay mode or the other. This method of scanning was

demanded from the scanners and most effectively followed by

them.

In summary, the two main types of events scanned for were

characterized as follows. (See Appendix A, Figures 19-21.)

Type I

    1.   Any zero prong event _if_ the beam track is not heavily

        ionized within 2 cm (low magnification) of its end.

    2.   Any 1, 2, 3..... n prong interaction whose outgoing

        tracks satisfy all of the following.

        a. All outgoing tracks must stop in the chamber

and the last 2 cm (high magnification) must be
heavily ionized.

b.   No negatively charged prongs.

c.   The outgoing prongs must not interact or decay,
i.e., no abrupt change in ionization.

d.   A prong may scatter through any angle as long as
it satisfies (c) above <u>and</u> does not produce one
or more prongs at the point of scatter.

<u>Type II</u>

1.   The interaction has an outgoing negatively charged
prong longer than 4 cm (high magnification).

2.   The beam track is minimum ionizing in the last 2 cm
(low magnification) before interaction.

All the film was double scanned for Type I and Type II
events. The scanners were instructed to scan along the tracks
from the point where they entered the fiducial volume to the
point where they left it, typically a distance of $\sim$ 55 cms.
Only those tracks which entered the fiducial volume within
$\pm 6°$ of the average beam direction were scanned. Since the
huge fringing field of the chamber magnet bends the beam
through $\sim 80°$ before entering the fiducial volume, this rule
ensured that only "on momentum" tracks were scanned. All
disagreements from the double scan were checked and resolved
by a third party, either an experienced scanner or a physicist.

At the conclusion of both scans and the disagreement
check there were 29,444 recorded events. Of these 27,030
were Type I events and 2,414 were Type II events. This then

was the raw sample which had to be further classified.

The question of scanning efficiency for this experiment was important only to the extent that we would want the detection efficiency of charged decays to equal the detection efficiency of the neutral decays. Of the three predominant models[31] used in calculating scanning efficiencies, random-miss, correlated-miss, and two-scanner model, the random-miss model was employed for this experiment. This model is based on the hypothesis that all events are of equal difficulty for the scanner to detect and is the model most often used in bubble chamber work. Mathematically, the random-miss model treats all events missed by scanners as statistically independent events.

When double scanning film, as we did in this experiment, the scanning efficiency for each roll is greatly improved. If we let N_S be the number of events seen by a single scanner, N_B the number seen by both scanners, then $N_{SB} \equiv N_S + N_B$ is the number seen by either or both scanners. If the total number of events that could have been found, i.e., they passed the scan rules, is N_T then we can relate the above quantities to a single scan efficiency[*] e as follows:

$$N_S = 2N_T e(1 - e) \tag{3.1a}$$

---

[*]This method of calculation is particularly attractive when many different scanners have processed the film. The efficiency e is indicative of the results of all scanners combined and does not necessarily reflect the result of any one of the scanners.

$$N_B = N_T e^2 \qquad\qquad (3.1b)$$

$$N_{SB} = N_T[1 - (1 - e)^2] = N_T(2e - e^2) \quad.(3.1c)$$

The double scan efficiency E is just

$$\frac{N_{SB}}{N_T} = (2e - e^2) = E \qquad. \qquad\qquad (3.2)$$

Solving (3.1) for e and substituting in (3.2) we find

$$E = \frac{4N_{SB}N_B}{(N_{SB} + N_B)^2} \qquad. \qquad\qquad (3.3)$$

Using this expression the double scan efficiency for $K_S^o \to$ $\pi^+\pi^-$ events was .994 while the double scan efficiency for $K_S^o \to \pi^o\pi^o$ was .995. These correspond to single scan efficiencies of .923 and .929, respectively. Thus no scanning bias was detectable for the two scans.

3. EDITING

3.1 The K^+ Sample

A series of four edits was used to further classify the events. The rules governing these edits can be found in Appendix B. In the first edit all events found in the two scans were examined by experienced scanners. In the case of Type I events they checked to see that the charge exchange

vertex obeyed the scan rules and that there were no other Type I events within a distance of 10 cms on any of the four projected views. Ten centimeters on the scanning machine corresponds to ~ 20 cms in real space. If the event passed both these tests a template consisting of two concentric circles of radii 5 cms and 10 cms, respectively, was centered on the charge exchange vertex and the area within the outer circle scanned on all four views for one or more electron pairs. Note was taken of any electron pair with an apex within the 10 cm circle on all four views. At this point no judgment was made concerning the origin of the γ-ray. The only other test applied to the electron pair was that its entire track length could not fit within a square 1 cm on a side. This imposed a low energy cutoff of about 10 MeV on the accepted electron pairs. Events which passed these tests were denoted as "γ events" and were passed on to a second edit as such.

In addition to searching for electron pairs, the first editor also searched for V's whose apex lay within the 5 cm circle on all four views. Such events were noted as V events. In order not to miss V's with wide opening angles the first editor was instructed to count as V's stray tracks intersecting the 5 cm circle provided they were not obviously beam tracks or connected to beam tracks.

Events which passed both the γ-test and the V test were denoted as γ-V events.

In the case of Type II events the first editor examined them and classified them as described in Section 2 of this

chapter. Then the first editor searched for V's and electron pairs in the same way as for Type I events.

Physicists carried out a second edit of the film. We examined all γ events, V events, and γ-V events. We checked to see that the arms of each V were consistent with being $\pi^+\pi^-$ tracks and that the orientation of the V relative to the charge exchange vertex was consistent with conservation of momentum. All events whose arms were consistent with $\pi^+\pi^-$ tracks were accepted, and the distance between the charge exchange point and the apex of the V was noted. Those events whose orientation was inconsistent with the conservation of momentum were denoted as scattered V events.

In the case of γ events and γ-V events we examined each electron pair whose apex lay within the 10 cm radius on all four views to see if it had an origin other than the charge exchange vertex. The event remained a γ-event if there was at least one electron pair within the 10 cm radius for which no origin, other than the charge exchange vertex, could be found and provided the electron pair(s) could have come from within the 5 cm circle on all four views. Again, the separation between charge exchange point and the nearest γ was measured at the scan table and noted. It should be emphasized that the number of γ rays per event in no way influenced our raw count of neutral decays.

Table III contains a breakdown of all categories after the first two edits and the double scan. For the meaning of each classification see the edit rules in Appendix B.

TABLE III

DETAILED EVENT BREAKDOWN AFTER SECOND EDIT

Scan	First Edit Classification	Totals	Second Edit Classification	Totals
Confirmed Type I Events 27,030	Reject	868	Reject	108
	Neither V nor γ	9187		
	Associated V	6870	V good V fails Undecided	5979 875 23
	Associated γ(s)	5616	At least one good γ All γ's fail Undecided	4161 1394 33
	Associated V and associated $\overline{\gamma(s)}$	1628	γ(s) and V fail Good V, no γ Good γ(s), no V Both V and γ(s) good Undecided	311 1041 141 106 20
	2 Type I within 20 cm	3195		
	Undecided	8		
Confirmed Type II Events 2,414	τ decays	1230		
	π^- with K^+	62		
	π^- only	76		
	V on good Type I event with associated γ(s)	118	At least one good γ All γ's fail Undecided	21 93 1
	V on good Type I event with no associated γ	453	Good V Undecided	453 0
	e^- or $e^- e^+$ pair	26		
	e^- or $e^- e^+$ pair on bad Type I	79		
	$\pi^+ \pi^-$ on illegitimate Type I	22		
	Undecided	7		

To check the accuracy of these two major edits, we re-edited a 20% sample of the film and compared the results with the original edits. All conflicting categorizations were resolved by a third party during the fourth edit. In each event category we found errors ($\sim$ 3%) of both omission and comission approximately equal in numbers so that the corrections applied to each category for such errors are small. Table IV gives exact numbers for the re-edit-edit comparison. Classifications not listed in Table III showed no net change between edit and re-edit.

TABLE IV

TABULATION OF ERRORS FOUND BY RE-EDIT
OF 20% SAMPLE OF K^+ FILM

		Omission	Comission
V events	1st editor	15	4
	2nd editor	25	24
γ events		31	35
γ-V events		10	4
π^- only events		0	1
Neither a V or a γ events		56	67

The third edit was carried out by those scanners who had first edited the film and was twofold in purpose. Primarily we wanted to determine the distribution in spatial separation between the charge-exchange point and estimated copunctal

point for those events classified as associated γ events by the second editors. This distribution was to be checked later by Monte Carlo techniques described shortly. The secondary purpose of this edit was to insure that there indeed was no other Type I event within 10 cm of those events classified as 24, 25, and 26 by the first editor.

The fourth and last edit of the raw sample, carried on solely by physicists, was designed to serve several diverse purposes. All events in which the second editor had tossed out a V configuration were re-examined for possible regeneration effects (see Appendix C, Section 2) or K_S^o elastic scattering. A spot check was made of those events which, due to the first edit classification, were not passed on to the second edit and thus were not examined by physicists. In this spot check special attention was given to the distinguishing of any p^+ contamination from those events categorized as having neither an associated V or γ. As stated earlier all disagreements between editor and re-editor were resolved at this point. The final purpose of this fourth edit is related to a step in the analysis of the sample described in Section 4 of this chapter. This step was a further check of the V events obtained by measuring a randomly chosen sample of $\sim$ 2000 events and testing to see if they constrained (tests applied are explained in Section 4) to the decay $K_S^o \to \pi^+\pi^-$. If they did not constrain to this decay they were visually checked at this edit.

3.2 Editing of the π^+ Film

The π^+ sample went through the first two major edits only. All rules used in the K^+ edit applied to the π^+ edit with the exception that even if there was another Type 1 event within 10 cm of the vertex in question it was still accepted.[*] This was done since the important point was not which vertex the γ was associated with but that the γ was associated with either one. Table V contains a comparison of K^+ and π^+ sample after the first two edits. In this table the sample is already grouped into its major divisions.

TABLE V

DISPOSITION OF EVENTS IN THE K^+ AND π^+ FILM AFTER SECOND EDITING

	K^+ Film		π^+ Film	
V events including Type II events with $\pi^+\pi^-$ at interaction vertex	7381	(535)[**]	195	(195)
γ-V events	119	(22)	0	
Total V events	7500		195	
γ events including Type II events whose negative track is an electron at the interaction vertex	4280	(26)	1025	(28)
Type II events with π^- but no π^+ at the interaction vertex	76	(76)	275	(275)
Events with neither a V nor a γ	11747	(0)	1244	(0)
Total of all events	23527		2739	

[**]The numbers in parentheses denote the number of Type II events in each category.

---

[*]We also demanded that the γ point exactly to the C.E. point.

4. MEASURING

To further guarantee that those events categorized as "associated V" events by the second editor were indeed $K_s^o \rightarrow$ $\pi^+\pi^-$ decays, a random sample of 1000 (14%) such events were measured on digitized projection machines. These machines were equipped with encoding devices which transferred position measurements along with track and event identification to IBM cards for subsequent computer analysis.

The resulting punched cards were processed through CAST, a measurement-checking program for Datex-machine measurements of bubble chamber events written at the University of Michigan. This program checks both for illegal and illogical control information on every card and compiles data for the event as a whole. Then CAST checks the event for consistency and unmeasured vertex points are extrapolated. Badly measured points are determined using a sliding circle fit and excluded. Finally CAST produces output in the necessary form to serve as input to SHAPE.

4.1 Geometric Reconstruction

SHAPE[32] is a University of Michigan-created heavy liquid geometry program, designed to reconstruct the spatial coordinates of each measured track and to calculate, using range-energy relationships and the curvature implied by these spatial coordinates, the components of momenta and their associated errors plus all involved real space angles and errors. Briefly the structure of SHAPE is as follows.[33]

1. Reads all input constants which may vary from experiment to experiment and prints them.

2. Reads in the data (CAST output) for each event.

3. Tries to reconstruct all vertices as corresponding points.

4. Reconstructs tracks in three dimensions by calling, among other things, CURFIT--a large package of routines which obtain kinematical variables (range, angles, momenta) from the real space points of the track.

5. Reconstructs gamma tracks from e^+e^- pairs.

6. Controls the calling of print and tape writing routines and further calculations.

7. When all events have been processed prints a list of events passed and events failed.

4.2 Kinematic Fitting

Fitting to the $K_S^0 \rightarrow \pi^+\pi^-$ hypothesis was accomplished with the program UKFIT written especially for this reaction and based on the deduction that the vector ($\vec{S} = \hat{S}|S|$) from charge exchange point to V-vertex should lie in the same direction as the vector ($\vec{R} = \hat{R}|R|$) found to be the kinematical vector sum of the $\pi^+\pi^-$ system. Thus

$$\hat{S} \cdot \hat{R} = 1.0 \qquad (3.4)$$

was one requirement for fitting the hypothesis. A second test

required that the effective mass of the $\pi^+\pi^-$ system equal the
mass of the K° within 1 S.D. Of the 1000 events initially
measured, 240 failed one or both of these tests and were sub-
sequently visually examined. This rather high rate of failure
(24%) is a consequence of the relatively poor reconstruction
available for slow and extremely short tracks in heavy liquids
plus the fact that we purposely set the requirements very
tight so that any dubious events would be subject to re-
examination.

CHAPTER IV

CHECKS AND CORRECTIONS OF THE RAW SAMPLE

1. MONTE CARLO TECHNIQUE[*]

In addition to the check on the charged sample provided

by the measurement described at the end of the last chapter,

it is also possible to use Monte Carlo techniques to check

both our samples. Monte Carlo may be defined as the use of

the statistical properties of random numbers to solve prob-

lems. In this case we are trying to simulate the statistical

nature of the K_S° decay so that the application of Monte Carlo

methods is particularly well suited and consequently easy to

apply.

We used the kinematic properties determined from the

random sample of measured charged decays as input to our

Monte Carlo program. For each event that passed the fitting

program we took the charge exchange point and momentum vector

of the K°. The program then carried out the following steps.

1. Starting at the charge exchange space point the

"particle" was stepped along its given direction

.5 cm at a time. At each point a probability to

decay is determined from the relation $P_{DK} =$

$1 - e^{-(\ell/\gamma\beta c\tau)}$; a random number, r, is then gener-

ated and compared to P_{DK}. If $P_{DK} < r$ then the

"particle" has decayed and the program moves on to

----

[*]An excellent reference for Monte Carlo techniques if F. James,
Monte Carlo for Particle Physicists, CERN Reprint.

Step 2, while if $P_{DK} > r$ Step 1 is repeated until it does decay.

2. We now have the decay point which is the apex of the V for the charged decay and the point of creation for the two π°'s of the neutral decay. Aside from geometrical projections and scaling factors to get from a 3-space point in the chamber to the screen of our measuring machines, we are now finished with the "particle" as a charged decay since we only need the projected distance from charge exchange point to decay point for comparisons. For the neutral decays, however, we are just beginning. Using $K_S^\circ \rightarrow \pi^\circ \pi^\circ$ center of mass kinematics, we randomly decay (in terms of φ and cos θ) each π° to two gammas. Due to the extremely short π° lifetime[7] (τ_{π° = .89 x 10^{-16} sec), we assume the K° decay point and π° decay points as identical.

3. Each of the four gammas is now stepped along its random, though kinematically constrained, direction until a comparison of its conversion factor[34] and a random number dictates a $\gamma \rightarrow e^+ + e^-$ conversion or a compton conversion. Naturally a check is made at each point to insure that the γ is still within the boundaries of the chamber.

4. Having determined all items of interest--K_S° decay point (V apex), the four gamma conversion points, and distributions of kinematical variables of the

particles involved--all 3-space points were projected

to the screen of the scanning machine and relevant

distances determined.

Based on the quantities determined with this Monte Carlo

method we made the checks and some of the corrections to be

discussed directly.

2. THE CHARGED DECAYS

2.1 Verification

To determine the purity of our sample of observed charged

decays we pursued two courses; the experimental determination

of well known kinematic characteristics for the decay $K_S^0 \rightarrow$

$\pi^+ + \pi^-$ and comparison of observed distributions with Monte

Carlo predicted distributions. First we measured and kinema-

tically checked a random sample of charged decays as described

at the end of the last chapter. Of the 2200 events measured[*],

1940 events passed the kinematic checks or subsequent visual

examination. In Figure 5 the effective mass of the $\pi\pi$ system

is presented. There are 235 (12%) events in the central bin

which runs from .49 to .50 BeV while 892 events lie to the

left of this bin and 813 events fall to the right. Thus the

mean value of the distribution gives a mass of $\approx$ .495 BeV for

the $\pi^+\pi^-$ system with a full width at half-maximum of .050 BeV.

---

[*]In addition to the sample of 1000 events measured, fit, and
visually inspected, a second sample of ~ 1200 events was
measured and those that passed both fitting criteria were
used to increase the statistics of our effective mass plot
and proper time distribution. There was no further treat-
ment of this second sample.
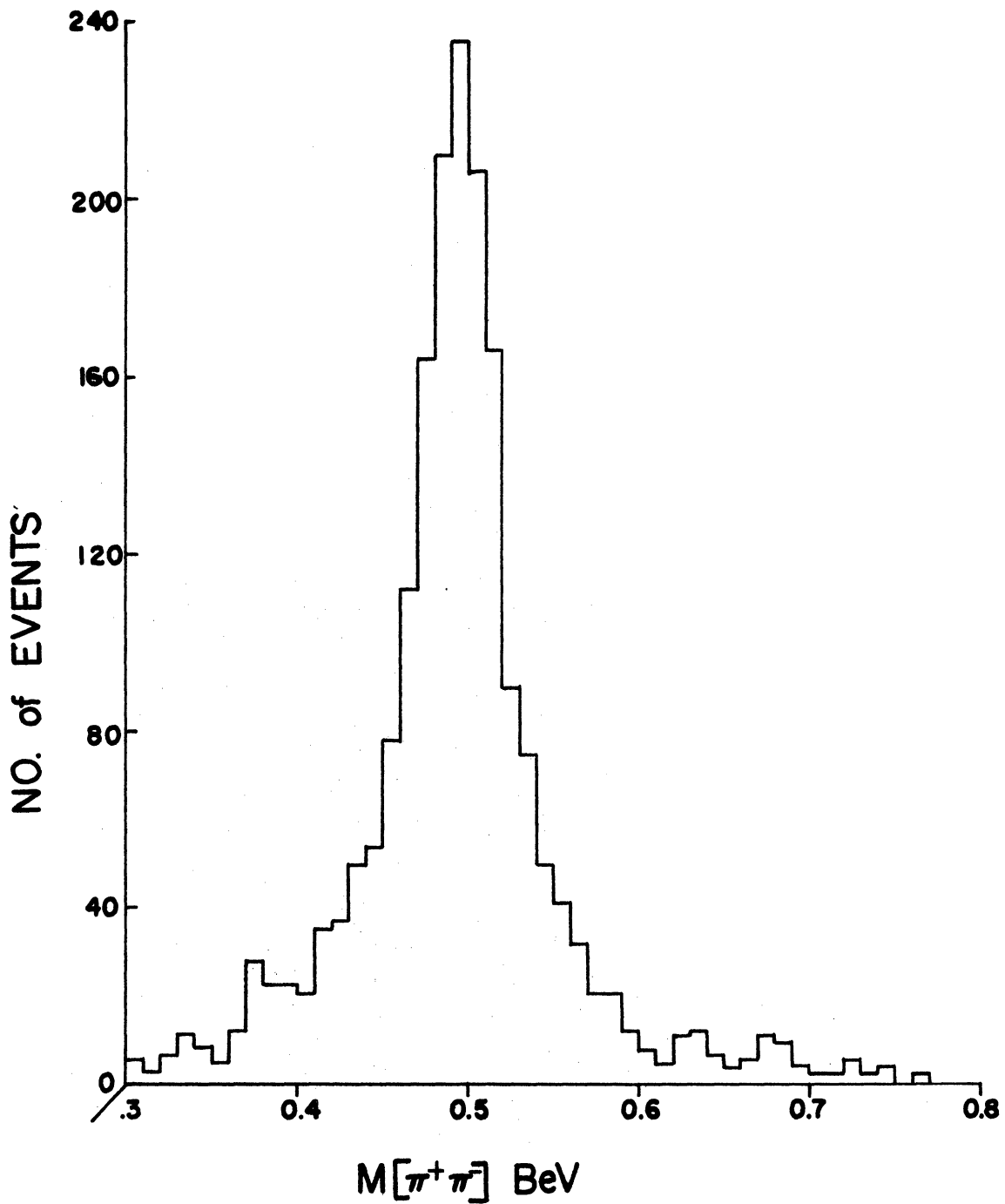
Figure 5. Distribution of the measured effective mass of
the $\pi^+\pi^-$ system. Each bin is 10 MeV^2 wide. The center of
the peak is at $\approx$ 0.495 BeV with FWHM of $\approx$ 0.050 BeV.

This effective mass of the $\pi^+\pi^-$ system is to be compared with the mass[7] of the $K^\circ = (.49776 \pm .00016)$ BeV.

The proper time of each of these decays was also computed and the resulting distribution is presented in Figure 6. A straight line was visually fit to the points, and the intersecting dashed lines give the e^{-1} point and the corresponding lifetime. This admittedly crude procedure yields a value for $\tau(K_S^\circ)$ of $.83 \times 10^{-10}$ sec to be compared with[7] $(.862 \pm .006) \times 10^{-10}$ sec.

Of the 1940 kinematically checked $K_S^\circ \rightarrow \pi^+\pi^-$ decays, 580 were picked at random and used as input for the Monte Carlo program described above.* The momentum distribution of the 580 events chosen is shown in Figure 7. Since each event went through the procedure 20 times, the number of K° decays generated was 11,600. The distribution of (charge-exchange-point)-($\pi^+\pi^-$-vertex) separation of the generated sample is compared to the distribution of distances noted during the second edit in Figure 8. The distributions are normalized to the first two bins, and it is found that the statistics match extremely well except for the last four bins. It is found that there is a $\sim$ 195 event surplus of actual events over predicted events; since 40% of these excess events occur in the last four bins this excess might be attributed to regeneration phenomena.

---

*Monte Carlo programs are notoriously inefficient and consequently outrageously expensive. This is the reason why we generated such a small sample.
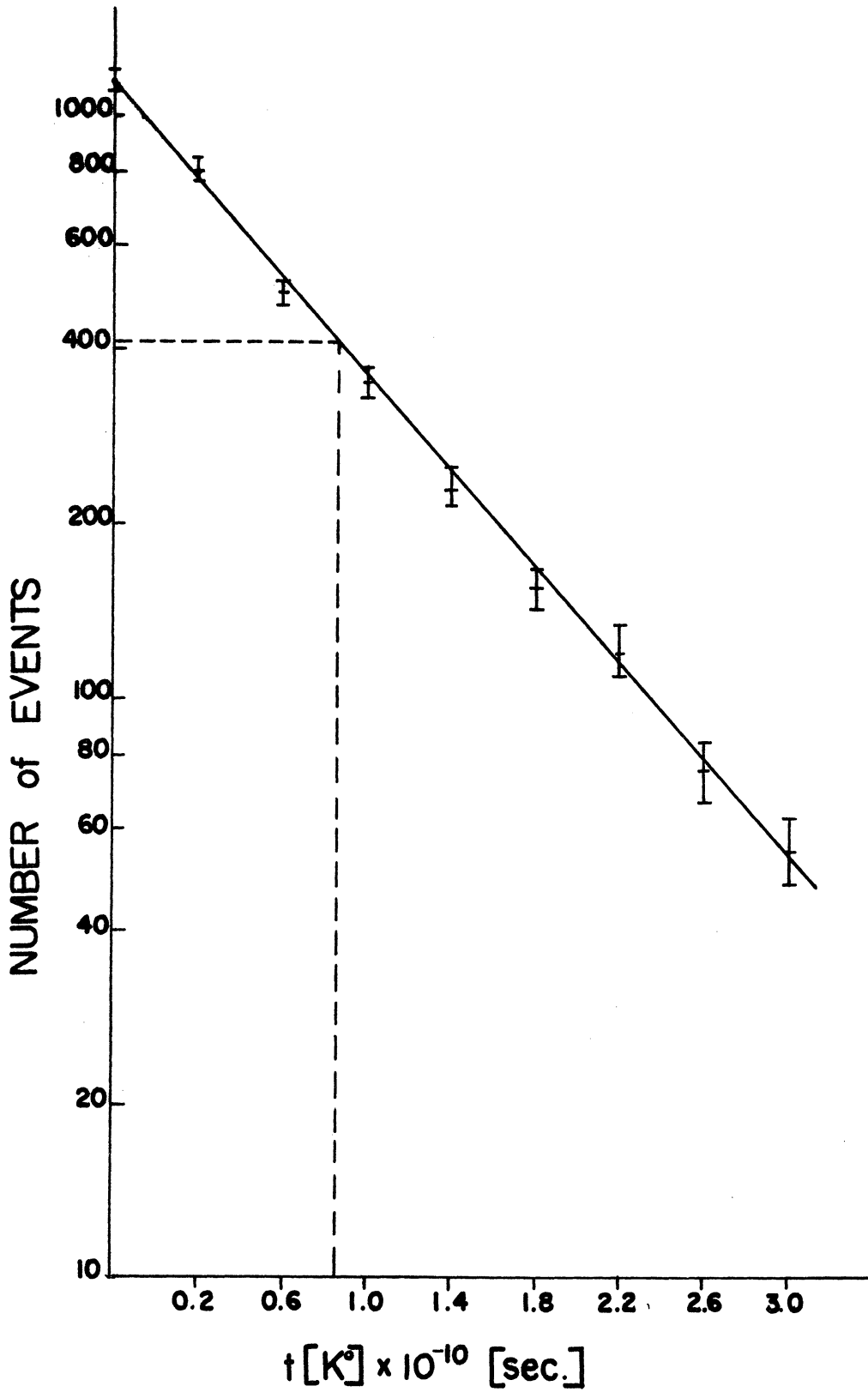
Figure 6. Proper time distribution of measured sample
$K^{\circ} \to \pi^{+} + \pi^{-}$. The intersecting dashed lines give the e^{-1}
point and the corresponding lifetime.
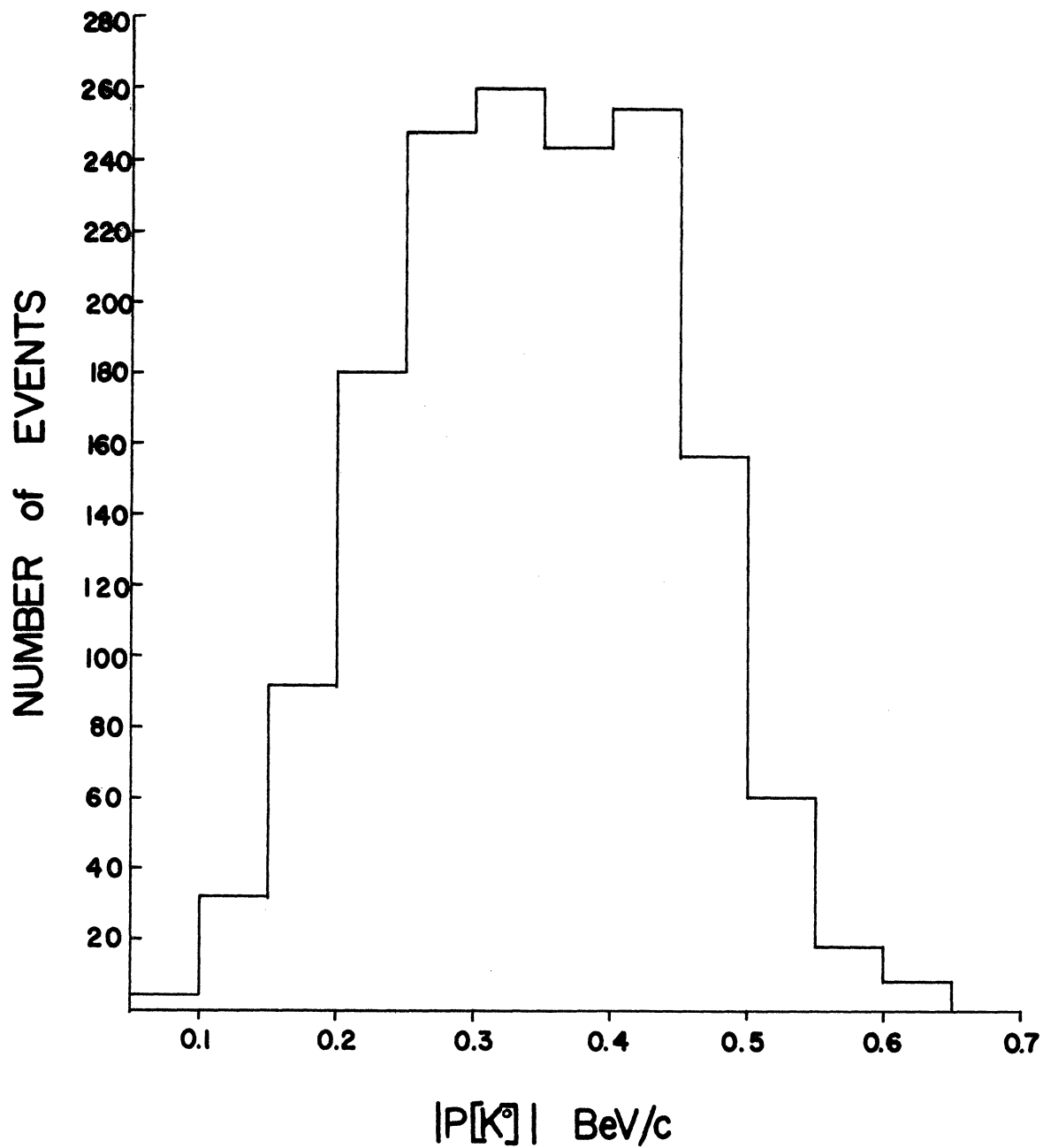
Figure 7. Distribution of lab momentum for K°'s produced via K⁺ charge-exchange reaction.
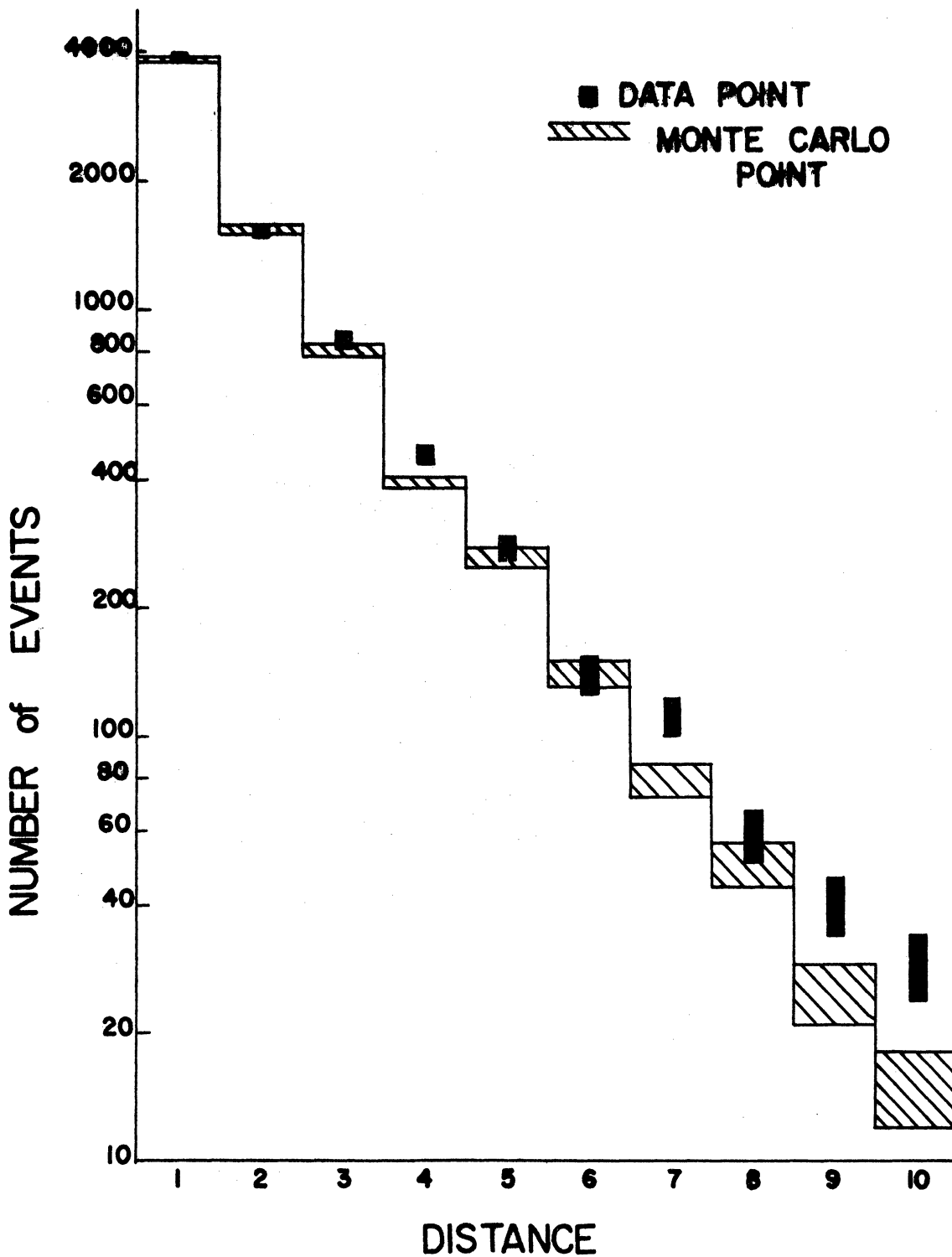
Figure 8. Distribution of separation between charge-exchange (C.E.) point and V-vertex as observed and as predicted via Monte Carlo methods. Each unit of distance is 0.5 cm on the scan table which is ≈ 1.0 cm in real space.

2.2 Corrections to the Charged Sample

It was found necessary to make four minor corrections to the raw sample of 7500 charged decays. Table VI summarizes these corrections.

TABLE VI

CORRECTIONS TO $K_S^o \rightarrow \pi^+\pi^-$ SAMPLE

Total V events from 2nd edit	7500 ±87
Scattered V events	242 ±15
Due to π^+ contamination	-53 ± 8
Total edit corrections	90 ±45
Due to K_L^o-K_S^o interference	-43 ± 7
Total $K_S^o \rightarrow \pi^+\pi^-$ events	7736 ±99

The largest correction was for scattered K^o particles which subsequently decayed as $K_S^o \rightarrow \pi^+\pi^-$. This class of events contains both K_S non-regenerative scatters and incoherent regenerative effects. Our neutral sample includes such events while scattered K^o events decaying by the charged mode within the 5 cm scanning circle would most likely be eliminated at the second edit. To correct for this we examined all V events rejected by the second edit to find out how many were charged decays which had failed the second edit because their configuration relative to the charge exchange point was inconsistent with the conservation of momentum. Of the 1126

events examined, 242 were found to be of this type and were

consequently measured. The effective mass of the $\pi^+\pi^-$ system

is shown in Figure 9d. Of these 242 events, 80 were found to

have a short proton track located close to the vertex of the

V. The distribution of the projected distances of these

scattered events from the charge exchange vertex is shown in

Figure 9a, 9b, and 9c, respectively, for events with observed

proton recoil, without observed recoil (containing those events

scattering off neutrons and those events scattering off protons

but imparting insufficient energy to the proton to render it

visible), and total. These distributions are consistent with

a flat distribution of K_L regenerative effects plus the super-

position of an expeonential fall-off from K_S scatters. An

extremely crude visual estimate of the relative magnitudes of

these two effects would attribute 150 to K_L regeneration and

the balance (92) to K_S non-regenerative scattering[*]. Because

our neutral sample includes such scattered events we must

therefore add 242 ±15 events to our raw sample.

A second correction takes into account the results of

both the sample measurement and the re-edit check. All of

the 240 events which failed one or both of the fit require-

ments in the initial 1000 event sample were examined by phys-

icists and in all but 22 of these cases the events were

thought to be good K° decays into $\pi^+\pi^-$, having failed the

kinematics tests either because of a measurably difficult

---

[*]We attempt a more precise calculation of these two effects
in the next chapter.
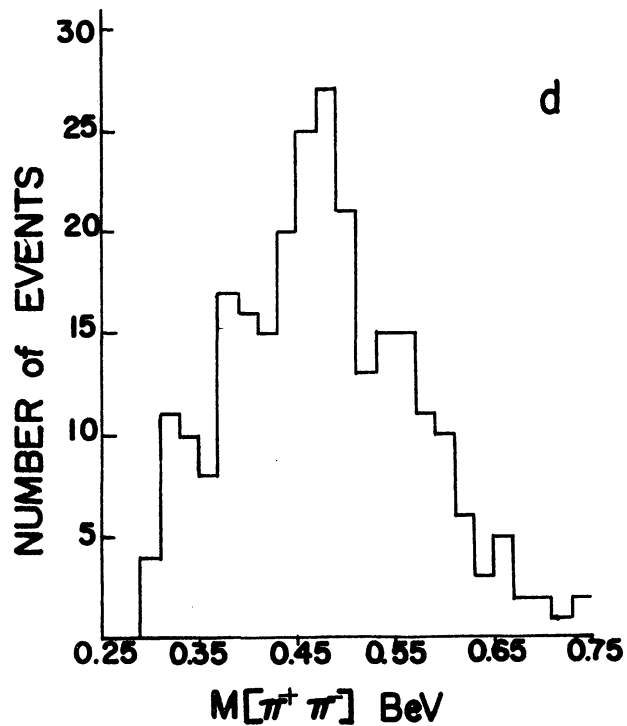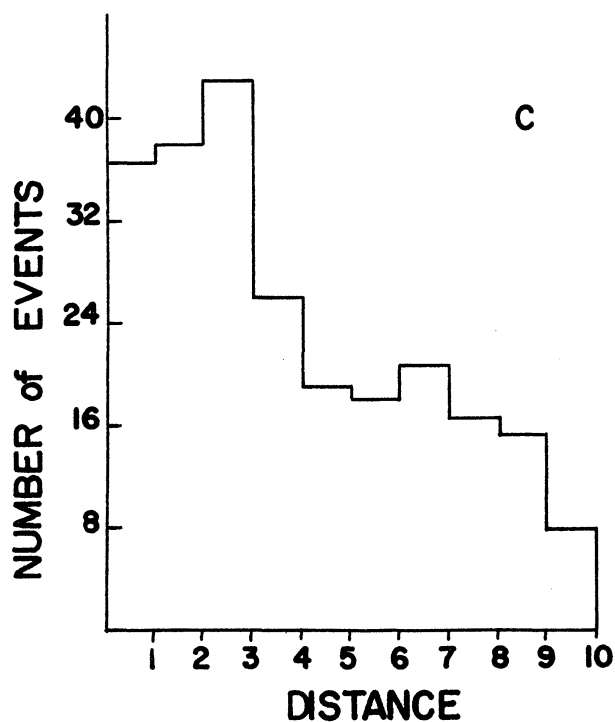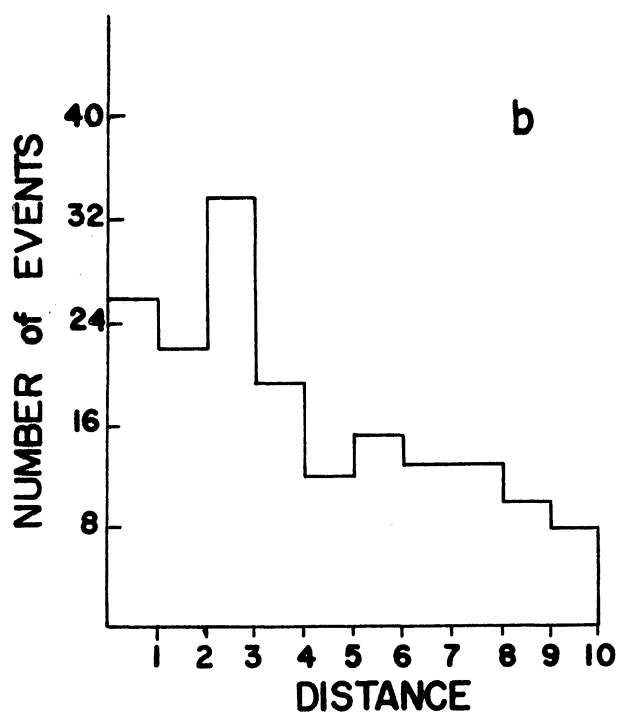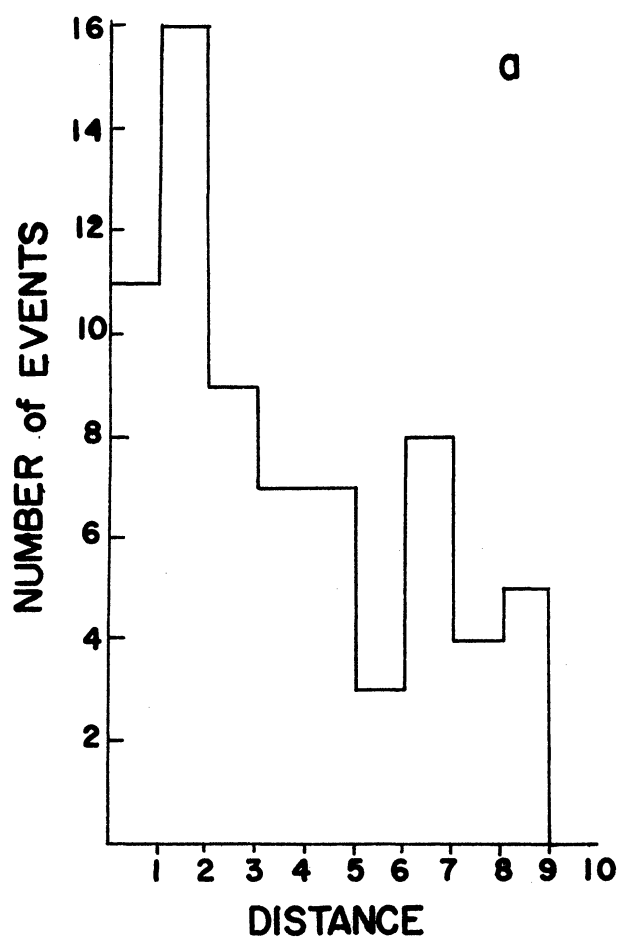
Figure 9. Characteristics of "scattered-V" sample. Separation between C.E. point and V-vertex for: a) events with observed point of scatter; b) events without observed point of scatter; c) total events observed. Figure 9d gives the measured effective mass for the scattered V sample.

configuration such as a steeply dipping or scattered track or because of a slight K° scatter before decay. The 22 failing events could in most cases be traced to errors by the second editor. The complement of this measurement check of the charged decays was executed when we examined all V's failing the second edit for the scattered K° correction described above. It was found that 113 events went from rejected V's to good V's. In summary, the measurements showed that 22 events out of 1000 (13.5% of the 7500 initial V's) were incorrectly called charged decays while the re-examination of the rejected V events (the total sample of them) showed that 113 events were incorrectly called failing V's. We can now compare these results for consistency with the re-edit findings given in Table V. It is obvious that the 22 events of the 13.5% sample measurement is consistent with the 24 errors of comission by the second editor uncovered by the re-edit of the 20% sample. We also note that the 113 events which went from rejected V's to good V's is perfectly consistent with the 25 errors of omission uncovered by the sample re-edit. We have thus determined our V classification efficiency in two independent manners and found them to be consistent. Combining the results we apply a net correction of 90 ±45.

The third correction applied to the charged sample accounts for the very minor π^+ contamination of the beam. From Table IV we see that 76 "π^- only" events were found in the K^+ sample compared to 275 found in the sample of π^+ film scanned, and since these events can be produced only by π^+

interactions we deduce that the K^+ film contained a contamination of π^+ mesons equal to $76/275 = .276 \pm .032$ of the π^+ film. The π^+ film contained 195 events simulating V events[*], hence the K^+ film would be expected to contain $195 \times .276 = 53 \pm 8$ events due to π^+ contamination which must be subtracted.

Another correction to be considered is the possibility of interference between the $K_L^0 \to 2\pi$ and $K_S^0 \to 2\pi$ amplitudes. If it is determined that $\eta_{oo} = \eta_{+-}$ then this correction is unnecessary; however, since $|\eta_{oo}|$ is poorly known we are compelled to include the effect. From Appendix C, expression (C.41), we see that the integrated time dependence of the decay rate in the $\pi^+\pi^-$ channel (assuming only $\varphi_\rho \approx 0$) contains the major contribution

$$M_{+-} \equiv |\rho|^2 \frac{(1.0 - e^{-\Gamma_S T})}{2}$$

and a correction term due to interference effects

$$C_{+-} \equiv |\eta_{+-}\rho| [\alpha \cos \varphi_{+-} - \beta \sin \varphi_{+-}]$$

where

$$\frac{\alpha}{(\beta)} = e^{-\Gamma_S/2\, T} [\sin \left(\frac{\Gamma_S}{2} T\right)_{(+)} - \cos \left(\frac{\Gamma_S}{2} T\right)_{(-)} + 1.0] \quad .$$

---

[*]An event such as $\pi^+ n \to \pi^+\pi^- p$ simulates a good Type II event and would thus enter our charged sample.

For our fiducial volume $T = 6\tau_s$ so that

$$M_{+-} = (4.988 \times 10^{-1})|\rho|^2 \quad .$$

Then using[7] $|\eta_{+-}| = (1.92 \pm .04) \times 10^{-3}$ and[35] $\varphi_+ = 40° \pm 6°$ we can calculate the correction term to be .

$$C_{+-} = (2.84 \, {}^{+0.07}_{-0.10} \times 10^{-3})|\rho|$$

so that the <u>percentage</u> of ultimately detected $\pi^+\pi^-$ decays due to interference effects will be $(.57 \, {}^{+.01}_{-.02})/|\rho|$. The magnitude of the regeneration constant ρ, as defined here, can be expressed in terms of the matrix elements $R_{ij}(x)$ as defined in Appendix C, Section 2, to be

$$\rho \approx \frac{1.0 + R_{12}}{1.0 - R_{12}} \quad .$$

Upon solving for ρ using heavy freon characteristics, we find $\rho(CF_3Br) = 1.04$ which implies that the actual percentage is $(.55 \, {}^{+.009}_{-.018})$. Using the subtotal of 7804 events (raw sample plus all previous corrections), it is found that 43 ± 7 must be subtracted as arising from interference effects.

The final corrected number of $K_s^o \rightarrow \pi^+\pi^-$ decays was 7736 ±99 events.

3. THE NEUTRAL DECAYS

The initial sample of events stood at 4280 ±65 and, as in
the charged decays, certain corrections had to be made to this
quantity. Since visual observation of the decay process
$K_S^o \rightarrow \pi^o + \pi^o$ is contingent upon the detection of one of the
ultimately produced gammas, checks and corrections are very
difficult and must reflect this uncertainty with larger assigned
errors. A summary of all corrections for the neutral sample
is given in Table VII.

TABLE VII

CORRECTIONS TO $K_S^o \rightarrow \pi^o \pi^o$ SAMPLE

Total γ events from 2nd edit	4280 ± 65
Due to imperfect detection efficiency	101 ± 28
Edit corrections	-20 ± 40
Due to π^+ contamination	-284 ± 36
Due to background γ's	-284 ± 35
Outside fiducial volume	-109 ± 11
Due to K_L^o-K_S^o interference	-30 ± 30
Total $K_S^o \rightarrow \pi^o \pi^o$ events	3654 ±100

The techniques for reconstructing and fitting gamma con-
versions in heavy liquids need much improvement; therefore
any checks that were made had to be made via Monte Carlo

predictions. We feel justified in pursuing this course since very few sources of extraneous γ's are available. Even with the Monte Carlo predictions there is no off-hand check on the neutral sample because of the very intimate relationship between the corrections and these checks. To illustrate this Figure 10 presents the distance between charge exchange point and nearest γ as determined by both the second editor and the Monte Carlo methods. The two distributions are normalized to the total number of events so that there is surprisingly good agreement for the first two bins; however, beyond this, as the distance increases, predictions and reality tend to diverge. This does not indicate that there is a basic fault with our neutral sample. On the contrary, since the Monte Carlo points as plotted assume perfect (100%) gamma detection efficiency, we would be at a loss to explain agreement at this stage. Thus our first correction to the neutral sample, a positive correction for unobserved gamma events, should result in a more meaningful check between observed and predicted gamma distributions.

The probability of none of the four gammas from the neutral decay converting within the 10 cm (projected on the scan table) scanning circle is only about 1%. However, not all of the converted gammas will be observed by the editors. Some will be missed because they are dipping steeply in the chamber, others because their energy is too low. It is an important advantage of this experiment that this correction remains small even when low scanning efficiencies are assumed.
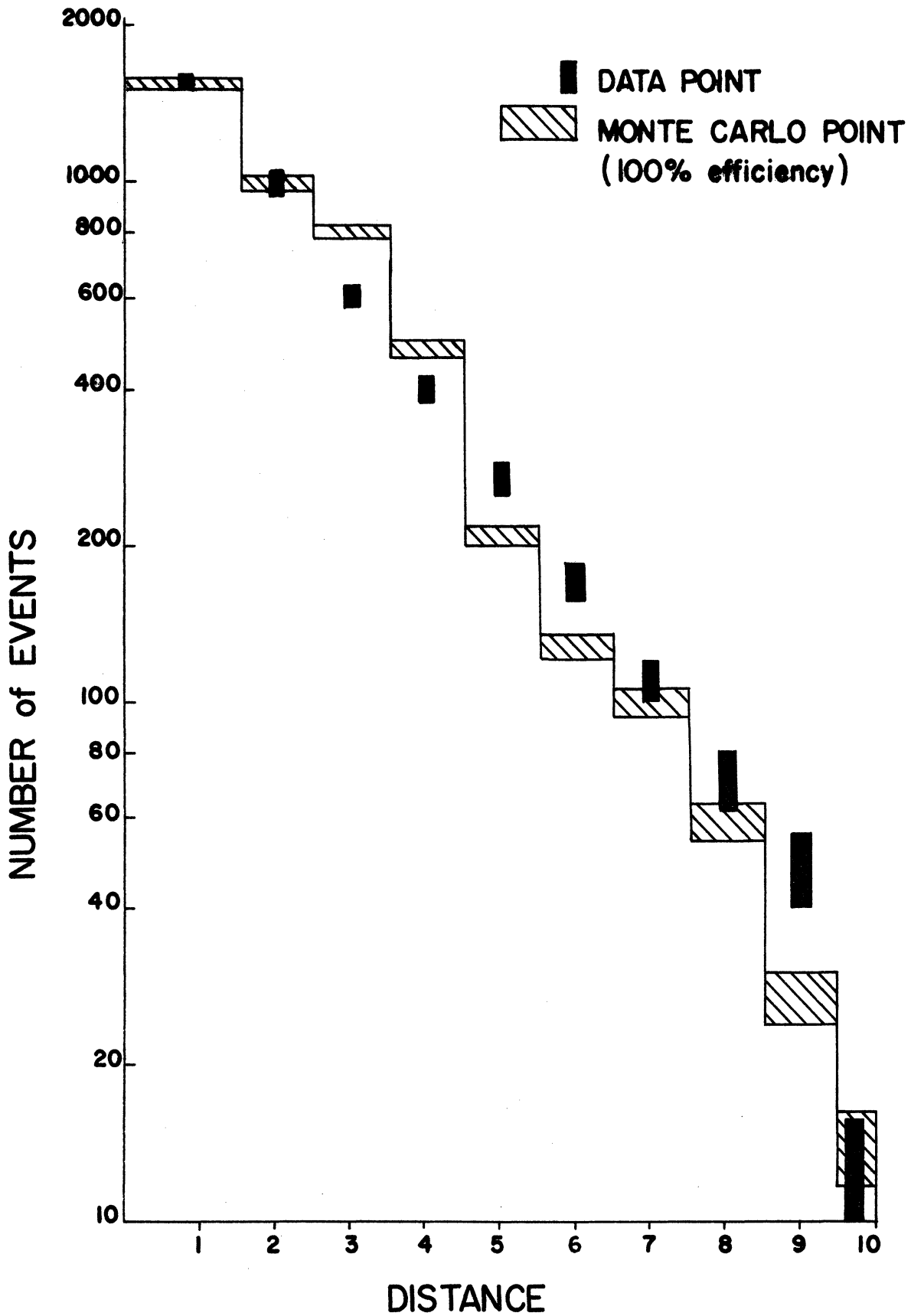
Figure 10. Separation between C.E. point and conversion point (nearest e^+e^- pair) as observed and as predicted by unweighted Monte Carlo. One unit of distance is $\approx$ 2 cm real space.

To determine this correction a small sample (12%) of neutral decays was examined by those scanners who were responsible for detecting the gammas initially. They were instructed to scan within a 10 cm radius of the charge exchange point and count the number of gammas. We then hypothesized three scanning models whose ultimately predicted gamma detection efficiency depended on a weighted product of a dip factor and an energy factor. Hypothesis A assumed that the detection efficiency for electron pairs varies between 0.0 and .95 as the gamma energy varies from 0 to 80 MeV but never gets above 0.95. Also the detection of dipped electron pairs is further inhibited by a factor which varies from 1.0 to 0.0 as the dip (measured up from the xy plane) varies from $30°$ to $90°$. Hypothesis B was designed similarly except that the energy factor reached 0.95 at 40 MeV and the dip factor was 1.0 until $60°$. Hypothesis C assumed that the detection efficiency was both energy- and dip-independent and assumed a straight 95% detection efficiency. Figure 11 gives the distribution in dip of the gammas as predicted by the Monte Carlo program. Also contained in Figure 11 is a graphical description of the dip factor as used in the three hypotheses. Figure 12 gives the gamma ray energy distribution, again Monte Carlo predicted, as well as a graphical representation of the energy factor for the three hypotheses. Each of the hypotheses was subjected to Monte Carlo methods which resulted in a prediction for the number of unobserved gamma events, the ratio of $4\text{-}\gamma$ to $3\text{-}\gamma$ events and the ratio of $(4\text{-}\gamma + 3\text{-}\gamma)$ to $(2\text{-}\gamma + 1\text{-}\gamma)$ events as
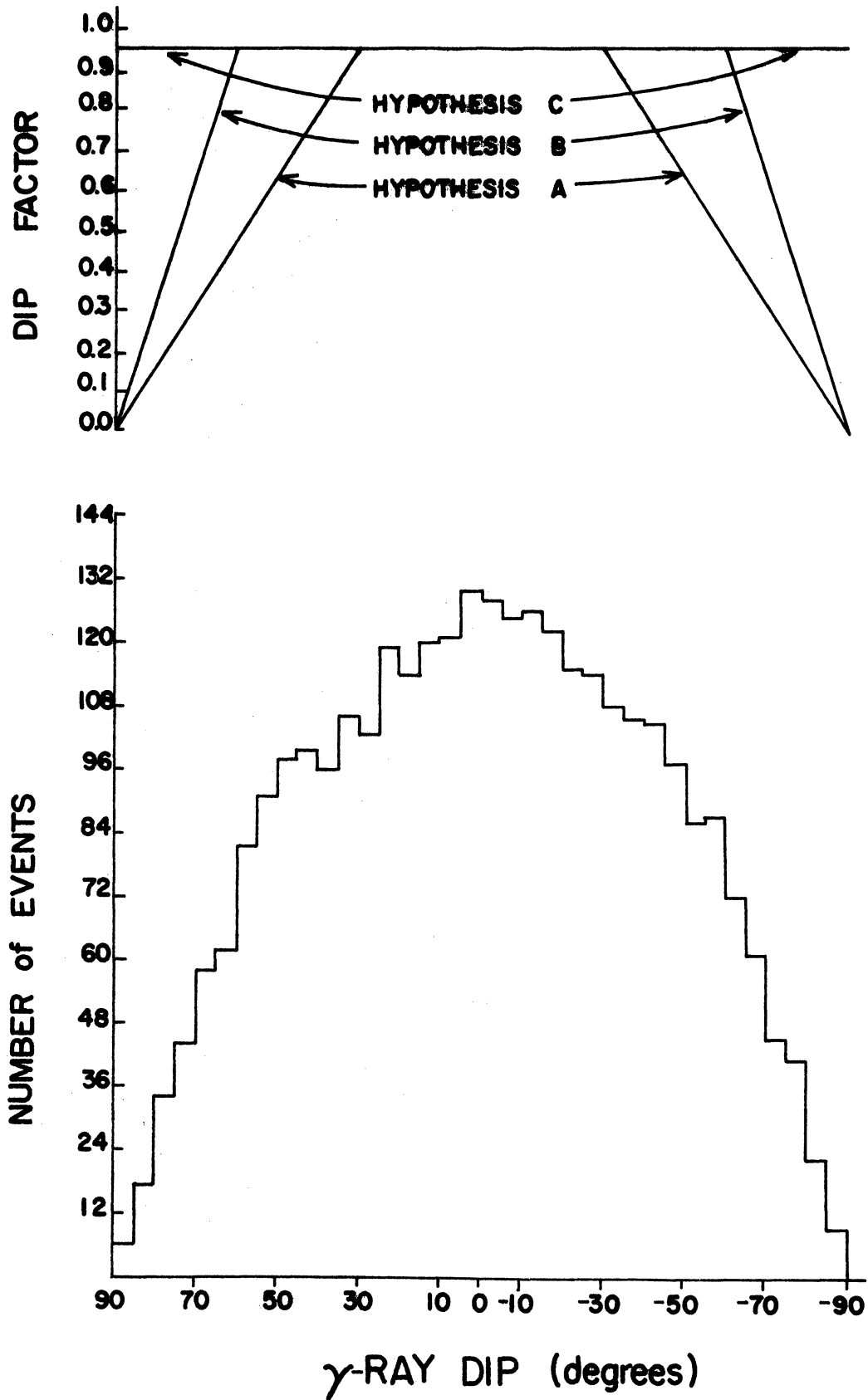
Figure 11. Predicted γ-ray dip and three hypotheses used to determine detection efficiency. Weighting factor varies linearly from 0.0 to 0.95. 100% detection efficiency was assumed to yield distribution.
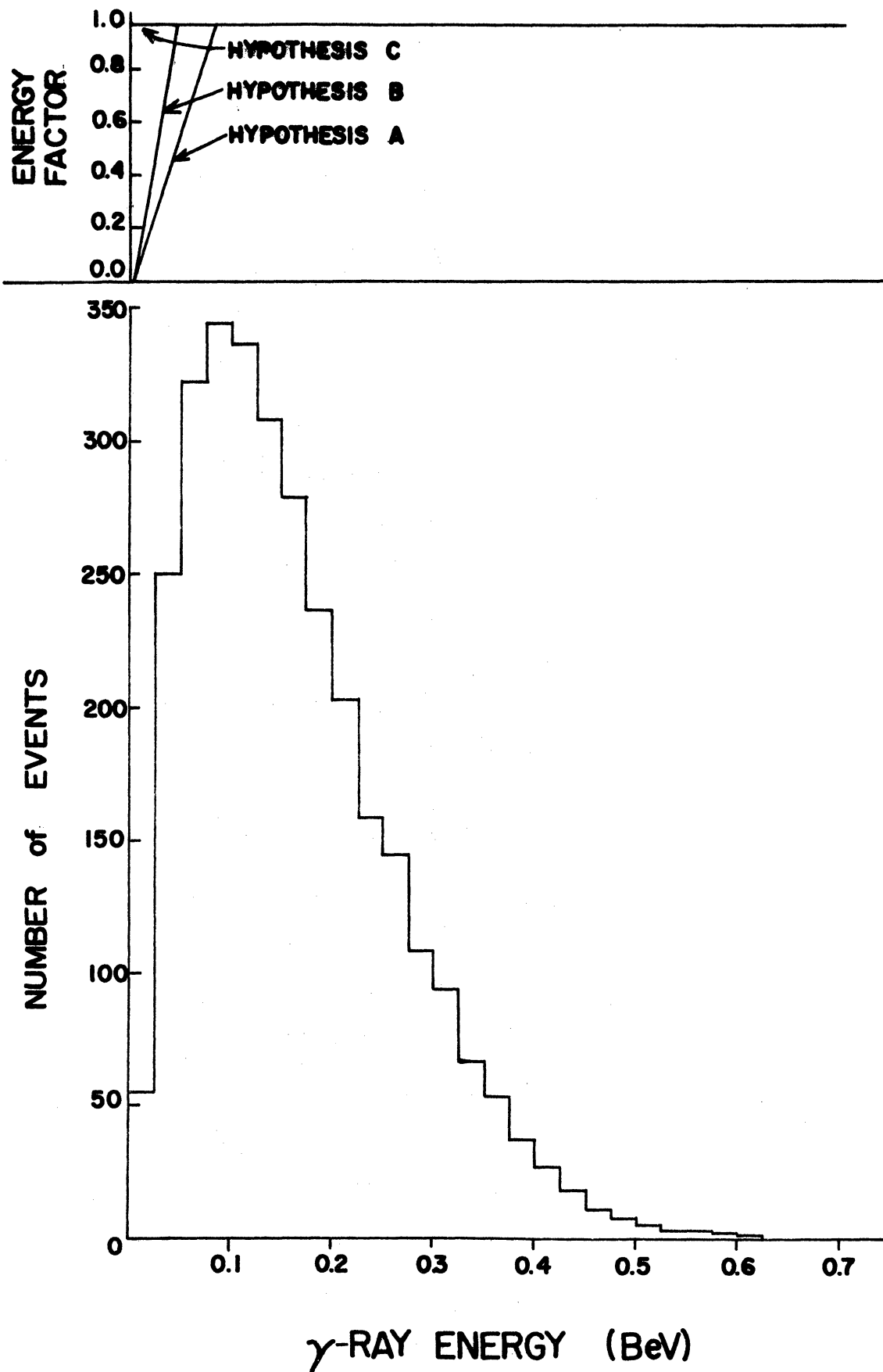
Figure 12. Predicted γ-ray momentum and weighting factor for three hypotheses. 100% detection efficiency was assumed to yield distribution.

well as the distribution of distances between charge exchange point and nearest γ. The results for the three hypotheses as well as the ratios observed in the sample scan are summarized in Table VIII.

TABLE VIII

DETECTION OF γ CONVERSIONS

	Hypo-thesis A	Hypo-thesis B	Hypo-thesis C	Observed
$4\gamma/3\gamma$ ratio	.242	.422	.553	.401 ±.050
$(4\gamma + 3\gamma)/(1\gamma + 2\gamma)$	.456	1.06	1.425	1.053 ±.085
Number of γ events missed	286	96	50	

It was then trivial to interpolate between the Monte Carlo predictions to arrive at our final correction for unobserved gamma events. From the 4γ to 3γ ratio, $103\,^{+27}_{-20}$ unobserved gamma events were predicted, while from the $(4\gamma + 3\gamma)$ to $(2\gamma + 1\gamma)$ ratio a consistent number $98\,^{+15}_{-13}$, of unobserved gamma events resulted. Thus, to the raw sample, $101\,^{+28}_{-20}$ gamma events were added.

We can now also see how the unobserved gamma factor affects the distribution of nearest gammas as in Figure 10. Using the distribution of nearest γ distances as predicted by Hypothesis B we find the distribution of Figure 13 which also contains the unweighted Monte Carlo points for ease in

comparison. As can be seen, agreement between the observed and predicted distributions has improved perceptibly.

The next correction accounted for edit misclassifications as uncovered by the sample re-edit. From Table V this correction can be calculated to be minus 20 ±40 events.

A correction for π^+ contamination had to be made for the neutral sample as well as the charged sample. Using the same procedure as before and the results of Table IV we find that the number of γ-events in reality due to π^+ interactions was .276 x 1025 = 284 ±36 events.

A further correction to the neutral sample is that which must be made to compensate for the background, unassociated γ-rays which came from sources other than $K_S^o \rightarrow \pi^o \pi^o$ decay. These background gammas have the following sources: (1) totally external γ production; (2) π^o production along with the charge exchange; (3) a $\bar{K}$ interaction producing a Λ which decays by the neutral mode $n\pi^o$; and (4) K_L^o decay into three neutral pions. Of these effects, (4) is negligible within the fiducial volume we are considering.[*] Sources (1) and (2) can be compensated for by realizing that $\gamma + K_L^o$ events, which make up the first two sources, should occur 1.47 (assuming charged to neutral ratio of about 2.12 and K_L^o to K_S^o ratio of 1:1) times as often as the $\gamma + V$ events which we have counted and corrected. Hence we would expect sources (1) and (2) to

---

[*] A K_L^o with a mean momentum of .325 BeV/c will decay into its $3\pi^o$ mode within the first 10 cm after production only $\sim$ 0.2% of the time. If we then fold in conversion probabilities we can safely ignore this correction.
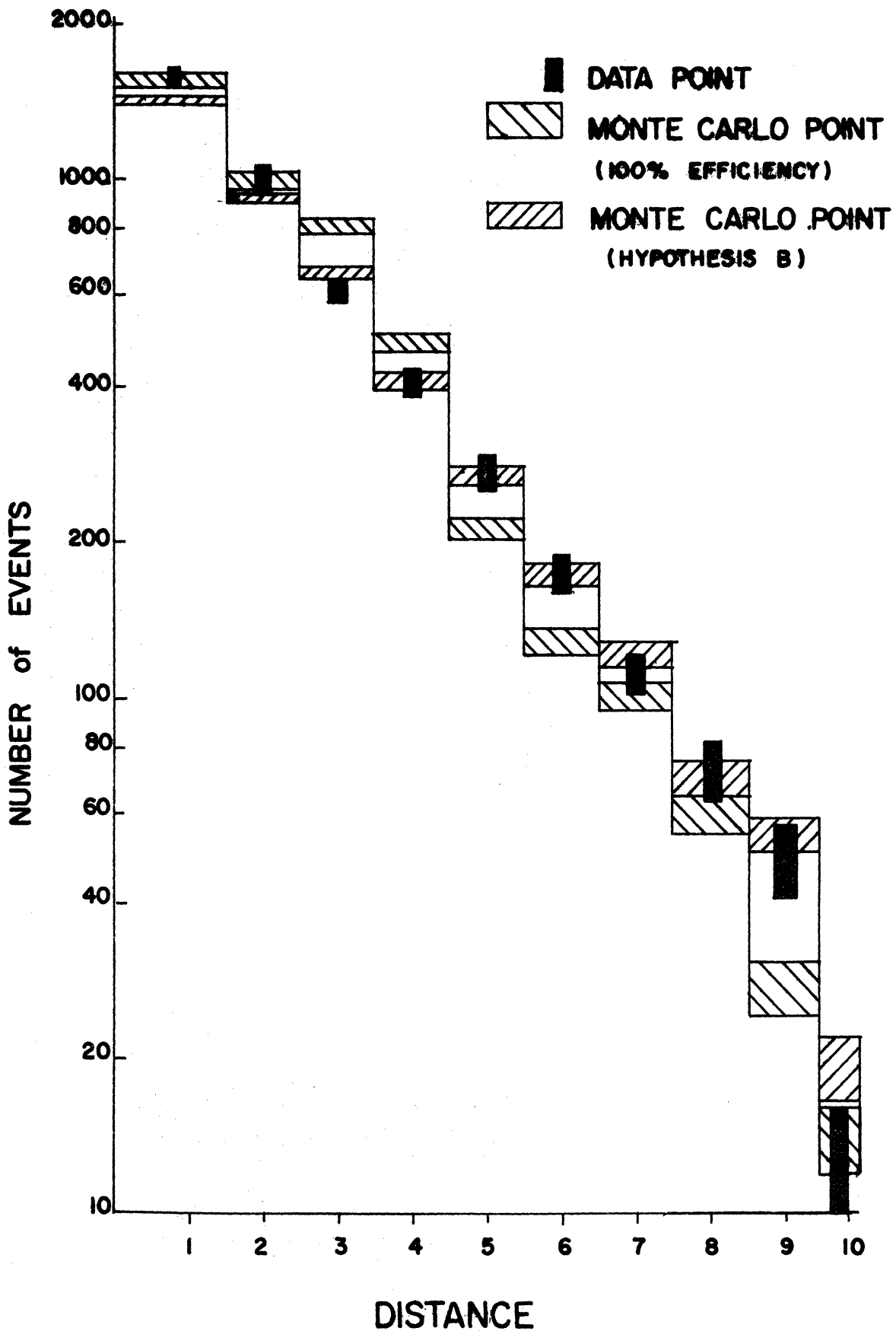
Figure 13. Separation of C.E. point and nearest e^+e^- pair as observed, as predicted by unweighted Monte Carlo, and as predicted using Hypothesis B.

contributed $(149 \pm 22) \times 1.47 = 219 \pm 32$. Source (3), Λ decays, was accounted for by scanning a sample of the film for the charged Λ decay $(\Lambda \rightarrow p\pi^-)$. For the sample scanned 30 ± 10 charged Λ decays were found which would indicate $\sim 112 \pm 22$ in the whole sample. Taking the charged to neutral branching ratio[7] of the Λ° as $1.88 \pm .02$ we estimate the number of $\Lambda^\circ \rightarrow n\pi^\circ$ decays as 65 ± 12 events. Thus the total necessary correction for stray γ's is 284 ± 35 events.

The complementary correction to the question of stray γ's is the correction for an actual $K_s^\circ \rightarrow \pi^\circ\pi^\circ$ decay whose only qualifying gammas have false alternate origins.* To estimate this correction a sample of $K_{\pi 2}^+$ decays in flight were found. In the decay $K^+ \rightarrow \pi^+\pi^\circ$ the decay vertex and thus the origin of the two γ's is easily defined. Hence we know the true origin of the gammas and we could then find any alternate origins which also fit the gammas. A total of 1466 $K_{\pi 2}$ events were initially found and subjected to an edit which cut all but 461 of them. Next these 461 events were measured and geometrically reconstructed using CAST-SHAPE as described earlier; 309 passed the measurement stage. These 309 events were put through a $K_{\pi 2}$ constraint program which gave positive fits on 243 of them for a final sample of 486 gammas. It was found that 62 of these gammas had alternate origins which would seem to imply that we should increase our 1-γ events by

*A full report of this phase of the experiment is contained in University of Michigan Bubble Chamber Group Research Note No. 14/69 by K. Bartley.

14.6%, our 2-γ events by 2.1% (14.6% squared), our 3-γ events by 0.31%, and our 4-γ events by 0.045%. However, to perform this correction meaningfully, the distributions in θ, φ, and $\vec{P}$ should be identical for the $K_{\pi 2}$ gammas and the $K_S^\circ \to \pi^\circ \pi^\circ$ gammas. When the necessary cuts are imposed on the $K_{\pi 2}$ sample to meet this condition it is found that the sum total (1-γ + 2-γ + 3-γ + 4-γ events) of gamma events missed in this manner is insignificant and thus negligible.

The next correction to the neutral sample makes use of the fact that in the $K_S^\circ \to \pi^\circ \pi^\circ$ events we do not observe the point of decay but rather the point of conversion for one or more of the resultant gammas. For this reason a separate check must be made to insure that we are using the same fiducial volume for both charged and neutral decays. To guarantee this <u>all</u> events accepted in the neutral sample were examined by experienced scanners or physicists with the sole purpose of determining the copunctal point (point of origin) or distance of closest approach for 1-γ events and then measuring the distance between charge exchange point and copunctal point. Monte Carlo methods were used to predict what the distribution should resemble, and the results, both observed and predicted, are presented in Figure 14. From the observed distribution we see that 109 ±11 gamma events[*] must be subtracted from the gamma total to insure equal fiducial volumes. Another interesting feature of Figure 14 is its consistency with Figure 8

---

[*] We have already subtracted the 284 stray γ events before arriving at this figure.
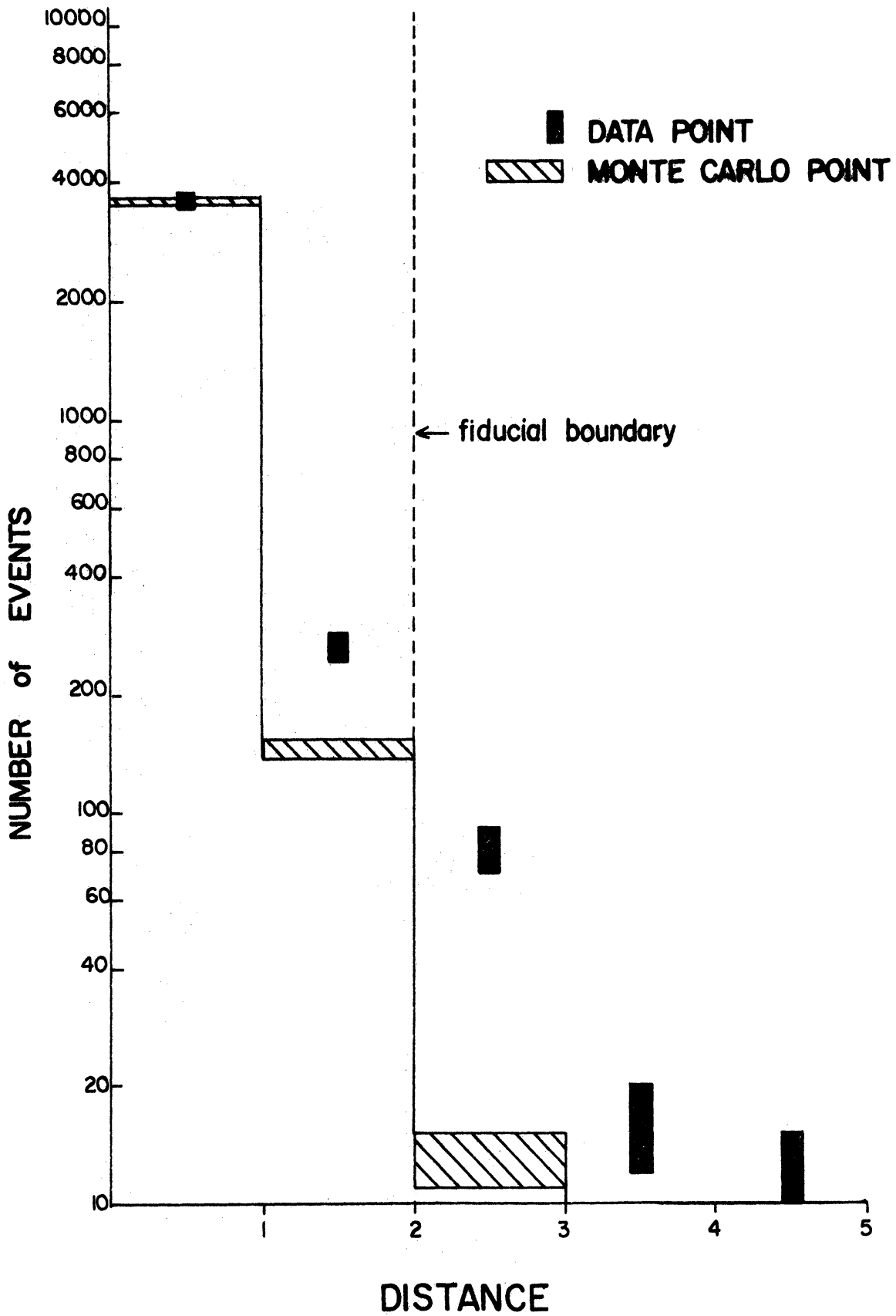
Figure 14. Separation of C.E. point and neutral decay point as observed and as predicted by Monte Carlo technique. One unit of distance is $\approx$ 5 cm real space.

(charge exchange-V vertex separation) in terms of the various

pheonomena (both regenerative and non-regenerative scattering)

we would most likely observe in the last half of our fiducial

volume. To confirm that these various effects are not biased

toward one or the other of the decay modes we can determine

the branching ratio for the last half of the fiducial volume

and compare it with the overall branching ratio. In the

last 10 cm (real space) there are 378 ±19 V events and 288 ±17

γ events. Correcting each sample as described throughout

this chapter we obtain corrected samples of 455 ±21 V events

and 227 ±19 γ events. The resulting branching ratio is 2.00

±0.19; certainly consistent with our overall branching ratio.

As in the charged decays, a certain small percentage of

those events we have detected are due to interference effects

between the $K_L^o \rightarrow 2\pi^o$ and $K_S^o \rightarrow 2\pi^o$ amplitudes. In this

case we are interested in the parameters $|\eta_{oo}|$ and φ_{oo}.

Since these quantities are very poorly known as of now, the

error on this correction is quite large. Following the same

procedure as used for the charged decays we find that 30 ±30

events must be subtracted from the neutral sample.

Thus, with all correction considered, the final neutral

sample stood at 3654 ±100 events.

4. THE K_L^o SAMPLE

As a further check on our experimental method a count of

K_L^o decays (charge exchange with neither V nor γ associated)

was made. It follows[36] from the CPT theorem that the originally produced K° in the charge exchange reaction $K^+ + n \rightarrow K^\circ + p$ has an equal chance of decaying as a K_S° or as a K_L°. Thus, aside from uncalculable regeneration effects, the corrected number of K_S° decays should equal the corrected number of K_L° decays at the termination of our experiment. Table IX summarizes the K_L° decays.

TABLE IX

CORRECTIONS TO K_L° SAMPLE

Total with neither V nor γ from 2nd edit	11747 ±108
Due to π^+ contamination	-344 ± 19
Due to background γ's	+284 ± 35
Due to missed γ conversions	-101 ± 28
Scattered V events	-242 ± 15
Re-edit corrections	-55 ± 55
Total K_L° observed	11289 ±134

The raw sample stood at 11747 ±108. The corrections to this sample are straightforward and in all cases except two are compensations for events shifted to or from the K_S° decays in correcting the charged and neutral samples. The first exception is the correction for π^+ contamination of the beam.

Following procedures previously established for the K_S^o decays
and using Table IV we must subtract 344 ±19 events from the
raw sample. The other exception is the edit corrections.
From Table V we see that the sample must be diminished by
55 ±55 events for this correction. The only other corrections
are as follows: (1) 284 ±35 events which were determined to
be K_L + stray γ and subtracted from the neutral sample are
added here; (2) 101 $^{+28}_{-20}$ events which were undetected as neutral
decays because of imperfect gamma detection efficiency were
added to the sample of neutral decays and must be subtracted
from the K_L decays; (3) 242 ±15 events whose associated V's
failed to conserve momentum at the scan table were originally
classified as K_L decays. They have since been added to the
charged sample and must therefore be subtracted from the K_L^o
sample. The final K_L^o sample thus stands at 11264 ±134 events.

CHAPTER V

RESULTS AND CONCLUSIONS

1. THE K_s^o CHARGED TO NEUTRAL BRANCHING RATIO

From Table VI the corrected total of $K_s^o \rightarrow \pi^+ + \pi^-$

decays found in this experiment is 7736 ±99, while from Table

VIII we note that the total $K_s^o \rightarrow \pi^o + \pi^o$ decays stands at

3654 ±100. From these final figures we determine the K_s

charged to neutral branching ratio to be

$$R = \frac{\Gamma(K_s^o \rightarrow \pi^+ + \pi^-)}{\Gamma(K_s^o \rightarrow \pi^o + \pi^o)} = \frac{7736 \pm 99}{3654 \pm 100} = 2.117 \pm 0.064 \quad .$$

This is approximately two standard deviations away from 2.0

which we should obtain if the decay is pure $\Delta I = 1/2$. It then

appears that the odds are twenty to one in favor of some com-

bination of $\Delta I = 3/2$ and $\Delta I = 5/2$ amplitude in the K_s^o decay.

Note also that although this result is consistent with the

weighted average of the old generation experiments (2.16 ±.08)

it is ≈ 2.5 standard deviations away from the only other com-

pleted recent experiment of Gobbi et al. (2.285 ±.055).

Therefore, an immediate and obvious result of this experiment

is to point out the necessity for further high accuracy exper-

iments to resolve the current substantial deviation in repor-

ted values. There are several attempts reported underway at

this time. Of these the Hungarian group, Bozoki et al.[37]

has released the <u>preliminary</u> value of 2.12 ±.17 in a recent preprint. Though it is questionable as to what value a weighted average of three such widely varying (2.285 ±.055, 2.160 ±.080, and 2.117 ±.064) quantities is, the average obtained is 2.201 ±.071.

It is now possible, using expression (1.14),

$$R - 2 = 6\sqrt{2}\ Re(\frac{A_2}{A_o})\ \cos\ (\delta_2 - \delta_o) \qquad (5.1)$$

as derived in Chapter I, to determine various quantities of interest depending on what we assume as known.

1.1 $\pi\pi$ s-wave Phase Shifts

If we assume that there is <u>no $\Delta I = 5/2$ component</u> of the decay amplitude, then it is possible to determine $Re(A_2/A_o)$, as done in Chapter I, to be 0.044. Using this quantity, our value of R and expression (5.1) we can now solve for the difference in $\pi\pi$ s-wave phase shifts $|\delta_2 - \delta_o|$ at $E_{cm} = M_{K^o}$, where the subscripts indicate the isospin of the $\pi\pi$ final state. It follows that

$$\cos\ (\delta_2 - \delta_o) = \frac{R - 2}{6\sqrt{2}\ Re(\frac{A_2}{A_o})} = \frac{.117\ \pm.064}{.373} = .314\ \pm.172$$

which implies that the difference in s-wave phase shifts is

$$|\delta_2 - \delta_o| = (72 \, ^{+10}_{-11})° \quad .$$

The $\pi\pi$ s-wave phase shifts can be independently measured by studying the strong interaction

$$\pi + N \rightarrow N + (n\pi) \quad .$$
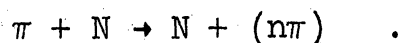
Unfortunately the phase shifts derived, both experimentally and theoretically, are strongly model-dependent (as will be shown in Appendix D), so that agreement among various reported values is in even greater turmoil than the branching ratio we have determined. Table X summarizes the most recently reported experimental values, as well as those values predicted theoretically using current algebras, Veneziano and phenomenological S-matrix techniques. As can be seen, $|\delta_2 - \delta_o|$ can range all the way from $(28 \pm 10)°$--using the Hagopian et al. value of δ_o^o and the Baton et al. value of δ_o^2--to $(73 \pm 10)°$ using the Biswas et al. value of δ_o^o and the Malamud et al. value of δ_o^2. An attempt at finding some sort of mean value for these widely varying results ends with a value of $\approx(50 \pm 15)°$ for the difference in phase shifts $|\delta_2 - \delta_o|$. This value covers the entire range of theoretical values, from Arnowitt's current algebra prediction of $(35 \pm 4)°$ to Tryon's value, using a unitarized Veneziano partial wave analysis, of $\sim (60 \pm 8)°$. A complete review of the current state-of-the-art in $\pi\pi$ phase shifts as well as a description of some of the theoretical models and experiments can be

TABLE X

REPORTED VALUES OF δ_0^0 AND δ_0^2

Reference	δ_0^0 (Degrees)	δ_0^2 (Degrees)	$\delta_0^0 - \delta_0^2$ (Degrees)
Gutay[38] and Carmony[39]	19 ±6 (52 ±10)		
Biswas et al.[40]	56 ±10	-6 ±3	62 ±10
Malamud and Schlein[41]	41 ±5	-17 ±3	58 ±6
Hagopian et al.[42]	23 ±10 (75 ±10)		
Cline[43]	50 ±17	-10 ±3	60 ±17
Scharengiuel et al.[44]	42 ±7	-7 ±3	49 ±8
Saxon et al.[45]	27 ±7 (50 ±8)		
Baton and Laurens[46]		-5 ±3	
Katz et al.[47]		-8.7 ±0.9	
Smith and Manning[48]		-9.8 ±0.7 (-15.4 ±1.1)	
Current Algebra[49]			35 ±4
Veneziano[50]	54 ±5, 52 ±9	-7 ±3	59 ±9, 61 ±6

found in Appendix D of this paper.

There are several implications of the quantity $|\delta_2 - \delta_o|$ which we have determined and quoted as $|\delta_2 - \delta_o| = (72 \pm 10)°$. First, and most important, is that in arriving at our value for $|\delta_2 - \delta_o|$ we assumed that the $\Delta I = 5/2$ component of the decay amplitude was zero. If further experimentation shows that the $|\delta_2 - \delta_o|$ lies in the vicinity of the mean value we have determined--$(50 \pm 15)°$--or even lower, then only an admixture of $\Delta I = 5/2$ amplitude will reconcile this lower value of $|\delta_2 - \delta_o|$ and our experimental result for the K_S^o charged to neutral branching ratio. This point will be examined in detail shortly. A second point of particularly current interest in which both our value of R and $|\delta_2 - \delta_o|$ play a part is the question of time reversal invariance in the decay of $K^o \rightarrow 2\pi$. The breakdown of CP invariance for this decay has been experimentally[51] known for some time. Thus, accepting the validity of the CPT theorem[52], the violation of T invariance seems insured. Recently, however, R. C. Casella has shown[53-55] how, with the use of quantities determined from K^o decays, T invariance can be tested independently of CPT. Employing two related methods, a modified Wu-Yang triangle and the Bell-Steinberger[56] sum rules, Casella assumes T invariance and upon this assumption arrives at contradictions with the data.

Since the method employing the modified Wu-Yang triangle can be shown to include the Bell-Steinberger sum rule analysis, we will briefly examine Casella's first method only. The

original Wu-Yang[57,16] triangular relations were based on the assumption that the 2π decays were mainly responsible for the CP breaking effects (i.e., no large amount of $K_S^o \to 3\pi$), the validity of CPT, and the dominance of $\Delta I = 1/2$ transitions in the $K \to 2\pi$ decay. The resulting relations are

$$\eta_{+-} = \epsilon + \epsilon' \qquad\qquad (5.2)$$

$$\eta_{oo} = \epsilon - 2\epsilon' \qquad\qquad (5.3)$$

where ϵ and ϵ' are related to the coefficients of K_S and K_L (p and q in Appendix C) in the $K^o(\overline{K^o})$ state. The phase of ϵ and ϵ' are given by

$$\theta_\epsilon = \tan^{-1}\left[\frac{2(m_L - m_S)}{\Gamma_S - \Gamma_L}\right] + \Delta\theta_\epsilon \qquad\qquad (5.4)$$

and

$$\theta_{\epsilon'} = -(\delta_o - \delta_2) + 90^\circ \ (+180^\circ) \quad . \qquad (5.5)$$

It is possible to modify these relations so that instead of being based on the validity of CPT, they are based on T-invariance. The new relations

$$\eta_{+-} = \overline{\epsilon} + \overline{\epsilon}'$$

$$\eta_{oo} = \overline{\epsilon} - 2\overline{\epsilon}'$$

incorporate phases for $\bar{\epsilon}$ and $\bar{\epsilon}'$ which are rotated $90°$ from the CPT phases

$$\theta_{\bar{\epsilon}} = \theta_{\epsilon} - 90°$$

$$\theta_{\bar{\epsilon}'} = \theta_{\epsilon} - 90° \quad .$$

These modified triangular relations are solved by putting in the measured value of $\theta_{\bar{\epsilon}} = -47° \pm 10°$ and value of

$$r \equiv \frac{\eta_{oo}}{\eta_{+-}}$$

which then results in a range of values for $(\delta_o - \delta_2)$ where the triangle does not achieve closure, hence implying T-noninvariance. Thus, with our value of the branching ratio which reaffirms $\Delta I = 1/2$ dominance--one of the bases for this whole analysis--and our value for $|\delta_o - \delta_2|$ it can be shown that T-noninvariance is ascertained for all values of $r < 3.5$ if $(\delta_o - \delta_2) > 0$ and for all values of $r < 1.8$ if $(\delta_o - \delta_2) < 0$.

1.2 The Quantity $Re(A_2/A_o)$ and $\Delta I > 1/2$ Transitions

It is also possible using expression (5.1) to obtain the value of $Re(A_2/A_o)$ by assuming that the phase shift $\delta_2 - \delta_o$ is known. For the sake of simplicity we will initially use the mean value of $|\delta_2 - \delta_o| = (50 \pm 15)°$ quoted in the last

section for computations and generalize the results to cover
the full range of $|\delta_2 - \delta_o|$ later. We thus want to solve the
equation

$$Re\left(\frac{A_2}{A_o}\right) = \frac{R - 2}{6\sqrt{2} \cos (\delta_2 - \delta_o)} \tag{5.6}$$

using $R = 2.117 \pm .064$ and $|\delta_2 - \delta_o| = (50 \pm 15)°$. We find

$$Re\left(\frac{A_2}{A_o}\right) = 0.022 \pm 0.014$$

where the large error is basically due to the fact that it is
the quantity $\underline{R - 2.0}$ that determines the admixture of $I = 0$
and $I = 2$ states. Figure 15 generalizes this result in that
it graphically shows how $Re(A_2/A_o)$ behaves as a function of
the difference in phase shift $|\delta_2 - \delta_o|$. Our error in $R - 2$
has already been folded in and is shown by the lower curve
which gives the effective lower limit of $Re(A_2/A_o)$ for any
given value of $\delta_2 - \delta_o$.

1.3   Ratio of $\Delta I = 5/2$ to $\Delta I = 3/2$ Amplitudes

If we now assume that the $Im(A_2/A_o)$ is less than 10^{-3}
(recent measurements of $|\eta_{oo}|$ imply that $Im(A_2/A_o) < 3 \times 10^{-4}$)
then we can find $|A_2/A_o|$ from the value of $Re(A_2/A_o)$ we deter-
mined in the last section. Having this quantity and using
the $K^+ \rightarrow \pi^+\pi^o$ decay rate as input we can determine the ratio
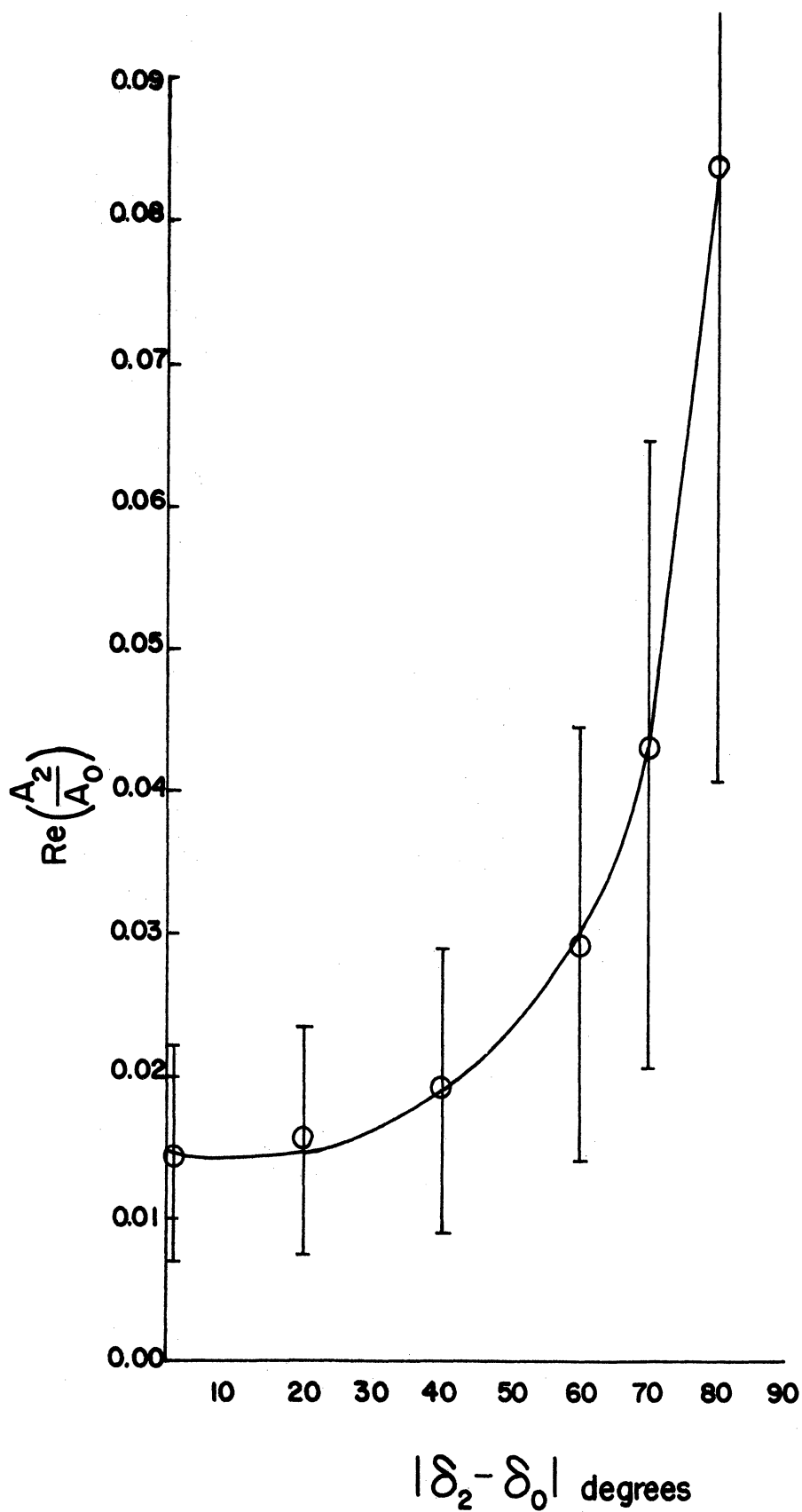
Figure 15. Dependence of $Re(A_2/A_o)$ on value of $|\delta_2 - \delta_o|$ using our value of $R \pm \Delta R = 2.117 \pm 0.064$. Only median value and lower limit (1 S.D.) are drawn.
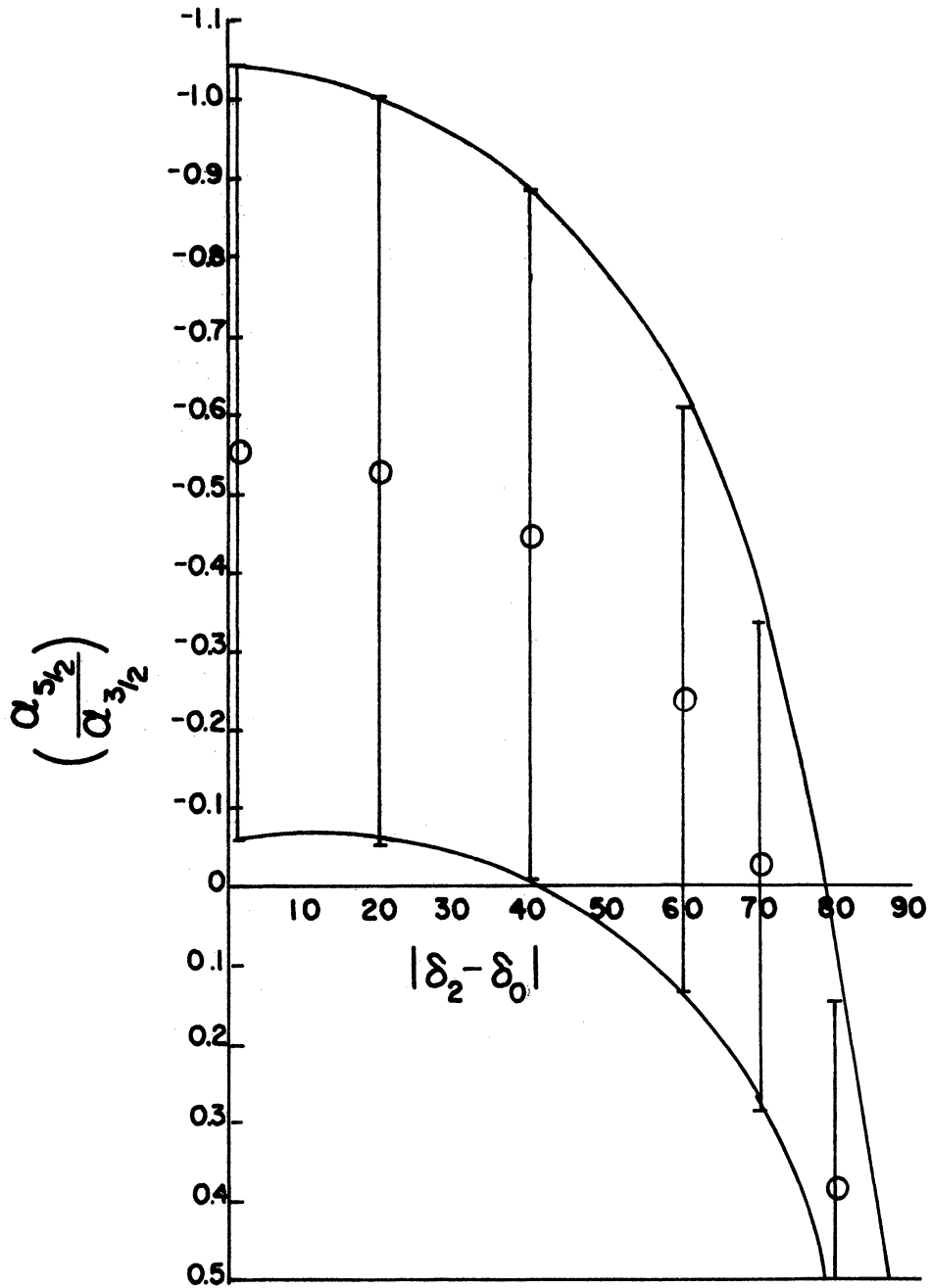
Figure 16. Dependence of $\dfrac{\alpha_{5/2}}{\alpha_{3/2}}$ on value of $\mid \delta_2 - \delta_o \mid$ using our value of R $\pm \Delta R = 2.117 \pm 0.064$. Circles represent median values while upper and lower limit curves are at ± 1 S.D. The equation yielding the smaller value for $\left| \dfrac{\alpha_{5/2}}{\alpha_{3/2}} \right|$ was used in determining the above curves.

of $\Delta I = 5/2$ to $\Delta I = 3/2$ amplitudes as shown in Chapter I.

We are again hampered by the large error in the quantity $R - 2$

($\approx 55\%$) and the large error in cos $(\delta_2 - \delta_o)$ ($\sim 35\%$) and the

fact that the resultant of these two errors, added in quadra-

ture, appears both in the numerator and denominator of $\left(\dfrac{\alpha_{5/2}}{\alpha_{3/2}}\right)$.

Assuming the amplitudes are <u>real</u>, the two solutions are

$$\left(\frac{\alpha_{5/2}}{\alpha_{3/2}}\right) = -0.391 \pm 0.510 \quad ; \quad \left(\frac{\alpha_{5/2}}{\alpha_{3/2}}\right) = -2.18 \pm 2.85 \quad .$$

It is obvious that although these values are consistent with

no $\Delta I = 5/2$ transitions, the necessarily large errors preclude

any positive statement. We have arbitrarily chosen the root

smallest in magnitude for further calculations. Figure 16

generalizes our results and gives $\dfrac{\alpha_{5/2}}{\alpha_{3/2}}$ as a function of

$\left| \delta_2 - \delta_o \right|$.

2. RATIO OF K_L^o TO K_S^o PRODUCTION

From Tables VI and VIII, the total corrected number of

$K_S^o \rightarrow 2\pi$ decays is 11390 $\pm$141, while from Table IX we see

that the total corrected number of K_L^o decays is 11289 $\pm$134.

Thus our final value for the ratio $R_{L,S}$ is

$$R_{L,S} = \frac{N(K_S^o)}{N(K_S^o) + N(K_L^o)} = \frac{11390 \pm 141}{22679 \pm 195} = 0.503 \pm 0.008$$

while the absolute difference in the number of K_S^o and K_L^o

TABLE XI

SUMMARY OF TOTAL K_S^o AND K_L^o PRODUCTION

Corrected Sample - $K_S^o \rightarrow \pi^+ + \pi^-$	7736 ± 99
Corrected Sample - $K_S^o \rightarrow \pi^o + \pi^o$	3654 ± 100
Total K_S^o Decays	11390 ± 141
Corrected Sample - $K_L^o \rightarrow$ all	11289 ± 134
Corrected Total K^o Production	22679 ± 195

$$\frac{\Gamma(K_S^o \rightarrow 2\pi)}{\Gamma(K_S^o \rightarrow 2\pi) + \Gamma(K_L^o \rightarrow \text{all})} = 0.503 \pm 0.008$$

TABLE XII

$Re(A_2/A_o)$ AND $\dfrac{\alpha_{5/2}}{\alpha_{3/2}}$ FOR THREE VALUES OF R

R	$Re(A_2/A_o)$	$\dfrac{\alpha_{5/2}}{\alpha_{3/2}}$
2.117 ± 0.064	0.023 ± 0.014	-0.391 ± 0.510
2.201 ± 0.071 (Weighted Average)	0.037 ± 0.018	-0.110 ± 0.092
2.285 ± 0.055 (Gobbi et al.)	0.052 ± 0.020	-0.098 ± 0.064

Assuming $|\delta_o^2 - \delta_o^o| = (50 \pm 15)^\circ$

produced is

$$N(K_S^o) - N(K_L^o) = 101 \pm 195 \quad .$$

The question then becomes what we expect the ratio $R_{L,S}$ to be. As was mentioned earlier, incoherent regeneration phenomena will tend to reduce the number of K_L^o that we detect while supplementing the number of K_S^o decays by a similar amount. In the case of coherent regeneration, however, the observed number of K_S^o particles can <u>either</u> be enhanced or reduced depending on the regeneration phase $\theta_{S,L}$. Since the regeneration phase in heavy freon (CF_3Br) is an unknown (we will shortly derive an estimation of $\theta_{S,L}$) we will, at this point, merely set limits on $R_{L,S}$. In Appendix C, Section 2, we estimate that coherent effects can cause as much as a $\pm 4.2\%$ difference between the number of K_S^o observed in vacuum and the number observed in our experiment. We have estimated the incoherent effects (Section 3.2 of this chapter) to be a 2.2% enhancement of the number of observed K_S^o at the expense of the K_L^o sample. Thus, without prior knowledge of the coherent regeneration phase, the sum total of regeneration effects can cause as much as a 6.4% enhancement or 2% depletion of observed (in freon) K_S^o events over the corresponding number in vacuum. The limits on $R_{L,S}$ are then

$$0.49 < R_{L,S} < 0.53 \quad .$$

Our measured value of $R_{L,S} = 0.503 \pm 0.008$ does fall safely within this limit.

3. SUMMARY OF RESULTS: CONCLUSIONS

In summary, the basic results of this experiment are as follows.

1.
$$R = \frac{\Gamma(K_S^o \to \pi^+ + \pi^-)}{\Gamma(K_S^o \to \pi^o + \pi^o)} = 2.117 \pm 0.064 \quad .$$

2. Assuming no $\Delta I = 5/2$ transitions,

$$|\delta_2 - \delta_o| = (72 \, {}^{+10}_{-11})^o \quad .$$

3. Assuming a mean experimental value of the phase shift difference $|\delta_2 - \delta_o| = (50 \pm 15)^o$

a.
$$Re\left(\frac{A_2}{A_o}\right) = 0.022 \pm 0.014 \quad ,$$

b.
$$\frac{a_{5/2}}{a_{3/2}} = -0.391 \pm 0.510 \quad .$$

4. In freon

$$R_{L,S} = \frac{N(K_S^o)}{N(K_S^o) + N(K_L^o)} = 0.503 \pm 0.008 \quad .$$

3.1 Branching Ratio and Associated Quantities

There are several obvious conclusions to be drawn from these results. Strictly from the necessarily low accuracy of

our quoted values it may be surmised that more high precision determinations of the K_s^o charged to neutral branching ratio are needed. They are necessary not only to resolve the final value of R, but also to reduce the error in R still further. Note that even though we have measured R to an accuracy of ~ 3%, because of the value of R itself we have measured the quantity R - 2 to only ≈ 55%. Since R - 2 is the quantity of interest we should aim for an experimental determination of this quantity to within 10% if not less. Figure 17 indicates the type of accuracy needed in determining R to yield 1%, 10%, or 25% accuracy in determining R - 2. As can be seen, if R is indeed ~ 2.1 then to measure R - 2 to 25%, 10%, or 1% we must measure R to 1.2%, .48%, or .048%, respectively. An analysis of our 3% error shows that the neutral sample contributes 2.75% in quadrature while the charged sample contributes ~ 1.25%. If we in turn now break down each of these errors we find that we are essentially no longer statistics-limited in terms of minimum error attainable. We are rather at the stage where the necessary corrections dictate the major part of the error. Therefore, though it may be still possible to measure R to the accuracy necessary to determine R -2 to ~ 25% with the present methods, it is almost inevitable that other techniques need be used if we wish to measure R - 2 to 10% or less.

The attainment of 10% accuracy in the measurement of R - 2 will be a major step forward in eventually determining the quantity $Re(A_2/A_o)$ to a desirable accuracy; however, it
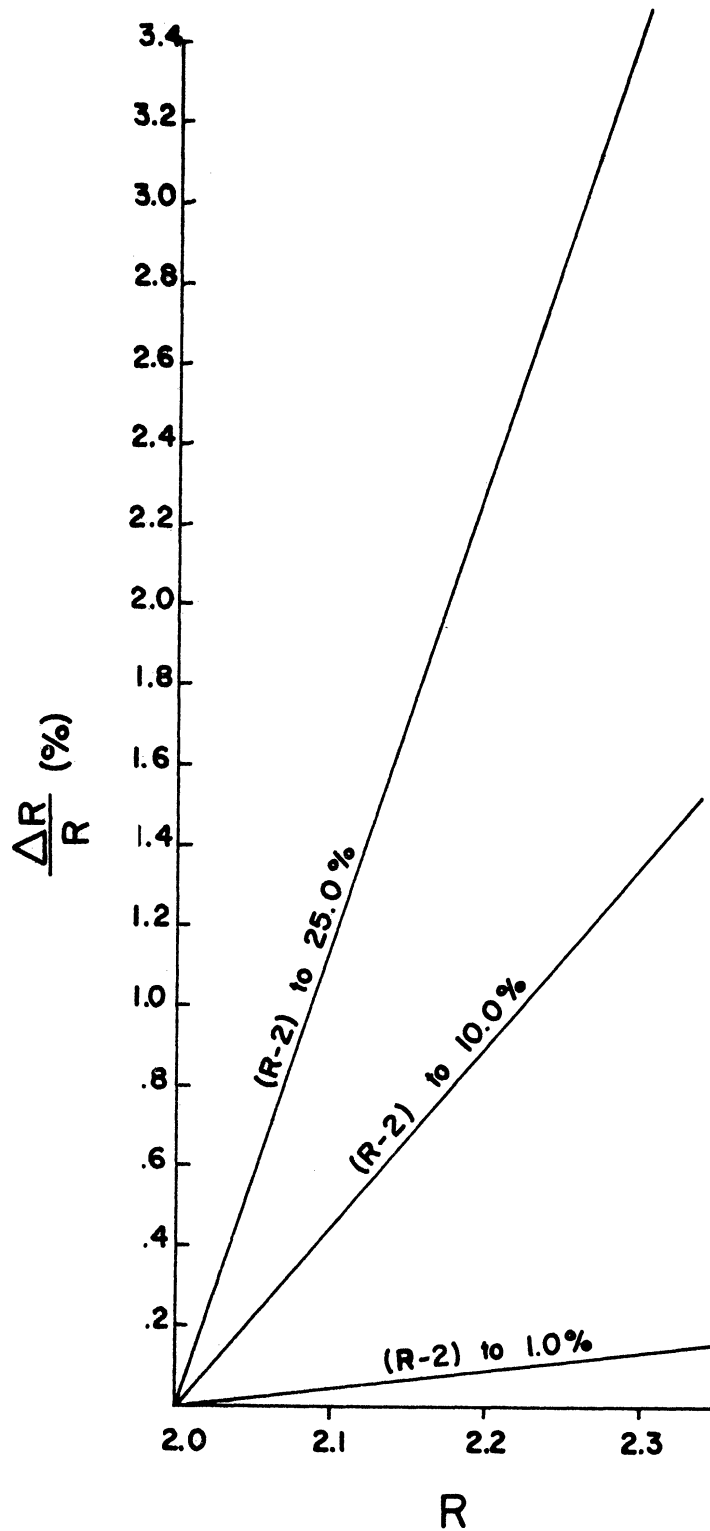
Figure 17. The necessary accuracy of the quantity R to determine R - 2 to 1.0%, 10.0%, and 25.0%.

alone will not be sufficient to attain this goal. The present

wide variance in the difference of $\pi\pi$ s-wave phase shifts,

$|\delta_2 - \delta_o|$, must also be resolved. In using the mean value

$|\delta_2 - \delta_o| = 50 \pm 15°$ we are introducing a 35% error in

cos $|(\delta_2 - \delta_o)|$ which appears in the denominator of the expres-

sion for $Re(A_2/A_o)$. This error plus our huge error in R - 2

combine to give us a 61% error in the value of $Re(A_2/A_o)$.

Figure 18 shows the dependence of the percentage error of

$Re(A_2/A_o)$ on the percentage error of cos $(\delta_2 - \delta_o)$ for differ-

ent values of the percentage error in (R - 2). We see from

these curves that if R - 2 can be measured to 10% then the

$Re(A_2/A_o)$ can be determined to within 11% if cos $(\delta_2 - \delta_o)$ is

known within 5%. A similar analysis can be carried out for

the ratio of $\Delta I = 5/2$ to $\Delta I = 3/2$ amplitudes $\frac{\alpha_{5/2}}{\alpha_{3/2}}$, but it

only reconfirms the necessity for resolving the quantities

R - 2 and $\delta_2 - \delta_o$ to a much higher accuracy than available now.

Very little can be said about the quantities $Re(A_2/A_o)$

and $\frac{\alpha_{5/2}}{\alpha_{3/2}}$ as determined by this experiment for obvious reasons.

If the phase shift difference $\delta_2 - \delta_o$ is ultimately found to

be $\sim 50°$ then $\Delta I = 1/2$ dominance is insured to the 97% level

(from $Re(A_2/A_o)$ as determined from expression (5.6)). However,

it is still too early to make such claims. The $\sim 130\%$ error

necessarily attributed to $\frac{\alpha_{5/2}}{\alpha_{3/2}}$ precludes any discussion of the

result other than what was given at the time we calculated

this quantity; thus although this ratio is consistent with

0 (i.e., no $\Delta I = 5/2$ transition) it also brackets 0.90.

To show how the branching ratio itself can influence the
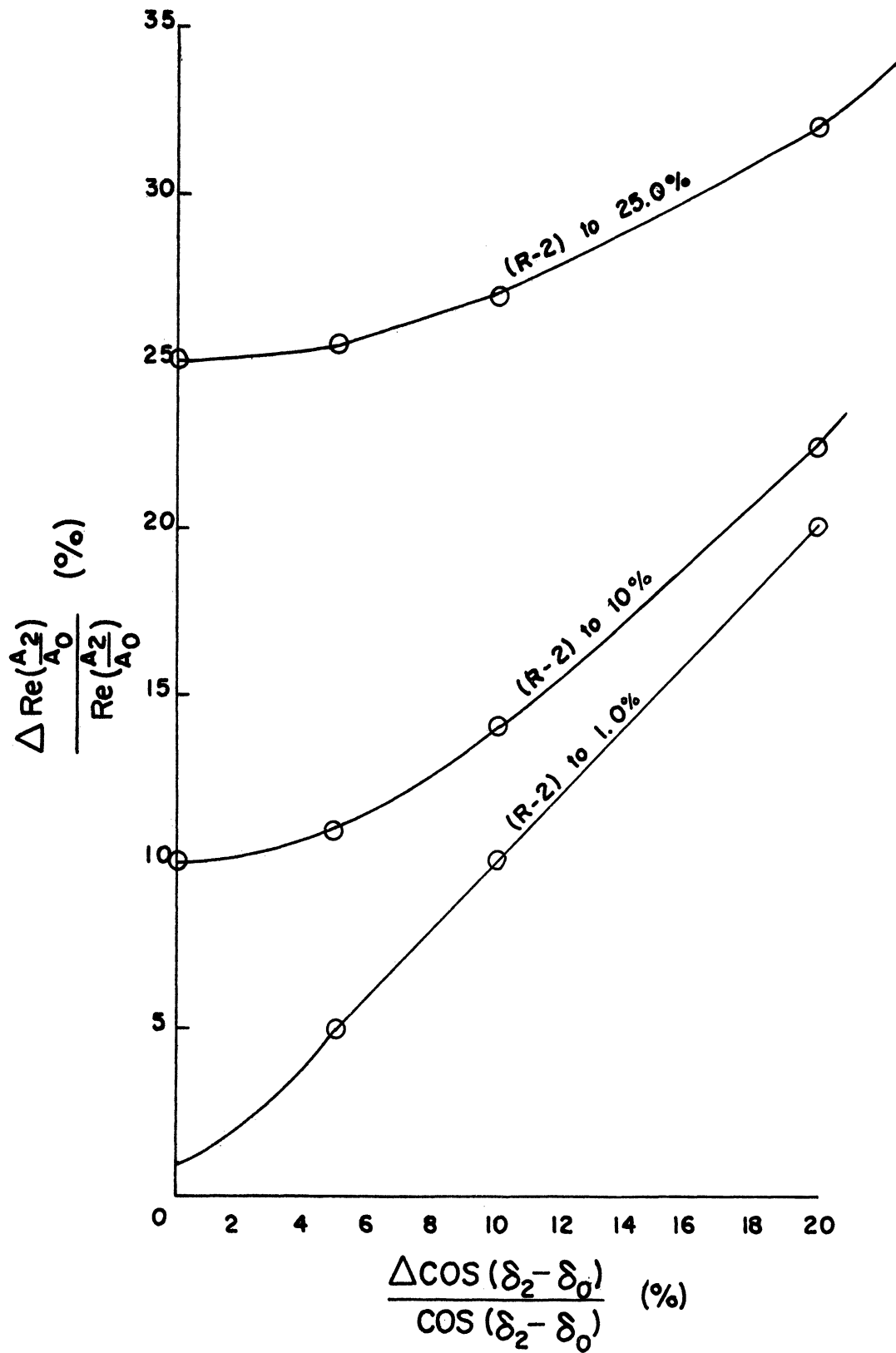
Figure 18. The behavior of the percentage error in $Re(A_2/A_o)$ as a function of the percentage error of $R - 2$ and $\cos(\delta_2 - \delta_o)$.

quantities $Re(A_2/A_o)$ and $\dfrac{\alpha_{5/2}}{\alpha_{3/2}}$ we can calculate these quantities

using the weighted average for R determined as 2.201 ±0.071

and the Gobbi et al. value of 2.285 ±.055. We again use the

mean value $|\delta_2 - \delta_o| = (50 \pm 15)°$. Table XII summarizes the

results for all three values of R. Under the assumption made

about $(\delta_2 - \delta_o)$, it can be seen that both the weighted average

and the Gobbi et al. value are consistent with a small frac-

tion of $\Delta I = 5/2$ transition, while $\Delta I = 1/2$ dominance is only

assured at the 92% level. If indeed $\Delta I = 1/2$ rule is shown

to be so violated then the T-invariance arguments of Casella

based on the modified Wu-Yang triangle and presented earlier,

are better replaced by the arguments incorporating the Bell-

Steinberger sum rules and not based on $\Delta I = 1/2$ dominance.

3.2 The Coherent Regeneration Phase, θ_{SL} in CF_3Br

We have found it possible to estimate the coherent regen-

eration phase, θ_{SL}, for CF_3Br. We emphasize the fact that

although the value we obtain is a probable value for θ_{SL}, due

to the great sensitivity in θ_{SL} for the difference in $N(K_S^o)$

and $N(K_L^o)$ a separate confirming experiment is most definitely

needed.

From Appendix C we see that the intensity of K_S^o as a

function of ℓ, the distance from origin in mean decay lengths,

is

$$I_S(\ell) = \text{Constant} \times [e^{-\ell} + 3.6 \times 10^{-2}(e^{-\ell}\cos\theta$$
$$- e^{-\ell/2}\cos(\theta - \delta_{\ell})] \quad . \quad (5.7)$$

Thus, at any point ℓ, the correction to a pure exponential decay law is determined as

$$C(\ell) = 3.6 \times 10^{-2}(e^{-\ell}\cos\theta - e^{-\ell/2}\cos(\theta - \delta\ell)) \quad (5.8)$$

whereas the pure exponential decay contributes the term

$$E(\ell) = e^{-\ell} \quad . \quad (5.9)$$

Upon integrating over our fiducial volume we find

$$E = \int_{\substack{\text{Fid.}\\\text{Vol.}}} E(\ell)\, d\ell = \int_{o}^{6} e^{-\ell}\, d\ell$$

and

$$C = \int_{\substack{\text{Fid.}\\\text{Vol.}}} C(\ell)\, d\ell = 3.6 \times 10^{-2} \int_{o}^{6} [e^{-\ell}\cos\theta$$

$$- e^{\ell/2}\cos(\theta - \delta\ell)]\, d\ell \quad .$$

Upon integration we find

$$E = 0.9975 \quad (5.10)$$

and

$$C = 0.0395\cos\theta - 0.0144\sin\theta \quad (5.11)$$

so that the fraction of events due to the correction term is

$$F = \frac{C}{E} = 0.0396 \cos \theta - 0.0145 \sin \theta \quad . \qquad (5.12)$$

We can determine F for our experiment by examining our totals of K_L^o and K_S^o. From Table XI the corrected number of K_S^o particles (N_S) is 11390 ±141 while the similar total for K_L^o is N_L = 11289 ±134. However, N_S contains a correction of 242 ±15 events for "scattered V events" which contains scattered K_S^o events plus <u>large angle incoherent regeneration</u> effects. Thus, for the determination of F, these particles created as K_L^o but decaying as K_S^o must be subtracted from N_S and added to N_L. In Chapter III we estimated that 150 of these 242 events were due to incoherent scatters of 15° or more.

It is possible to make a rough numerical calculation of the relative amounts of K_S^o scatters and incoherent effects to check our visual estimates. Let Y be the number of V's within two mean path lengths from the origin and X be the number of V's between two mean path lengths and the end of our fiducial volume. S_x and S_y are the number of K_S^o scatters in regions X and Y, respectively, while L_x and L_y are the number of K_S^o incoherently regenerated from K_L^o particles. Then

$$X = S_y + L_x$$

and

$$Y = S_y + L_y \quad .$$

Since the scattering is relatively low energy, we assume it is isotropic so that those K_s^o scatters detected still roughly follow an exponential distribution law, hence

$$\frac{S_x}{S_y} = \frac{e^{-2.0} - e^{-6.0}}{1.0 - e^{-2.0}} = \frac{0.14}{0.86} = 0.162 \quad .$$

The distribution of incoherently regenerated K_s^o's should remain flat over our fiducial volume so that

$$\frac{L_x}{L_y} = 2.0 \quad .$$

We thus have four equations and four unknowns and we can solve for

$$L = (L_x + L_y) = 1.635 \; X - 0.265 \; Y \quad .$$

From Figure 9 we find $X = 115 \pm 11$, $Y = 127 \pm 11$ so that the total number of <u>large angle</u> incoherently regenerated K_s^o's which decay via the charged mode are calculated to be

$$L = (158 \pm 18) - (34 \pm 3) = 154 \pm 18$$

which agrees quite well with our visual estimate. To this

total we must add the estimated number of small angle ($\lesssim 15°$)
incoherent regenerations which were not caught at the edit
stage. From our Gaussian approximation in Appendix C, Section 2,
we find that the ratio of scatters of $< 15°$ to scatters of
greater than $15°$ is $\approx 1{:}10$, hence the total number of regener-
ations is estimated to be 170 ±18 events. This would imply
that the number of neutral decaying regenerations is

$$\frac{170 \pm 18}{2.117 \pm .064} = 80 \pm 9$$

and the total number of incoherent regenerations is

$$250 \pm 20 \quad .$$

This quantity must be subtracted from N_S and added to N_L.
The corrected numbers for the two samples are

$$N_S^C = 11140 \pm 142$$

and

$$N_L^C = 11539 \pm 132$$

with the difference in the two samples being

$$N_S^C - N_L^C = -399 \pm 196 \quad .$$

We propose that the difference between D as calculated above and D as predicted by CPT ($D = 0$) is due <u>entirely</u> to <u>coherent</u> regeneration effects, all other effects being corrected for. Assuming our proposition, the quantity of CF_3Br contained in our fiducial volume (a sphere of radius 10 cm) acted as an "anti-regenerator" subtracting 200 ±98 events from our K_S^o sample and adding them to our K_L^o sample. This being the case we determine F to be

$$F = \frac{-200 \pm 98}{(11140 \pm 142) + (200 \pm 98)} = -0.0176 \pm 0.0086 \quad .$$

From expression (5.12) we have

$$-0.0176 \pm 0.0086 = 0.0396 \cos \theta - 0.0145 \sin \theta \quad (5.13)$$

so that the quadratic equation for $\cos \theta$ is

$$5.73 \cos^2 \theta + (4.5 \pm 2.21) \cos \theta + (0.33 \pm 0.98). \quad (5.14)$$

Upon solving (5.13) for θ and using the relation

$$\theta_{SL} = \theta - \frac{3\pi}{4}$$

we find the only solution for θ_{SL} compatible with expression (5.13) is

$$\theta_{SL} = (-40 \pm 25)° \ (+90°) \quad .$$

We submit this then as a possible value of the phase for coherent regeneration in CF_3Br. This result can be compared with experimental determinations of the regeneration phase in other materials:

$$\theta_{Cu} = (-36 \pm 12)° \quad (+90°) \quad ,$$

$$\theta_{C} = (-43 \pm 8)° \quad (+90°) \quad ,$$

$$\theta_{H} = (-28 \pm 18)° \quad (+90°) \quad .$$

These phases for copper (C. Alff-Steinberger et al., Phys. Letters 20, 207), carbon (M. Bott-Bodenhauser et al., Phys. Letters 20, 212), and hydrogen (M. Lusignoli et al. to be published in Nuovo Cimento) as well as our value in freon are only defined to within +90° because of the behavior of the cosine of the phase.

APPENDIX A

CHARGE EXCHANGE SCAN RULES

These are the scan rules as used by the scanners in this experiment.

1. Beam Tracks. If a track satisfies all of the following, it is a beam track:

   a. Use the beam track template to determine whether a track enters the fiducial volume and has the correct entrance angle.

   b. The track must not be separated by more than 1 cm in views 1 and 4 at the point where the track enters the fiducial volume. Perform this test on low magnification with both views 1 and 4 on simultaneously.

   c. The track must be minimum ionizing at the point of entrance of the fiducial volume.

2. Primary Interactions. Scan EVERY beam track along the path of flight (i.e., start at the point where it enters the fiducial volume and follow it as it moves deeper into the chamber) for a primary interaction. A primary interaction is any one of the following.

   a. Any scatter of the beam track of more than 10°.

   b. Any 0, 1, 2, 3, ... prong interaction. Note that delta rays ("boil off" electron) are not considered prongs.

   c. Any decay of the beam track.

d. Any abrupt change in bubble density of the track.
The importance of along-the-path scanning cannot be
emphasized enough. Please strictly follow the above
procedure.

3. Types of Recordable Events. If the primary interac-
tion falls into any one of the following classes of
interactions, record it on a mark sense card.

a. Record any zero prong beam track interaction if
the beam track is not heavily ionized within 2 cm
of its end on low magnification. This is a Type 1
interaction. Figure 19 shows this type of event
with a $K_s^o \rightarrow \pi^o + \pi^o$ decay.

b. Record any 1, 2, 3, 4, ... prong interaction if
all of the outgoing tracks satisfy all of the
following.

i. All outgoing tracks must stop in the cham-
ber, and the last 2 cm on high magnifica-
tion of all prongs must be heavily ionized.

ii. There are no negatively charged prongs
(see (c) below).

iii. The outgoing prongs must not interact or
decay; thus, they may not have any abrupt
change in ionization.

iv. A prong may scatter through any angle as
long as it satisfies the change in ioniza-
tion criteria above (iii) and as long as it
does not produce one or more additional

112
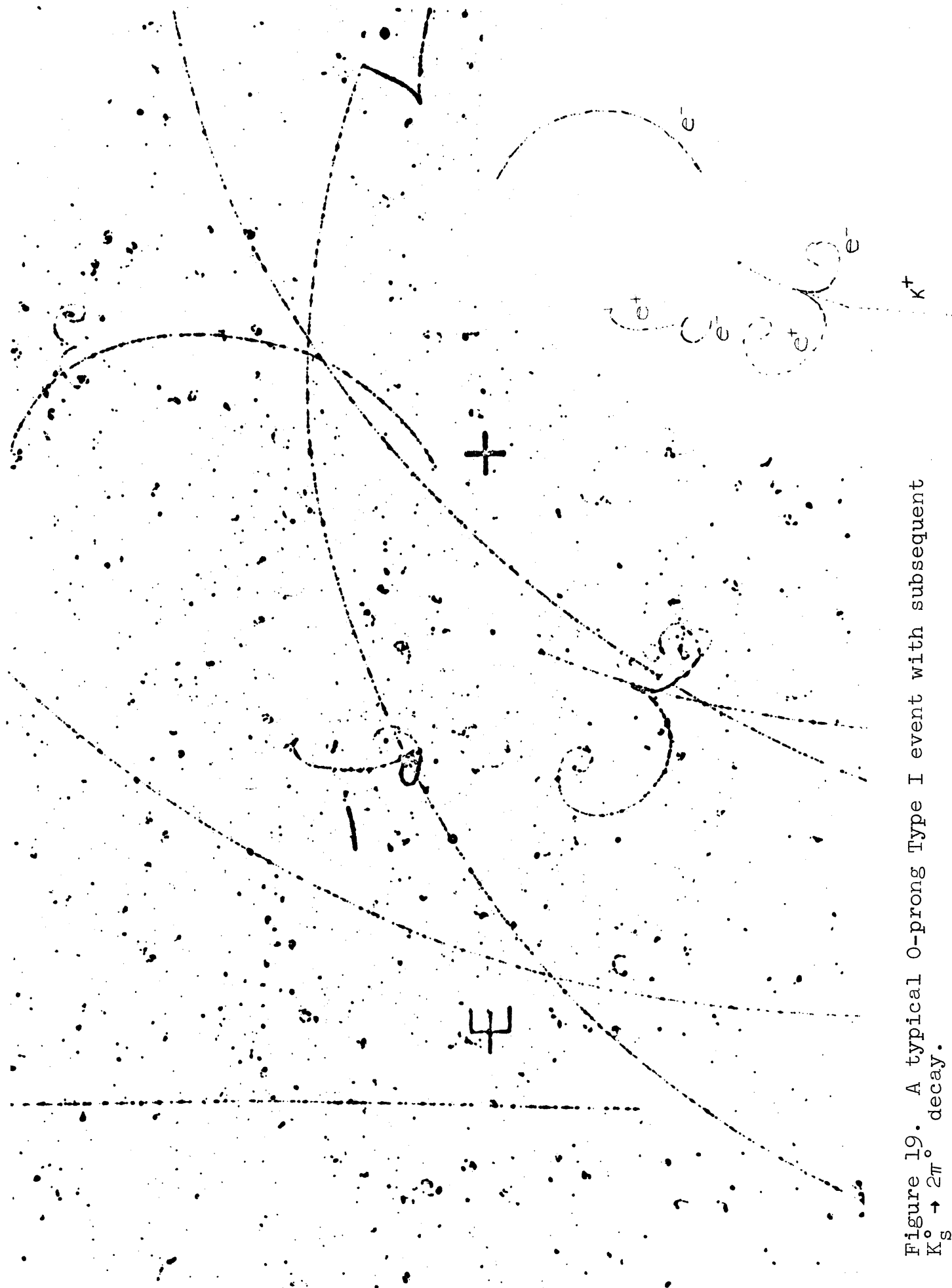
Figure 19. A typical 0-prong Type I event with subsequent $K_S^0 \to 2\pi^0$ decay.

prongs at the point of scatter.

If a primary interaction satisfies all of the above criteria (i, ii, iii, and iv) it is recorded as a Type 1 interaction. Figure 20 shows a typical one prong event with associated V.

c. Record any primary interaction with a negatively charged prong that satisfies both of the following.

    i. The beam track must be minimum ionizing in the last 2 cm before interaction on low magnification.

    ii. The negatively charged prong must be longer than 4 cm on high magnification in any view.

If an interaction satisfies both of the criteria above, it is recorded as a Type 2 interaction. Figure 21 shows a typical Type 2 event with V superimposed on charge exchange point.

While performing disagreement scans for the charge exchange experiment, it has been noted that there are several criteria in the scan rules that are too subjective. Because of these points the scanners are "missing" events or recording extra events. These events which they are missing in no way reflect their true ability to find the desired topologies. Thus, the purpose of this paper is to try and make these offending criteria more objective.

1. Fiducial Volume - Left-hand Entrance Boundary.

Because of the uncontrollable difference between
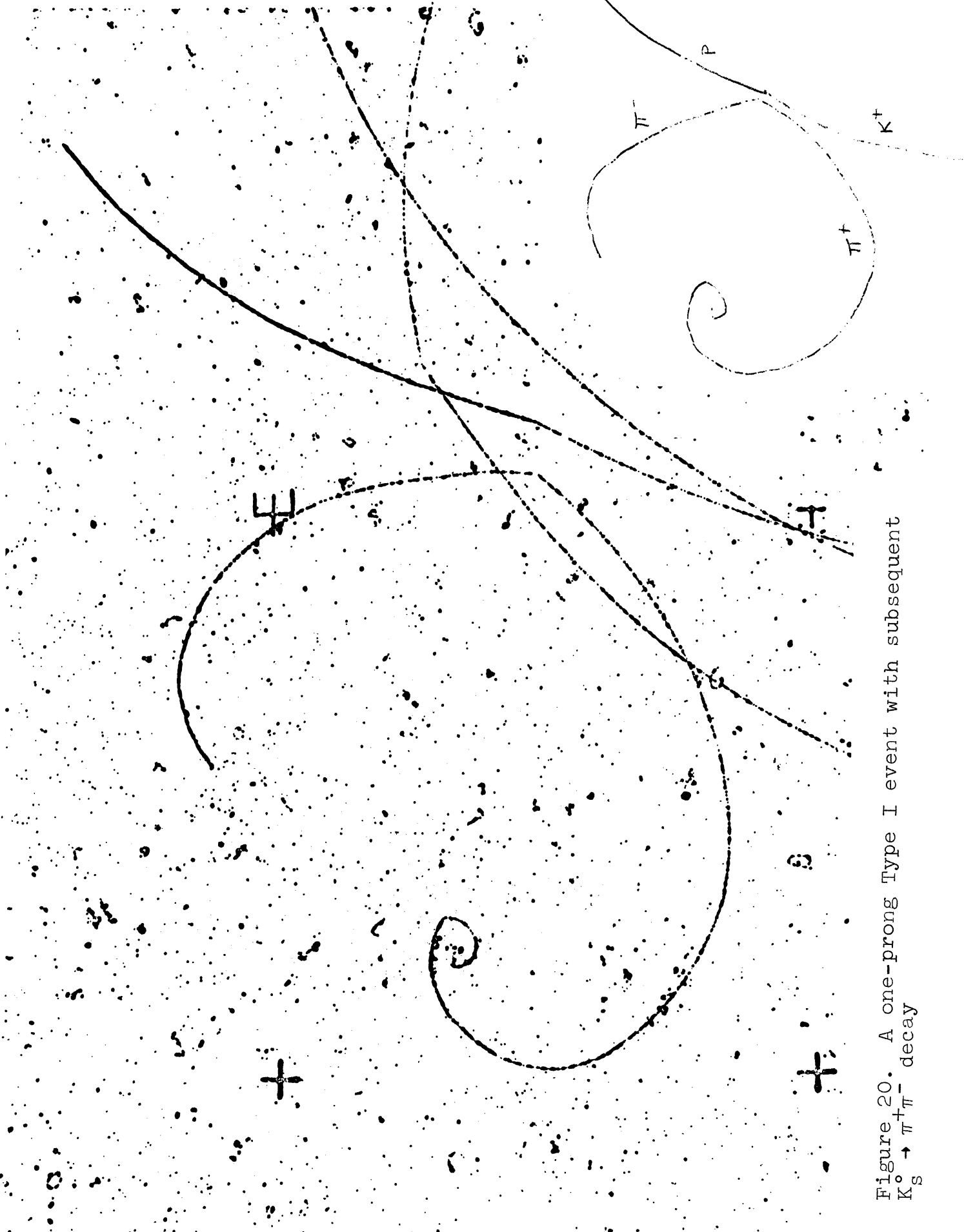
Figure 20. A one-prong Type I event with subsequent $K_S^o \rightarrow \pi^+ \pi^-$ decay
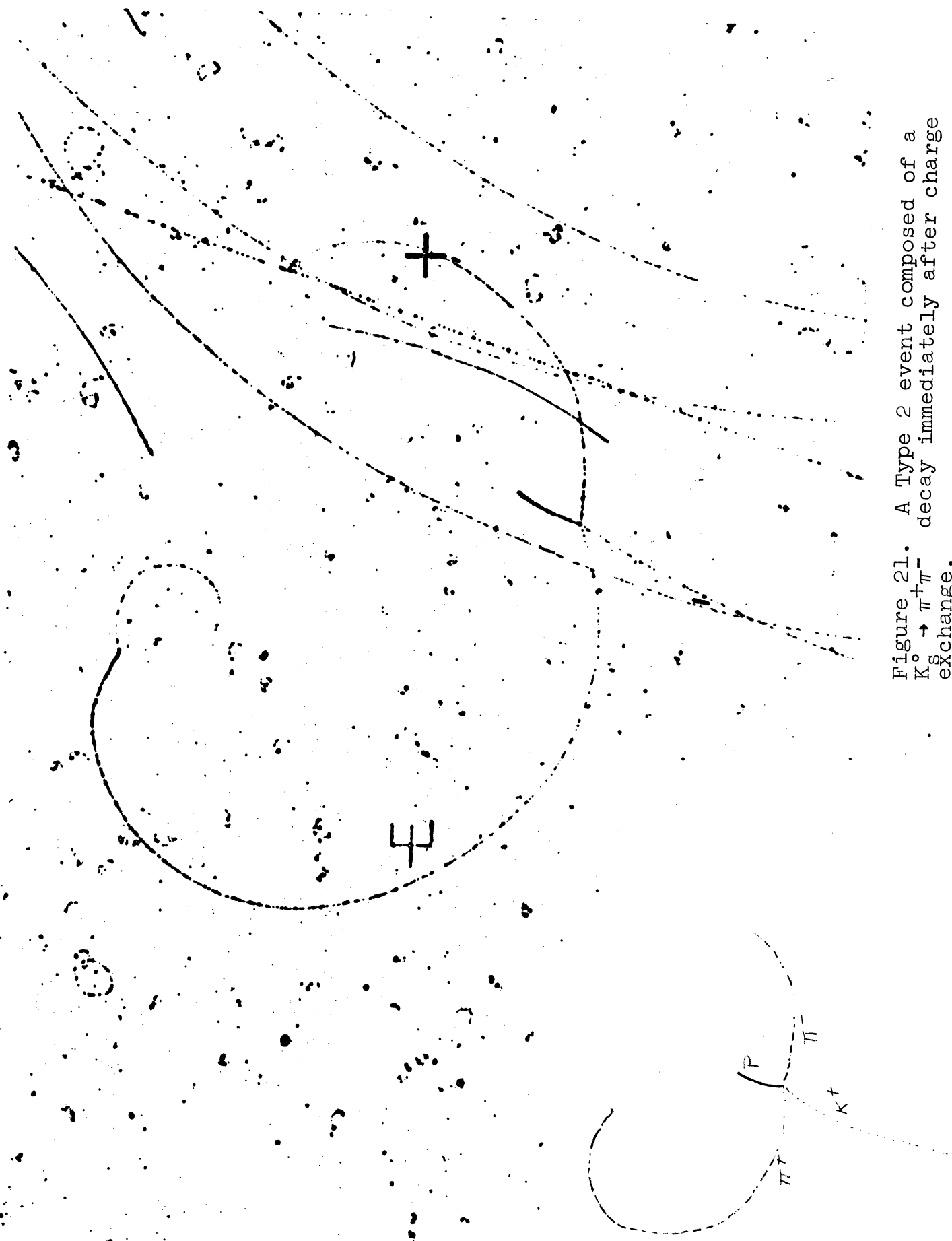
Figure 21. A Type 2 event composed of a $K_S^0 \to \pi^+ \pi^-$ decay immediately after charge exchange.

machine settings and templates, the templates presently provided do not give the same fiducial volume from machine to machine. To clear up this point, the left-hand boundary for entrace into the fiducial volume will be drawn from the frame itself rather than the template. A track will be considered within the fiducial volume at the left-hand limit if, at the point of entrance, it is still visible as a black track on a white background.

2. Pseudo One Prongs. In some instances a track may enter the fiducial volume and satisfy the beam criteria. It then appears to "come to rest" somewhere within the fiducial volume. Many scanners are listing these as Type 1, one prong interactions with questionable vertex. To remove these disagreements, I stress the fact that one must be able to detect an obvious vertex which correspons in at least two views. By obvious vertex we mean a change in direction of the track (angle change) or a definite, unquestionable change in density.

In many cases, these pseudo one prongs are protons, so when these cases arise check the bubble density carefully and compare with other tracks on the same frame.

3. When and When Not are Two Vertices Connected. This question arises in two contexts. The first, and most important, is differentiating between a true 0

prong and the case where the last few bubbles of a track are missing. First of all, a general rule to follow is if two distinct vertices are obviously not connected in any one view then they are not connected. Conversely, two vertices must be connected in all four views to be deemed connected. To determine in any one view if two vertices are connected, use one of the three inscribed curves on the "angle definer" part of the template. If, when you match the curvature of the beam to the template, both vertices fall on the inscribed curve of the template, then the two vertices are connected in that particular view. Check all four views in this manner.

The second context in which this arises is in distinguishing Type 1's from Type 2's. First of all, we have changed the scan program so that a scanner will no longer be charged with a miss if he or she incorrectly labels the event type. Let it suffice to say that the general rules--must be connected in all four views to be deemed connected--still hold. If with this general rule you still cannot decide which type it is, write down your best guess and put a 1 in the picture column.

4. When Does Prong Leave Chamber. When you encounter a very steep track (moves around a lot from view to view) you might question whether it goes out the front or back of the chamber. To determine if it

goes out the front, measure the distance between the end of the prong and a convenient fiducial in view 4. Then in view 1 do the same with the corresponding fiducial. If the distance measured in view 1 is within 1 mm of the distance measured in view 4 then the prong goes out.

5. Ionization. This has proven to be the most subjective criteria of all. What is "heavily ionized" and an "abrupt change in ionization" eludes exact definition since it can vary from roll to roll, even frame to frame.

To help clarify these points a scanner can use the following guides. The end of a prong is "heavily ionized" if the end of no other track on the same frame is obviously darker. If you have to stop and carefully compare the darkness of two tracks, then one is not obviously darker than the other.

As to the question of an "abrupt change of density", let me begin by saying that an abrupt change occurs at a single point--from one bubble to the next --and cannot be spread out over even a 1/2 cm. Secondly, an abrupt change in density is repeated at other points along the track it is not an abrupt change. Note that decays usually have a heavy ionization to minimum ionization type change, while fast prongs that interact usually have a light ionization to medium ionization type change.

6. Finally note that the 4 cm rule for the negative
    track of Type 2's include <u>all</u> segments of the nega-
    tive track if it should happen to scatter.

    In conclusion, if after applying the above clarifi-
cations to any particular case you still have a question,
<u>record the event--do not throw it out</u>. Also, we have
noted that a majority of missed events have occurred at
the extremes of the fiducial volume, either just after
entering or at the left-hand boundary. This indicates
to me that the scanners are not following the procedure
of along-the-track scanning. Be sure to follow every
track that has any possibility of being a good beam from
the point it enters the fiducial volume to the point where
it leaves the fiducial volume if necessary.

APPENDIX B

EDIT RULES

1. FIRST EDIT RULES

These edit rules, as written by Daniel Sinclair[58], were
to be applied to the film after it had been scanned twice and
all disagreements resolved.

In order to make a decision as to the first edit classi-
fication, apply the following tests.

1. Check to see that the event has been correctly iden-
    tified by going over all of the scan rules except
    those concerned with beam position and entry angle.

2. In order to determine whether or not the event has
    a θ associated with it, apply template to charge
    exchange point. Template has two circles radius
    10 cm and 20 cm (real sphere equivalent). The event
    has a θ if the apex of any "V" can be found within
    the 10 cm circle on all four views. A "V" is any
    V-shaped track configuration which is not directly
    connected to a beam track. One of the tracks should
    be negative and the other positive, but if they are
    so short that you cannot be sure of their sign, give
    them the benefit of the doubt. Be on the look-out
    for wide angle V's which might look like a single
    track with no apex. Study all such tracks carefully
    and if you think there might be an apex, include it.

3. In order to determine whether or not the event has

a γ associated with it, place the template on the
charge exchange point. Look on all four views to
see if there is a γ vertex <u>either</u> within the 10 cm
circle <u>or</u> within the 20 cm circle and pointing to
within the 10 cm circle. Accept the γ ray whether
or not it has an alternate origin. It should obey
these rules on all four views.

4. If the event is Type 1 and has no θ and no γ's, check
to see if another Type 1 is within 20 cm (real space
projected) on <u>at least</u> one view. (See Second Edit
Rules.)

1.1 Type 1 Events

If the event is checked to be neither a Type 1 or Type 2
then no further work need be done and the first edit classifi-
cation is 00. If the event is determined to be a Type 1,
decide on one of the following first edit classifications.

a. Event is checked to be a Type 1 but has no
    θ or γ pair associated with it and has no
    other Type 1 interaction with with 20 cm
    on any view..................................... 10

b. Event is checked to be Type 1 and has a θ
    associated with it, but no γ.................... 13

c. Event is checked to be a Type 1 and has a
    γ but no θ associated with it................... 14

d. Event is checked to be a Type 1 and has
    both a θ and a γ associated with it............ 15

e. Event satisfies (a) except that it <u>has</u> a

Type 1 interaction with 20 cm on <u>at least</u>

one view.. 16

f. It is impossible to make a decision on this

event.. 19

1.2 Type 2 Events

If, on the other hand, the event is checked out to be a

Type 2 event examine the interaction vertex to identify the

secondaries and search for a θ and γ as described above. Then

classify it as follows.

a. τ^+ in flight................................. 20

b. π^- with K^+................................. 21

c. π^- secondary with <u>no</u> associated θ or K^+........ 22

d. π^- secondary <u>with</u> an associated θ.............. 23

e. $\pi^+\pi^-$ on legitimate Type 1 with an associated

γ.. 24

f. $\pi^+\pi^-$ on legitimate Type 1 and no associated γ.. 25

g. e^- or e^-e^+ pair on legitimate Type 1............ 26

h. e^- or e^-e^+ pair on illegitimate Type 1......... 27

i. $\pi^+\pi^-$ on illegitimate Type 1.................... 28

j. A decision cannot be made....................... 29

By "legitimate Type 1" is meant an event which would fit the

rules for a Type 1 interaction but for the presence of the

e^- or e^-e^+ pair or $\pi^+\pi^-$.

2. SECOND EDIT RULES

The events to be examined in the second edit are those classified as 13-15, 23-25 in the first edit.

If for some reason the second editor wishes to reject the event, the classification will be 000. To ultimately classify the event one or more of the following tests will have to be applied.

1. Second Edit θ-Test. This test has three parts to it.

    a. The positive and negative track should be consistent with being pions.

    b. The straight line jointing the K^+ charge exchange point to the apex of the V should be contained in the arms of the V.

    c. If one pion is obviously faster than the other then the faster pion should make the smaller angle with the straight line joining the charge exchange point to the apex.

2. Measurable Test for θ's. Both the π^+ and π^- tracks must be measurable; that is, they must either stop without any inelastic interaction or they must have at least 15 cm of chord length (projected) on at least one view before interacting. (Note: 15 cm = 7.5 cm low magnification.)

3. Second Edit γ. The test proceeds thus. First find that (those) $\gamma(s)$ which either lies within the 10 cm circle, or lies within the 20 cm circle and points to within the 10 cm circle on all four views. Place

the "pointing template" on each γ in turn and check
to see if any γ has an alternate origin consistent
with all four views. If at least one of these γ's
can be found <u>without</u> an alternate origin then the
event has passed. Otherwise it has failed. An alter-
nate origin may be the following.

a. The interaction or decay of a beam track except
    when the interaction is another Type 1 meeting
    the requirements of

b. The interaction or decay of a secondary except
    simple proton scatters.

c. The stopping point of a π^- (but not a π^+).

d. The stopping point of a K^+ (but not of a proton).

e. The tangent line to any electron or positron
    track from any source.

f. The interaction point of π^+ or π^- tracks from any
    source.

g. Any neutron star except single proton.

For events which pass the test an estimate should be
made of the total number of copunctal γ's. To do
this, scan the whole picture, not just the 20 cm
circle. Use judgment as to the origin of a γ-ray.
A γ-ray with an alternate origin may be included in
this count if, in the editor's opinion, it is more
likely to be a member of the copunctal set than it is
to be associated with the alternate origin because of
the longer conversion distance to the alternate origin.

4. <u>Measurement of Distances.</u>

    a. For θ's measure the longest projected distance between the apex of the θ and the charge exchange interaction in millimeters on low magnification.

    b. For γ's measure the distance between the charge exchange point and the apex of the closest γ. Make the measurement in centimeters on low magnification and on that view in which the distance is longest. Round off to the nearest centimeter.

5. <u>Searching for Another Type 1 within 20 cm.</u> Place the template on the event and search within the 20 cm circle on all views. Accept any event within this circle on at least one view whether or not it meets the fiducial volume and angle requirements of the scan rules. However, it must be a legal Type 1 in all other respects. See Figure 22 for this topology.

2.1 With V

For events classified as 13 or 23 by the first edit, the following tests should be applied.

    1. Second edit θ-test; does it pass?

    2. Is the θ measurable? (See later instructions.)

    3. Is there another Type 1 vertex within 20 cm on any view?

Code your result as follows:

    a. It is <u>not</u> a θ <u>and</u> there is no other Type 1 within 20 cm on any view...................... Oij
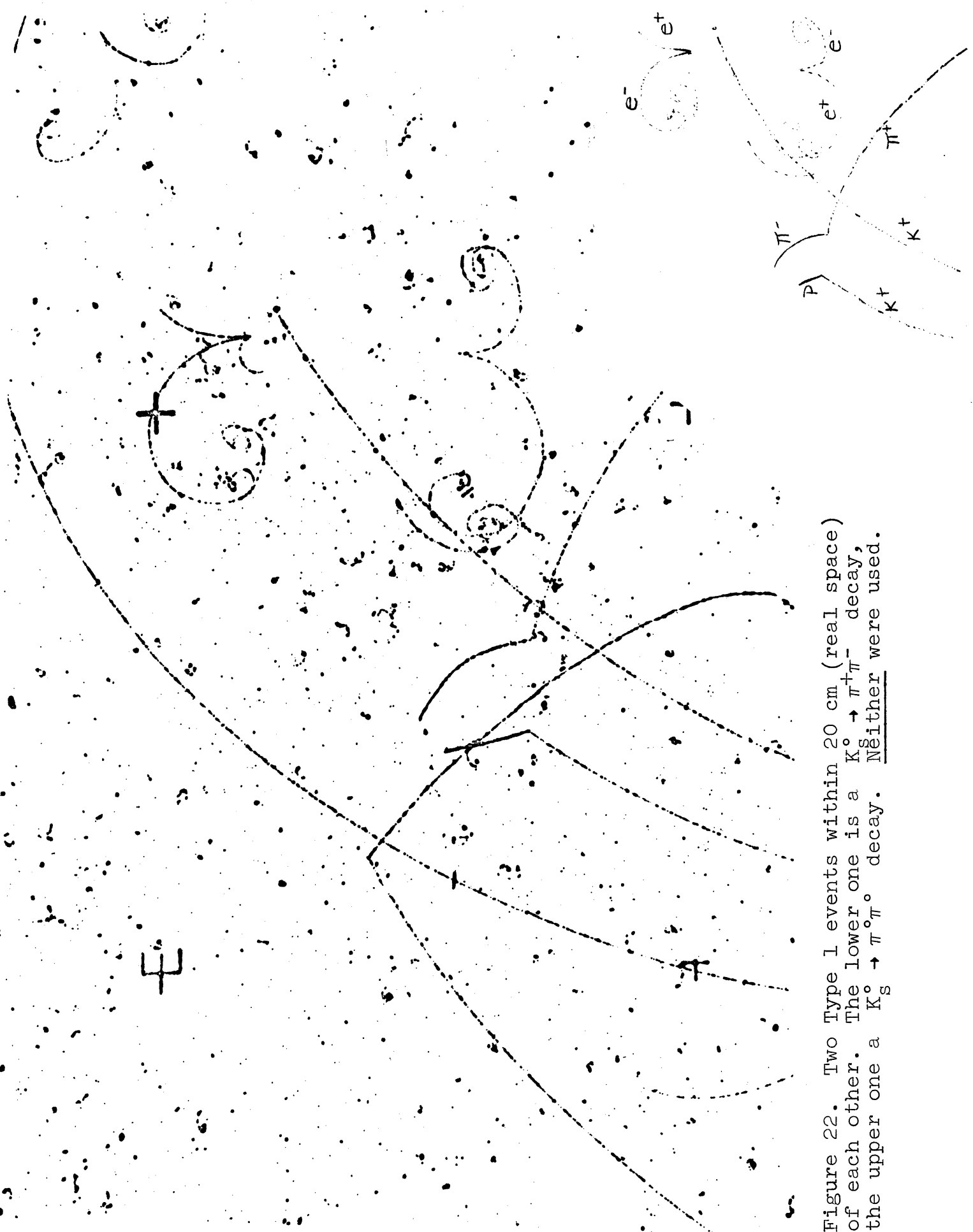
Figure 22. Two Type 1 events within 20 cm (real space) of each other. The lower one is a $K^0_S \to \pi^+\pi^-$ decay, the upper one a $K^0_S \to \pi^0\pi^0$ decay. Neither were used.

b. It <u>is</u> a θ <u>and</u> it <u>is</u> measurable and there

is <u>no</u> other Type 1 within 20 cm on any view.... 1ij

c. It <u>is</u> a θ, it <u>is</u> measurable, and there <u>is</u>

a Type 1 within 20 cm on some view............. 2ij

d. It <u>is</u> a θ, but it is <u>not</u> measurable and

there is <u>no</u> Type 1 within 20 cm on any view.... 3ij

e. It <u>is</u> a θ, but it is <u>not</u> measurable and

there is a Type 1 within 20 cm................. 4ij

f. It is <u>not</u> a θ and there <u>is</u> a Type 1 within

20 cm on some view............................. 5ij

The last two digits, i and j, are the distance from charge exchange point to the θ vertex. If no decision can be made the classification is 999.

2.2 With γ

For those events classified as 14 or 24 in the first edit apply the following tests.

1. Second edit γ-test. (See later instructions.)

2. Is there another Type 1 vertex within 20 cm on any view?

Code the first digit of the classification as follows. Enter the estimated number of γ's for events passing the test. If the event fails enter 0. Do not enter more than four unless, if the result of Test 2 is positive, add 5 to the entry. As the last two digits enter the distance of the closest γ passing the γ test. If none, enter 99. If no decision can be made, enter 999 as your final result. Fig. 23 shows <u>illegal</u> γ event.

128

Figure 23. An illegal γ event. A two-prong charge exchange with possible γ's. However, γ's come from nearby $K_{\pi 2}$ decay.

2.3 With V and γ

For those events classified as 15 in the first edit apply the following tests.

1. Second edit θ-test; does it pass?

2. Second edit γ-test.

3. Is the θ measurable?

4. Is there another Type 1 origin with 20 cm on any view?

If the event passes the θ-test and <u>no</u> γ's pass the γ-test, code your result as described in Section 2.1.

If the event fails the θ-test but passes the γ-test, code your classification as

    a. No Type 1 origin within 20 cm................... 5ij

    b. There is a Type 1 origin with 20 cm............ 6ij

where the distance of the shortest γ from the charge exchange point is digits ij.

If the event passes both the θ-test and the γ-test code your classification as

    a. There is no Type 1 origin within 20 cm......... 7ij

    b. There is a Type 1 origin within 20 cm.......... 8ij

where the distance of the shortest γ is again digits ij.

If the event passes neither the θ-test nor the γ-test, then enter 0 99 if no Type 1 within 20 cm; otherwise 088.

If no decision can be made enter 999.

Finally, if the first edit classification is 25, apply the "measurability test for θ's" to the $\pi^+\pi^-$ tracks leaving the origin. Code your result as follows.

    a. Fails the test and <u>no</u> Type 1 within 20 cm...... 200

b. Passes the test and <u>no</u> Type 1 within 20 cm..... 300

c. Fails the test and there <u>is</u> a Type 1 within

    20 cm.. 400

d. Passes the test and there is a Type 1 within

    20 cm.. 500

e. No decision can be made........................ 999

APPENDIX C

PHENOMENOLOGY OF $K^o_S \to 2\pi$ DECAY

1. THE DECAY $K^o_S \to 2\pi$

In this section we look at the K^o-$\overline{K^o}$ system from a
phenomenological point of view with special emphasis on the
2π decay of K^o_S. Only that analysis which bears direct effect
to our experiment will be presented. Our ultimate goal in
this section is to obtain the approximation formulated by
Abbud-Lee-Yang as

$$R - 2 = 6\sqrt{2} \; \mathrm{Re}\left(\frac{A_2}{A_o}\right) \cos\left(\delta_2 - \delta_o\right) + \left(\Delta_{em}\right) \qquad (C.1)$$

where:

$$R = \frac{\Gamma(K^o_S \to \pi^+\pi^-)}{\Gamma(K^o_S \to \pi^o\pi^o)} \; .$$

A_2 and A_o are the $I = 2$ and $I = 0$ standing wave decay ampli-
tudes, respectively, of $K \to \pi + \pi$; δ_2 and δ_o are the $\pi\pi$
s-wave scattering phase shifts for the $I = 2$ and $I = 0$ states
at $E = m_{K^o}$; Δ_{em} is the electromagnetic correction, mentioned
at the end of the first chapter, which is composed of three
factors: a) final state Coulomb interaction, b) radiative
correction (due to transverse photons), and c) corrections
from on-mass-shell decay of $K^o_S \to 2\pi\gamma \to 2\pi$, with correction

(a) being the most significant (see Chapter I, Section 4).
To derive this expression we will start with the initial time
dependent amplitudes of K° and $\overline{K^\sigma}$, and propagate them via a
modified Weisskopf-Wigner treatment.

The original Weisskopf-Wigner[59] description of unstable
states held only for nondegenerate eigenstates and resulted
in a differential equation for particle amplitude

$$- \frac{d}{dt} \psi(t) = \frac{\Gamma}{2} \psi(t) \tag{C.2}$$

where Γ is the total width of the state ψ which is the inverse
of the lifetime. In 1934 Breit and Lowen[60] modified the
original Weisskopf-Wigner formulation to include the possi-
bility of degeneracy and it is basically the Breit-Lowen
method we must use since the scalar formula (C.2) will not
describe the real and virtual transitions that cause K°-$\overline{K^\sigma}$
mixing. A detailed application of the Breit-Lowen method
(modified still further by Kallen[61] in 1958) to the K°-$\overline{K^\sigma}$
system, can be found in Kabir[62]. Essentially we must replace
the decay constant Γ with a 2 x 2 decay matrix whose off-
diagonal elements provide for the mixing phenomena, while
the general neutral K state becomes a vector in a two-
dimensional Hilbert space with basis states

$$|K^\circ\rangle = \begin{pmatrix} 1 \\ 0 \end{pmatrix} \quad ; \quad |\overline{K^\sigma}\rangle = \begin{pmatrix} 0 \\ 1 \end{pmatrix} \tag{C.3}$$

so that

$$|K(t)\rangle = a(t) \begin{pmatrix} 1 \\ 0 \end{pmatrix} + b(t) \begin{pmatrix} 0 \\ 1 \end{pmatrix} = \begin{pmatrix} a(t) \\ b(t) \end{pmatrix} \quad . \quad (C.4)$$

Thus the general Schrodinger type equation which governs this system will be of the form

$$- \frac{d}{dt} |K(t)\rangle = D|K(t)\rangle \quad . \quad (C.5)$$

If we denote the various channels of decay as f and $A_f(E) \, e^{-iEt}$ is the amplitude of the decay product in channel f with energy E, then equation (C.5) breaks down to two coupled Schrodinger equations (in the notation of Wu and Yang)

$$i \frac{d}{dt} K(t) = \sum_{f,E} H_{Kf}(E) \, A_f(E) \, e^{-iEt} \quad , \quad (C.6)$$

$$i \frac{d}{dt} \bar{K}(t) = \sum_{f,E} H_{\bar{K}f}(E) \, A_f(E) \, e^{-iEt} \quad (C.7)$$

with the amplitudes given by

$$\frac{\partial}{\partial t} A_f(E) = -ie^{iEt} [H_{fK}(E) \, K + H_{f\bar{K}}(E) \, \bar{K}] \quad . \quad (C.8)$$

The various $H_{fi} = \langle f|H_{wk}|i\rangle$ are the matrix elements which will later be expressed in terms of the decay and mass matrices so that further discussion of them will be left for that time.

Solving these via the modified Breit-Lowen treatment we obtain

$$\begin{pmatrix} K \\ K \end{pmatrix} = \psi_{\pm} e^{-1/2 \, \lambda_{\pm} t} \quad .$$

The amplitudes $\psi_{\pm}$ and decay constants $\lambda_{\pm}$ are given by the eigenvalue equation

$$(\Gamma + iM) \, \psi_{\pm} = \lambda_{\pm} \psi_{\pm} \quad . \qquad (C.9)$$

1.1 The Decay Matrix

The Hermitian matrix Γ is called the decay matrix and its matrix elements are related to the weak Hamiltonian by the perturbation formulae

$$\Gamma_{11} = \pi \sum_{f} \rho_f \, | \langle f | H_{wk} | K^\circ \rangle |^2 \quad ,$$

$$\Gamma_{22} = \pi \sum_{f} \rho_f \, | \langle f | H_{wk} | \overline{K}^\circ \rangle |^2 \quad , \qquad (C.10)$$

$$\Gamma_{21} = \Gamma_{12}^* = \pi \sum_{f} \rho_f \, \langle \overline{K}^\circ | H_{wk} | f \rangle \langle f | H_{wk} | K^\circ \rangle$$

where f again is the final state and ρ_f is the density of final states per unit energy. It is possible to perform these sums and express the Γ matrix as the sum of the contributions

from the $\pi\pi(I = 0)$, $\pi\pi(I = 2)$, leptonic, and 3π modes

$$\Gamma = \Gamma_o + \Gamma_2 + \Gamma_\ell + \Gamma_{3\pi}$$

where

$$\Gamma_o = \begin{pmatrix} A_o^2 & A_o^2 \\ A_o^2 & A_o^2 \end{pmatrix}$$

$$\Gamma_2 = \begin{pmatrix} A_2 A_2^* & A_2^2 \\ A_2^{*2} & A_2 A_2^* \end{pmatrix}$$

$$\Gamma_\ell = \begin{pmatrix} \alpha_\ell & x_\ell + iy_\ell \\ x_\ell - iy_\ell & \alpha_\ell \end{pmatrix}$$

$$\Gamma_{3\pi} = \begin{pmatrix} \alpha_{3\pi} & x_{3\pi} + iy_{3\pi} \\ x_{3\pi} - iy_{3\pi} & \alpha_{3\pi} \end{pmatrix}$$

The elements of Γ_o and Γ_2 were defined earlier. The elements of Γ_ℓ and $\Gamma_{3\pi}$ represent the general expressions from page 134 with the sum over possible leptonic and 3π final states, respectively.

1.2 The Mass Matrix

The Hermitian matrix M is called the mass matrix so that iM is an anti-Hermitian matrix which represents the effects of the mass shift. The elements of the mass matrix are much more complicated than those of the decay matrix since, in addition to the usual weak Hamiltonian perturbations, we now have both strong and electromagnetic couplings between various mass states. Thus we have (also in Wu-Yang notation)

$$M_{11} = m_K^\vee + \langle K^\circ | H_{wk} | K^\circ \rangle + \sum_n P \left(\frac{|\langle n | H_{wk} | K^\circ \rangle|^2}{(m_K^\circ - m_n^\circ)} \right)$$

$$M_{22} = m_K^\circ + \langle \overline{K}^\circ | H_{wk} | \overline{K}^\circ \rangle + \sum_n P \left(\frac{|\langle n | H_{wk} | \overline{K}^\circ \rangle|^2}{(m_K^\circ - m_n^\circ)} \right) \qquad (C.11)$$

$$M_{21} = M_{12}^* = \langle \overline{K}^\circ | H_{wk} | K^\circ \rangle + \sum_n P \left(\frac{\langle \overline{K}^\circ | H_{wk} | n \rangle \langle n | H_{wk} | K^\circ \rangle}{(m_K^\circ - m_n^\circ)} \right)$$

where

$$m_K^\circ = \langle K^\circ | H_{st} + H_\gamma | K^\circ \rangle = \langle \overline{K}^\circ | H_{st} + H_\gamma | \overline{K}^\circ \rangle$$

(assuming CPT allows the second equality). In the above elements P stands for the principle value while the sum over n extends over all unperturbed eigenstates of $H_{st} + H_\gamma$ with unperturbed energy m_n°.

The off-diagonal elements of M can be simplified by noting that the small mass difference between K_1^o and K_2^o suggests that $\langle \overline{K^o} | H_{wk} | K^o \rangle$ is essentially 0. This is also consistent with the hypothesis that the $|\Delta S| = 2$ component of the weak current J_μ^W is also essentially 0.

1.3 The States $|K_S^o\rangle$ and $|K_L^o\rangle$: Transition Matrix Elements

We can now construct the eigenvectors of the K^o-$\overline{K^o}$ system which, in the notation of Lee, Yang, and Oehme[63], take the form

$$\psi_{\pm} = (|p|^2 + |q|^2)^{-1/2} \begin{pmatrix} p \\ \pm q \end{pmatrix} \qquad (C.12)$$

where

$$p^2 = \Gamma_{12} + iM_{12} = A_o^2 + A_2^2 + x_\ell + iy_\ell + x_{3\pi}$$

$$+ iy_{3\pi} + iM_{12} \qquad (C.13)$$

and

$$q^2 = \Gamma_{21} + iM_{21} = \Gamma_{12}^* + iM_{12}^*$$

$$= A_o^2 + A_2^{*2} + x_\ell - iy_\ell + x_{3\pi} - iy_{3\pi} + iM_{12}^* \quad . \quad (C.14)$$

Thus, as our notation we shall take the K_S^o and K_L^o states to be:

$$|K_S^o\rangle = (|P|^2 + |q|^2)^{-1/2} \begin{pmatrix} P \\ q \end{pmatrix} \quad ,$$

$$\text{(C.15)}$$

$$|K_L^o\rangle = (|P|^2 + |q|^2)^{-1/2} \begin{pmatrix} P \\ -q \end{pmatrix} \quad .$$

There are several other common representations for these states in use in today's literature. Of these the two most predominant are $\epsilon = \dfrac{P - q}{2}$ in which case

$$|K_S^o\rangle = [2(1 + |\epsilon|^2)]^{-1/2} \begin{pmatrix} 1 + \epsilon \\ +(1 - \epsilon) \end{pmatrix}$$

and $r = P/q$ so that the K_S^o state becomes

$$|K_S^o\rangle = (1 + |r|^2)^{-1/2} \begin{pmatrix} 1 \\ +r \end{pmatrix} \quad . \qquad \text{(C.16)}$$

We are now in position to construct the 2π decay amplitudes of K_S^o. We need first the isoscalar ($I = 0$) and isotensor ($I = 2$) standing wave amplitudes a_o and a_2, respectively. Since

$$|\pi\pi(I = 0)\rangle = A_o \begin{pmatrix} 1 \\ 1 \end{pmatrix} \quad ,$$

$$|\pi\pi(I = 2)\rangle = \begin{pmatrix} A_2 \\ A_2^* \end{pmatrix} \quad .$$

Hence

$$a_2 = \langle \pi\pi(I = 2)|K_s^o\rangle = (A_2 A_2^*)(|P|^2 + |q|^2)^{-1/2} \binom{P}{q}$$

$$a_2 = (|P|^2 + |q|^2)^{-1/2} (A_2 P + A_2^* q) \tag{C.17}$$

and

$$a_o = (|P|^2 + |q|^2)^{-1/2} A_o (P + q) \quad . \tag{C.18}$$

We now construct the $\pi^+\pi^-$ outgoing wave amplitude using the Clebsch-Gordon coefficients. The $\pi^+\pi^-$ state is constructed as follows (states are $|I, I_3\rangle$):

$$\pi^+ = |1,+1\rangle \quad ; \quad \pi^- = |1,-1\rangle \quad .$$

Thus

$$|\pi^+\pi^-\rangle = \sqrt{\tfrac{2}{3}} \underbrace{|0,0\rangle}_{a_o} e^{i\delta_o} + \sqrt{\tfrac{1}{3}} \underbrace{|2,0\rangle}_{a_2} e^{i\delta_2} \tag{C.19}$$

and

$$\langle \pi^+\pi^-| I|K_s^o\rangle = (|P|^2 + |q|^2)^{-1/2} \Big\{ \Big[\sqrt{\tfrac{2}{3}} A_o e^{i\delta_o}$$

$$+ \sqrt{\tfrac{1}{3}} A_2 e^{i\delta_2}\Big] P + \Big[\sqrt{\tfrac{2}{3}} A_o e^{i\delta_o}$$

$$+ \sqrt{\tfrac{1}{3}} A_2^* e^{i\delta_2}\Big] q \Big\}$$

$$= [3(|P|^2 + |q|^2)]^{-1/2} \, e^{i\delta_o}$$

$$x \left[\sqrt{2} \, A_o(P + q) + (A_2 P + A_2^* q) \, e^{i(\delta_2 - \delta_o)} \right] .$$

Dropping the overall undetermined phase $e^{i\delta_o}$, we have

$$\langle \pi^+ \pi^- | I | K_S^o \rangle = [3(|P|^2 + |q|^2)]^{-1/2} \left[\sqrt{2} \, A_o(p + q) \right.$$

$$\left. + (A_2 P + A_2^* q) \, e^{i(\delta_2 - \delta_o)} \right] . \qquad (C.20)$$

Similarly,

$$\langle \pi^o \pi^o | I | K_S^o \rangle = [3(|P|^2 + |q|^2)]^{-1/2} \left[A_o(P + q) \right.$$

$$\left. - \sqrt{2} \, (A_2 P + A_2^* q) \, e^{i(\delta_2 - \delta_o)} \right] . \qquad (C.21)$$

Or, in the more contemporary 'r' notation

$$\langle \pi^+ \pi^- | I | K_S^o \rangle = [3(1 + |r|^2)]^{-1/2} \left[\sqrt{2} \, A_o(1 + r) \right.$$

$$\left. + (A_2 + A_2^* r) \, e^{i(\delta_2 - \delta_o)} \right] , \qquad (C.22)$$

$$\langle \pi^o \pi^o | I | K_S^o \rangle = [3(1 + |r|^2)]^{-1/2} \left[A_o(1 + r) \right.$$

$$- \sqrt{2} \; (A_2 + A_2^* r) \; e^{i(\delta_2 - \delta_o)} \Big] \qquad . \qquad (C.23)$$

By definition

$$R = \frac{\Gamma(K_S^o \to \pi^+\pi^-)}{\Gamma(K_S^o \to \pi^o\pi^o)} = \frac{\left|\langle \pi^+\pi^- | I | K_S^o \rangle\right|^2}{\left|\langle \pi^o\pi^o | I | K_S^o \rangle\right|^2} \qquad .$$

Thus

$$R = \frac{\left| \sqrt{2} \; A_o(1 + r) + (A_2 + A_2^* r) \; e^{i(\delta_2 - \delta_o)} \right|^2}{\left| A_o(1 + r) - \sqrt{2} \; (A_2 + A_2^* r) \; e^{i(\delta_2 - \delta_o)} \right|^2} \qquad . \qquad (C.24)$$

We now make the assumption, to be justified shortly, that the difference between r and 1 is negligible. Hence

$$R = \left| \frac{2\sqrt{2} \; A_o + 2 \; \text{Re} \; A_2 F}{2 \; A_o - 2\sqrt{2} \; \text{Re} \; A_2 F} \right|^2$$

where

$$F = e^{i(\delta_2 - \delta_o)} \qquad .$$

Then

$$R = \left| \frac{2\sqrt{2} \; [1 + \frac{1}{\sqrt{2}} \; \text{Re}(\frac{A_2}{A_o}) \; F]}{2[1 - \sqrt{2} \; \text{Re}(\frac{A_2}{A_o}) \; F]} \right|^2 \qquad ,$$

$$R = 2 \left| \frac{1 + \alpha}{1 - 2\alpha} \right|^2 = 2 \left[\frac{1 + 2 \text{ Re } \alpha + \alpha^2}{1 - 4 \text{ Re } \alpha + 4\alpha^2} \right]$$

where

$$\alpha = \frac{F}{\sqrt{2}} \text{ Re} \left(\frac{A_2}{A_o} \right) \quad .$$

Neglecting terms of order α^2 we find

$$R = 2 [(1 + 2 \text{ Re } \alpha)(1 - 4 \text{ Re } \alpha)^{-1}] \quad .$$

Expanding the denominator

$$R = 2 [(1 + 2 \text{ Re } \alpha)(1 + 4 \text{ Re } \alpha)]$$

$$= 2 [1 + 6 \text{ Re } \alpha + 8(\text{Re } \alpha)^2] \quad .$$

From the definition of α and F above,

$$\text{Re } \alpha = \frac{\cos (\delta_2 - \delta_o)}{\sqrt{2}} \text{ Re} \left(\frac{A_2}{A_o} \right) \quad .$$

Finally upon substitution, again neglecting terms of order α^2 or smaller,

$$R = 2 \left[1 + \frac{6}{\sqrt{2}} \text{ Re} \left(\frac{A_2}{A_o} \right) \cos (\delta_2 - \delta_o) \right]$$

$$R - 2 = 6\sqrt{2}\, \text{Re}\left(\frac{A_2}{A_o}\right) \cos\left(\delta_2 - \delta_o\right) \quad .$$

1.4 The Validity of the Abbud-Lee-Yang Approximation

In the preceding derivation we have assumed limits on several quantities. To justify these we need, in addition to the $K_S^o \to \pi^+\pi^-$ (henceforth denoted as S_c) and $K_S^o \to \pi^o\pi^o$ (S_n) amplitudes, the corresponding K_L^o amplitudes. These are:

$$L_c = \langle \pi^+\pi^- |I| K_L^o\rangle = [3(1 + |r|^2)]^{-1/2}$$

$$\times\ [\sqrt{2}\, A_o(1 - r) + (A_2 - A_2^* r)\, F] \quad ,$$

$$L_n = \langle \pi^o\pi^o |I| K_L^o\rangle = [3(1 + |r|^2)]^{-1/2}$$

$$\times\ [A_o(1 - r) - \sqrt{2}\, (A_2 - A_2^* r)\, F] \quad .$$

In addition we need the following numerical quantities[7]

$$|\eta_{+-}| = (1.92 \pm .04) \times 10^{-3} = L_c/S_c \quad ,$$

$$|\eta_{oo}| = (3. \pm 1.2) \times 10^{-3} = L_n/S_n^* \quad ,$$

$$R\ = 2.117 \pm 0.064 = S_c{}^2/S_n{}^2 \quad .$$

---

[*]We have set the error in $|\eta_{oo}|$ to reflect the significant deviations in reported values.

To determine the quantity r we use the four amplitudes L_c, L_n, S_c, and S_n as follows. Let

$$N = [3(1 + |r|^2)]^{-1/2} \quad .$$

Then

$$\frac{1}{3}(\sqrt{2}\, L_c + L_n) = NA_o(1 - r)$$

and

$$\frac{1}{3}(\sqrt{2}\, S_c + S_n) = NA_o(1 + r) \quad .$$

We define the quantity v, for later use, as

$$v = \frac{1 - r}{1 + r} = \frac{\sqrt{2}\, L_c + L_n}{\sqrt{2}\, S_c + S_n} \quad ,$$

$$v = \frac{\sqrt{2R}\, \eta_{+-} + \eta_{oo}}{\sqrt{2R} + 1} \quad . \tag{C.26}$$

Since we are interested in the magnitude of r and v and we experimentally measure $|\eta_{+-}|$ and $|\eta_{oo}|$ the best we can do is set an upper limit on v

$$|v| \leq \left| \frac{\sqrt{2R}\, \eta_{+-} + \eta_{oo}}{\sqrt{2R} + 1} \right|$$

$$|v| \leq \frac{\sqrt{2R} \; |\eta_{+-}| + |\eta_{oo}|}{\sqrt{2R} - 1} \quad . \tag{C.27}$$

This gives us a lower limit on r

$$|r| \geq \frac{1 - |v|}{1 + |v|} \quad .$$

Using the values above we find

$$|v| \leq 6.61 \times 10^{-3}$$

and

$$|r| \geq 0.987 \quad .$$

The validity of the Abbud-Lee-Yang approximation can be shown by solving for $\cos(\delta_2 - \delta_o)$ exactly, that is dropping no terms and assuming only that the CP violating component of the decay amplitude is small ($r = 1$). We find

$$\cos(\delta_2 - \delta_o) = \frac{R - 2 + (4R - 1)|\alpha|^2}{2\sqrt{2} \; (R + 1) \; Re(\frac{A_2}{A_o})} \tag{C.28}$$

which is quite similar to the Abbud-Lee-Yang form

$$\cos(\delta_2 - \delta_o) = \frac{R - 2}{6\sqrt{2} \; Re(\frac{A_2}{A_o})} \tag{C.28a}$$

since $|\alpha|^2 = 9.68 \times 10^{-4}$.

2. REGENERATION PHENOMENA

As early as 1955 regeneration of K_S^o from K_L^o was suggested by Pais and Piccioni[64]. Their basis for this hypothesis was the observation that if a K_L^o beam passes through matter its $\overline{K^o}$ component ($S = -1$) will be more strongly absorbed than the K^o amplitude ($S = +1$) since, due to strangeness arguments, $\overline{K^o}$ can make hyperons and hypernuclei while K^o can only elastic scatter and charge exchange. Hence, after traversing the matter, there will be relatively more K^o than $\overline{K^o}$ amplitude which is equivalent to an admixture of K_S^o.

2.1 Coherent Regeneration

Regeneration can occur with a scatter (incoherent regeneration) of the K_L^o beam or without a scatter (coherent regeneration). In coherent regeneration the amplitudes for K_S^o and K_L^o are obtained by solving a pair of coupled differential equations. Christenson et al.[65] give the solution in matrix form

$$\begin{pmatrix} K_S^o(x) \\ K_L^o(x) \end{pmatrix} = \begin{pmatrix} R_{11}(x) & R_{12}(x) \\ R_{21}(x) & R_{22}(x) \end{pmatrix} \begin{pmatrix} K_S^o(0) \\ K_L^o(0) \end{pmatrix} \qquad (C.29)$$

where

$$R(x) \equiv e^{-N\sigma_r(x/\tau^2)} \begin{pmatrix} e^{-\ell/2} & \dfrac{2\pi i N\Lambda_s f_{21}(0)(e^{-\ell/2} - e^{-i\delta\ell})}{K_s(-i\delta + \frac{1}{2})} \\ 0 & e^{-i\delta\ell} \end{pmatrix}$$

$$(C.30)$$

The terms in $R(x)$ are defined as follows:

$\Lambda_s = \gamma\beta C\tau_s \equiv$ mean decay length of the K_s,

$\delta \equiv K_s^o - K_L^o$ mass difference described earlier,

$\sigma_T \equiv$ total cross section in material averaged between K^o

and $\overline{K}^o$,

$\ell = X/\Lambda_s \equiv$ distance traversed by K in units of K_s mean

decay length,

$K_s = p_{K_s}/h \equiv$ wave number of K_s,

$N \equiv$ number of nuclei per unit volume of material,

$f_{21}(0) = 1/2 \ (f_K(0) - f_{\overline{K}}(0)) \equiv$ forward regeneration

amplitude of the nucleus of the material.

D. Sinclair[66] has applied these formulae specifically to

heavy freon (CF_3Br) by replacing $Nf_{21}(0)$ by $\Sigma\ N_j[f_{21}(0)]_j$

where the sum is over the different elements in the material.

Then putting in the initial condition

$$K_s^o(0) = K_L^o(0) = \frac{K(0)}{\sqrt{2}}$$

$$(C.31)$$

in equation (C.29), we have

$$K_S^o(x) = \frac{K(0)}{\sqrt{2}} [R_{11}(x) + R_{12}(x)] \quad . \qquad (C.32)$$

The resulting K_S^o intensity is given by

$$I_S(x) = |K_S^o(x)|^2 = \frac{I(0)}{2} [R_{11}(x)^2 + R_{12}(x)^2$$

$$+ 2Re\, R_{11}(x)\, R_{12}(x)] \quad . \qquad (C.33)$$

Since $|R_{12}(x)|^2$ is of order 10^{-4} it may be neglected and

$$I_S(x) = \frac{I(0)}{2} e^{-N\sigma_T x} \left[e^{-\ell} + \frac{4\pi N \Lambda_S\, f_{21}(0)}{K_S(\delta^2 + \frac{1}{4})^{1/2}} \right.$$

$$\left. x\, (e^{-\lambda} \cos\theta - e^{-\ell/2} \cos(\theta - \delta \ell)) \right] \quad . \, (C.34)$$

Following Sinclair's notation

$$\frac{4\pi N \Lambda_S\, |f_{21}(0)|}{K_S(\delta^2 + \frac{1}{4})^{1/2}} \rightarrow \frac{4\pi \Lambda_S}{K_S(\delta^2 + \frac{1}{4})^{1/2}} \left[N_C |f_{21}(0)|_C \right.$$

$$\left. + N_F |f_{21}(0)|_F + N_{Br} |f_{21}(0)|_{Br} \right]$$

and θ in (C.34) is defined as

$$\theta = \theta_{SL} + \frac{3\pi}{4}$$

where θ_{SL} is the phase of the regeneration amplitude. Upon substitution of numerical factors*

$$I_s(x) = \frac{I(0)}{2} e^{-N\sigma_T x} [e^{-\ell} + 3.6 \times 10^{-2}$$

$$x (e^{-\ell} \cos \theta - e^{-\ell/2} \cos (\theta - \delta\ell))] \quad . \quad (C.35)$$

Upon integrating (C.35) over our fiducial volume we can determine the correction to our K_S° sample for different values of the regeneration phase θ_{SL}. We estimate that this correction may result in as much as a 4.2% enhancement or reduction over the corresponding number of K_S° in vacuum and, although this factor does not affect our charged to neutral ratio directly, it does affect our K_S° / K_L° ratio.

2.2 Incoherent Regeneration

Incoherent regeneration arises since the cross section for K°-nucleus and $\overline{K^\circ}$-nucleus are different. The amplitude for scattering of the K_S° (per scattering center) is

$$\psi_{sc}(\theta,x) = \frac{1}{\sqrt{2}} [f_K(\theta) K(x) + f_{\overline{K}}(\theta) \overline{K}(x)] \quad . \quad (C.36)$$

Solving (C.29) for $K_S^\circ(x)$ and $K_L^\circ(x)$ and using the states

---

*D. Sinclair extrapolates between measurements given in Christenson et al.[65] and estimates errors at ~ 30%.

$$K(x) = \frac{1}{\sqrt{2}} [K_S(x) + K_L(x)]$$

$$\overline{K}(x) = \frac{1}{\sqrt{2}} [K_S(x) - K_L(x)]$$

equation (C.36) becomes

$$\psi_{sc}(\theta) = [f_{22}(\theta)(R_{11}|K_S(0)\rangle + R_{12}|K_L(0)\rangle)$$

$$+ f_{21}(\theta) R_{22}|K_L(0)\rangle]$$

$$\psi_{sc}(\theta,x) = [f_{22}(\theta)|K_S(x)\rangle + f_{21}(\theta)|K_L(x)\rangle]$$

where $f_{21}(\theta)$ is as defined before and

$$f_{22}(\theta) = \frac{1}{2} [f_K(\theta) + f_{\overline{K}}(\theta)] \quad .$$

Thus the intensity of scattered K_S is

$$I_S(\theta,x) = |\psi_{sc}(\theta)|^2 = N_{sc} \Big\{ |f_{22}(\theta)|^2 ||K_S(x)\rangle|^2$$

$$+ |f_{21}(\theta)|^2 ||K_L(x)\rangle|^2$$

$$+ 2\text{Re } f_{22}(\theta) f_{21}(\theta) \langle K_L^*(x)|K_S(x)\rangle \Big\} \quad .$$

We can remove the x-dependence by integrating over our fiducial volume

$$I_s(\theta) = \int_{\substack{Fid.\\Vol.}} I_s(\theta,x)\, dx = N_{sc}\left|f_{22}(\theta)\right|^2 N_s + \underbrace{N_{sc}\left|f_{21}(\theta)\right|^2 N_L}_{I_{Ls}}$$

$$+ 2N_{sc}\,Re\,f_{21}(\theta)\,f_{22}(\theta) \int \left\langle K_L^*(x)\,|K_s(x)\right\rangle dx$$

$$(C.37)$$

where N_{sc} is the total number of scattering centers, N_s the number of K_s^o, and N_L the number of K_L^o. The first term of (C.37) comes from scattering of the K_s intensity. The third term reflects the difference in cross section of K-nucleon and $\bar{K}$-nucleon and is insignificant when integrated over our fiducial volume. The second terms, however, come from regenerative scattering of the K_L intensity.

The quantity I_{Ls} can be calculated since every increment dx of the regenerator contributes at its end $(x = x_f)$ the following number of events per steradian

$$d\left(\frac{dN(\theta)}{d\Omega}\right) = N\left|f_{21}(\theta)\right|^2 e^{-(x_f-x)/\Lambda_s}\, dx \quad.$$

Upon integrating over our fiducial volume

$$I_{Ls} = N\Lambda_s(1.0 - e^{-6.0})N_L \int \left|f_{21}(\theta)\right|^2 d\Omega \quad.$$

The quantity $\left|f_{21}(\theta)\right|^2$ is, as of yet, undetermined in heavy freon; however, it can be approximated by a Gaussian[67]

$$\left|f_{21}(\theta)\right|^2 = \frac{d\sigma(\theta)}{d\Omega} \approx \frac{\sigma_o}{\sqrt{2\pi}\delta} e^{-\theta^2/2\delta^2} \quad .$$

We can then roughly determine the parameters σ_o and δ by demanding that at $\theta = 0$ we have $\left|f_{21}(0)\right|^2$ as given from the earlier discussion on coherent regeneration ($\left|f_{21}(0)\right|^2_{CF_3Br} \cong$ .58 x 10^{-24} cm^2)*, while at $\theta = \pi$ we let $\left|f_{21}(\pi)\right|^2$ be essentially $O(\left|f_{21}(\pi)\right|^2 \approx 1 \ \mu\text{barn})$. Under these conditions we find

$$\frac{d\sigma(\theta)}{d\Omega} \cong (.58 \times 10^{-24}) \ e^{-12.5\theta^2/\pi^2}$$

so that our expression for I_{Ls} becomes

$$I_{Ls} = 2\pi N \Lambda_s (.997) \ N_L (.58 \times 10^{-24}) \int e^{-12.5\theta^2/\pi^2} \sin \theta \ d\theta$$

$$= 1.95 \times 10^3 \int_o^\pi e^{-12.5\theta^2/\pi^2} \sin \theta \ d\theta$$

Thus this very crude approximation gives an estimate of 800 events due to incoherent K_L^o regeneration. This number is only a factor of three from the visual estimate of 250 events determined at the end of Chapter III. This discrepancy no doubt comes from the assumptions we have made to determine the parameters σ_o and δ in the Gaussian approximation, compounded

---

*We emphasize the fact that this is an extremely crude estimate since it is most likely that $\left|f_{21}(\theta)\right|^2$ is highly peaked at $0°$ and thus diverges from the Gaussian approximation.

by the approximation itself.

3. K_S^o-K_L^o INTERFERENCE

Since it is now known that K_L^o can decay into $\pi^+\pi^-$ and

$\pi^o\pi^o$ channels, constructive interference between $K_L^o \to 2\pi$

and $K_S^o \to 2\pi$ amplitudes may become an important factor

depending on the phase angle $\varphi_{+-} = \arg(\eta_{+-})$.
$\qquad\qquad\qquad\qquad\qquad\qquad\qquad\quad (oo)\qquad\quad (oo)$

If we have a choherent superposition of K_L^o and K_S^o

states in the form

$$|K^o\rangle = \frac{1}{\sqrt{1+\rho^2}} \left[|K_L^o\rangle + \rho|K_S^o\rangle \right] \qquad (C.38)$$

where ρ is a complex constant* characteristic of the regener-

ative properties of the material at hand. If we take the

eigenstates derived in the last section

$$|K_L(t)\rangle = \exp\left[-i(m_L - i\frac{\Gamma_L}{2})t\right] |K_L(0)\rangle$$

$$|K_S(t)\rangle = \exp\left[-i(m_S - i\frac{\Gamma_S}{2})t\right] |K_S(0)\rangle$$

then the time dependence of $K^o \to \pi^+\pi^-$ is given by

---

*P.K. Kabir[57], pp. 66-78. Explicitly $\rho = r(1 - e^{-(\gamma'+im')})$
where $\gamma' = \gamma_S - \gamma_L$ is the width of the eigenstates of K_S and
K_L in the material, $m' = m_S - m_L$ is the mass difference in
the material, and r accounts for the difference in cross
section between K^o and $\overline{K^o}$.

$$I_{+-}(t) = \left| e^{-i(m_L - i\Gamma_L/2)t} \langle \pi^+\pi^- |T| K_L \rangle \right.$$

$$\left. + \rho\, e^{-i(m_s - i\Gamma_s/2)t} \langle \pi^+\pi^- |T| K_s \rangle \right|^2$$

$$I_{+-}(t) \propto |\eta_{+-}|^2 e^{-\Gamma_L t} + |\rho|^2 e^{-\Gamma_s t}$$

$$+ 2|\eta_{+-}\rho|\, e^{-(\Gamma_L + \Gamma_s)t/2} \cos(\Delta mt - \varphi_{+-} + \varphi_\rho) \ .$$

$$(C.39)$$

Since $|\eta_{+-}|^2$ is on the order of 10^{-6}, we can ignore this term so that the integrated intensity for the $\pi^+\pi^-$ channel, assuming $\varphi_\rho \cong 0$, is

$$R_{+-} = \int_0^T I_{+-}(t)\, dt \cong \frac{|\rho|^2}{\Gamma_s}(1 - e^{-\Gamma_s T}) + \frac{2|\eta_{+-}\rho|}{\Gamma'^2 + (\Delta m)^2}$$

$$\times \left\{ \cos\varphi_{+-} \left[e^{-\Gamma'T}(\Delta m \sin(\Delta mT) - \Gamma' \cos(\Delta mT)) + \Gamma' \right] \right.$$

$$\left. - \sin\varphi_{+-} \left[e^{-\Gamma'T}(\Gamma' \sin(\Delta mT) + \Delta m \cos(\Delta mt)) - \Delta m \right] \right\}$$

$$(C.40)$$

where $\Gamma' = (\Gamma_L + \Gamma_S)/2$. Experimentally it has been shown that $\Delta m \approx \Gamma' \approx \Gamma_S/2 \equiv \Gamma'_S$, in which case

$$R_{+-} = \frac{1}{\Gamma'_S} \left[\frac{|\rho|^2}{2} (1 - e^{-2\Gamma'_S T}) + |\eta_{+-}\rho| \right.$$

$$\times \left\{ \cos \varphi_{+-} \underbrace{\left[e^{-\Gamma'_S T} (\sin (\Gamma'_S T) - \cos (\Gamma'_S T)) + 1 \right]}_{\alpha} \right.$$

$$\left. \left. - \sin \varphi_{+-} \underbrace{\left[e^{-\Gamma'_S T} (\sin (\Gamma'_S T) + \cos (\Gamma'_S T)) - 1 \right]}_{\beta} \right\} \right] .$$

$$(C.41)$$

For future use we need to know when the interference term will contribute the most as a function of φ_{+-}. It can be shown that R_{+-} is maximum when

$$\varphi_{+-} = \tan^{-1} \left(\frac{-\beta}{\alpha} \right) \qquad (C.42)$$

with the secondary condition

$$\tan \varphi_{+-} < \frac{\alpha}{\beta} \qquad (C.43)$$

where α and β are defined in (C.41).

For the case $K^\circ \to \pi^\circ\pi^\circ$, one need only substitute the

amplitudes $\langle \pi^\circ \pi^\circ | T | K^\circ_S \rangle$ for $\langle \pi^+ \pi^- | T | K^\circ_S \rangle$ in equation (C.39).
We find $\quad\quad\quad\quad\quad$ (L) $\quad\quad\quad\quad\quad\quad\quad$ (L)

$$I_{oo}(t) \propto \left| \eta_{oo} \right|^2 e^{-\Gamma_L t} + \left| \rho \right|^2 e^{-\Gamma_S t}$$

$$+ 2 \left| \eta_{oo} \rho \right| e^{-(\Gamma_L + \Gamma_S) t/2} \cos \left(\Delta m t - \varphi_{oo} + \varphi_\rho \right) \quad .$$

APPENDIX D

$\pi\pi$ PHASE SHIFTS[*]

The pi-nucleon interaction is certainly one of the most studied aspects of experimental elementary particle physics. Unfortunately, due to several severe experimental problems, the determination of $\pi\pi$ phase shifts has not fully benfitted from these years of study. As pointed out by Gutay[68] at a recent conference on $\pi\pi$ and $K\pi$ interactions, the two major problems currently haunting the experimentalists are:

1. One must <u>extract</u> the $\pi\pi$ phase shifts from inelastic πN scattering where the effects of the $\pi\pi$ scattering are often clouded by other inelastic processes.

2. Since the reaction we must use

$$\pi + N \rightarrow N + (n\pi)$$
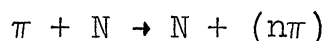
necessitates the involvement of a virtual pion, the angular distribution of the pions depends both on the effective mass of the dipion system <u>and</u> the square of the four-momentum transfer. Thus to extract the ℓth-wave contribution from background and absorption effects we must have knowledge of the $\pi\pi$ distribution as a function of four-momenta transfer squared (Δ^2) for each value of the dipion effective mass ($\sqrt{S}$).

---

[*]Much of the material in the first part of this resume comes from a paper delivered by L. J. Gutay at the recent Argonne Conference on $\pi\pi$ and $K\pi$ Interactions.

Gutay estimates that these restrictions demand more
than 50,000 events in the $N\pi\pi$ final state at any
single beam momenta; hence statistics are a problem.
Because of these difficulties all experiments to date have
used simplifying arguments to analyze the data. While the
resulting phase shifts are consistent for $I > 0$ channels, the
results for the s-wave zero isospin phase shift are as varied
as the methods used to obtain them.

1. THEORY

1.1 Partial Wave Analysis of $\pi\pi$ Elastic Interactions

The phase shifts themselves arise as a necessary param-
eter in the partial wave analysis of any given interaction
since the scattering process changes not only the amplitude
but the phase of the outgoing wave. Briefly, the principle
used is to construct asymptotic solutions to the wave equation
in regions far from the point of scatter so that the particle
wave functions (ψ) obey

$$\nabla^2 \psi + k^2 \psi = 0 \qquad\qquad (D.1)$$

where k is the momentum of the scattered particle. Following
the usual procedure[69] the asymptotic form of the scattered
wave is found to be

$$\psi_{sc} = \frac{1}{\sqrt{V}} f(\theta) \frac{e^{ik\pi}}{r} \qquad\qquad (D.2)$$

where V is the velocity of the particles and $f(\theta)$ is the scattering amplitude given by

$$f(\theta) = \sum_{\ell=0}^{\infty} (2\ell + 1) \, f_\ell \, P_\ell^0(\theta) \quad . \qquad (D.3)$$

In this last expression f_ℓ is usually referred to as the scattering function and is dependent on the phase shift in the form

$$f_\ell = \frac{\sin \delta_\ell \, e^{i\delta_\ell}}{k} \quad . \qquad (D.4)$$

We can easily apply this method to obtain the $\pi\pi$ phase shifts if we assume the following two things. First we assume that all pions are on the mass shell, while secondly we assume that all $\pi\pi$ interactions are elastic. Although the Chew-Low extrapolation technique has shown these assumptions ultimately unnecessary (at least for reactions dominated by single pion exchange), assuming them at this early stage facilitates the theoretical description of $\pi\pi$ scattering. Expressions (D.2)-(D.4) give a total description of the scattered wave function in "momentum-space"; however, to accommodate the various charge combinations of two pions it becomes convenient to introduce "iso-space" wave functions that are eigenstates of the total isospin. Using methods described earlier in Chapter I and Appendix C, we can construct the various 2π states to be

$(|I, I_3\rangle)$

$$|\pi^+\pi^-\rangle = |2,2\rangle \tag{D.5a}$$

$$|\pi^+\pi^o\rangle = \frac{1}{\sqrt{2}} [|2,1\rangle + |1,1\rangle] \tag{D.5b}$$

$$|\pi^-\pi^o\rangle = \frac{1}{\sqrt{2}} [|2,-1\rangle + |1,-1\rangle] \tag{D.5c}$$

$$|\pi^+\pi^-\rangle = \frac{1}{\sqrt{6}} |2,0\rangle + \frac{1}{\sqrt{2}} |1,0\rangle + \frac{1}{\sqrt{3}} |0,0\rangle \tag{D.5d}$$

which are the most often observed dipion states in the reaction

$$\pi^\pm p \rightarrow N\pi\pi \quad . \tag{D.6}$$

Combining the concept of isospin with the earlier constructed angular momentum states, equation (D.3) becomes

$$f^I(\theta) = \sum_{\ell=0}^{\infty} (2\ell + 1)[1 + (-1)^{I+\ell}] f_\ell^I P_\ell(\theta) \tag{D.7}$$

where now

$$f_\ell^I = \frac{\sin \delta_\ell^I \, e^{i\delta_\ell^I}}{k} \tag{D.8}$$

and k and θ are specifically the pion momentum and the scattering angle in the dipion rest frame. Using (D.7) and (D.8)

we can now construct the scattering amplitude for any 2π state following the isostate mixing as given in (D.5a-d). For example

$$f_{|\pi^+\pi^-\rangle}(\theta) = \frac{1}{k} \sum_{\ell=0}^{\infty} (2\ell + 1) \left\{ \frac{1}{6} e^{i\delta_\ell^2} \sin \delta_\ell^2 [1 + (-1)^\ell] \right.$$

$$+ \frac{1}{2} e^{i\delta_\ell^1} \sin \delta_\ell^1 [1 - (-1)^\ell]$$

$$+ \left. \frac{1}{3} e^{i\delta_\ell^0} \sin \delta_\ell^0 [1 + (-1)^\ell] \right\} P_\ell(\theta) \ . \quad \text{(D.9)}$$

Since we are primarily interested in the region $\sqrt{S} = m_{K^0}$ we may take advantage of the observation[70] that for energies such that $\sqrt{S} < m_\rho$ only the first two partial waves ($\ell = 0,1$) make any significant contribution. In this approximation the differential cross section obtained from (D.9) becomes

$$\frac{d\sigma}{d\Omega}(\theta)\bigg)_{\pi^+\pi^-} = \frac{1}{q^2} \left\{ (9 \sin^2 \delta_1^1) \cos^2 \theta \right.$$

$$+ 2[\cos (\delta_0^2 - \delta_1^1) \sin \delta_0^2 \sin \delta_1^1$$

$$+ 2 \cos (\delta_0^0 - \delta_1^1) \sin \delta_0^0 \sin \delta_1^1] \cos \theta$$

$$+ \frac{4}{9} [\sin^2 \delta_o^o + \cos (\delta_o^o - \delta_o^2) \sin \delta_o^o \sin \delta_o^2$$

$$+ \frac{\sin^2 \delta_o^2}{4}]\}} \quad . \qquad \qquad (D.10)$$

There are, of course, other representations than that used here. It has been shown that the differential cross section may be expressed in terms of density matrix elements as done by Jacob and Wick[71] or Csonka and Gutay[72].

1.2 The Chew-Low Extrapolation: One-Pion Exchange

Thus life would certainly be simple if pion targets were available and $\pi\pi$ elastic scattering dominated over a wider range of center-of-mass energies. Unfortunately such pion targets are not yet available. Because of these obvious limitations Goebel[73] and later Chew and Low[74] formulated a technique whereby $\pi\pi$ elastic scattering information could be extracted from higher energy inelastic πN scattering data. Basically, if one assumes that the process $\pi N \rightarrow N\pi\pi$ contains a one-pion exchange contribution then by extrapolating the observed cross sections to the unphysical point $\Delta^2 = m_\pi^2$ we obtain the $\pi\pi$ scattering amplitude. In theory this can be done with confidence since the extrapolation need be carried out over a relatively short distance $(m_\pi^2 = 0.02 \text{ GeV}^2/c^2)$. The relevant formulae can be derived from the one-pion exchange diagram (Figure 24). The contribution of this diagram to the
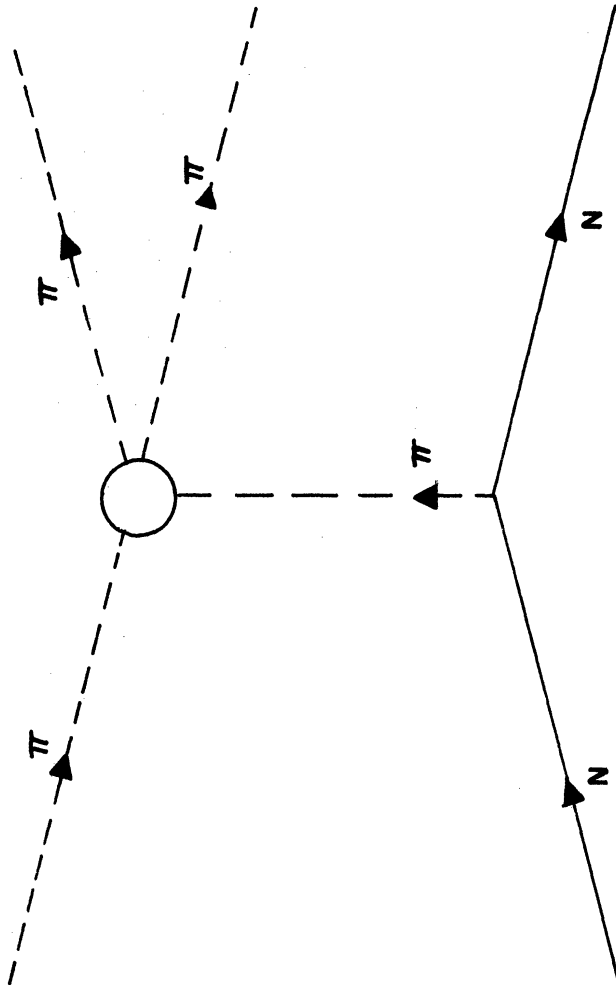
Figure 24. Standard one-pion exchange diagram for reaction
$\pi + n \rightarrow N + \pi + \pi$.

angular distribution of reaction (D.6) is found to be[75]

$$\frac{d^2\sigma(S_o, \Delta^2)}{d\Delta^2 dS_o} = - \frac{S_o^2 \Delta^2}{4\pi p_i^2 S} \frac{p_e g^2}{(\Delta^2 - m_\pi^2)^2} \sigma_{\pi^-\pi^+}(S_o, \Delta^2) F_{N\pi}^2(\Delta^2)$$

where $S_o \equiv \pi^-\pi^+$ rest mass, $p_i \equiv$ cm momentum of initial state, $p_e \equiv$ momentum of the exchanged pion and $g^2 \equiv N\pi p$ coupling constant. We are then left with two unknowns: $\sigma_{\pi^-\pi^+}(S_o, \Delta^2) \equiv$ the cross section for $\pi^-\pi^+ \to \pi^-\pi^+$ with one of the incoming pions being virtual and $F_{N\pi p}(\Delta^2) \equiv$ the "pionic" form factor of the nucleon. These must be "extrapolated".

1.3 Durr-Pilkuhn and Benecke-Durr Parameterization

The result of Chew-Low extrapolation which we have briefly described in the last section is strongly dependent on the choice of extrapolation function. Of the various types of extrapolation functions[76] the "linear" and the "quadratic" functions are those most often used by experimentors, and it has been found[77] that both functions fit the same data (for certain reactions) equally well yet yield widely variant extrapolated cross sections. Moreover Schlein et al.[78] has described a case where neither of the functions gives the correct result. Because of these ambiguities Durr and Pilkuhn[79] and recently Benecke and Durr[80] have proposed parameterization methods which relate off-shell to on-shell cross sections. The results have been quite reliable when the Benecke-Durr

vertex correction factors are combined with the Chew-Low one-pion exchange model extrapolation techniques.

1.4 Model Dependent Predictions

In Appendix C, Section 1, it was shown how the phase shifts δ°_o and δ^2_o enter the transition matrix elements for $K^\circ_S \to \pi^\circ + \pi^\circ$ and $K^\circ_S \to \pi^+ + \pi^-$. Since these are the only phase shifts which enter this particular analysis we will describe the application of current algebra and Veneziano techniques with emphasis on the derivation of these quantities.

1.4a Current Algebra Techniques[*]

There are two types of analysis that have been applied to $\pi\pi$ scattering. The first method involves the "soft-pion" calculations of Weinberg[81] and is based on four assumptions:

1. Conserved Vector Current (CVC) hypothesis.

2. The Partially Conserved Axial-Vector Current (PCAC) hypothesis.

3. Both vector and axial vector currents obey SU2SU2 equal time commutators.

4. A dynamical postulate restricting the change in the scattering amplitude if one restricts the pion momentum to zero, the "gentleness" hypothesis.

In addition Weinberg made an additional assumption concerning the nature of a particular commutator which when combined with

---

[*]As summarized by R. Arnowitt at the Conference on $\pi\pi$ and $K\pi$ Interactions, Argonne National Laboratory, 1969.

the first four assumptions led to a set of s- and p-wave scattering lengths. The second method was initiated in hopes of correcting errors introduced by the "gentleness" hypothesis of the soft-pion model. This new model, labeled the hard-pion method, substitutes the concept of vector dominance[82] for assumption number four. Weinberg's fifth hypothesis was modified only to the extent that it was made less stringent. The "hard-pion" results are simply the soft-pion calculations modified by a factor which represents the breakdown of Weinberg's "gentleness" hypothesis.

Arnowitt et al.[83] have performed hard-meson calculations at energies comparable to the K° mass. They have found that the scattering amplitude depends upon $\sim m_{\sigma}$ and Γ_{σ} which they set at $m_{\sigma} \cong 730$ MeV and $\Gamma_{\sigma} \cong 200$ MeV to obtain the best fit. With these parameters, the difference in phase shifts at the K° mass is found to be $\delta^{\circ}_{o} - \delta^{2}_{2} = (35 \pm 4)^{\circ}$.

1.4b   Veneziano Partial Wave Technique[84]

Lovelace[85] has proposed the following Veneziano representation for the $\pi\pi$ s-wave elastic amplitudes

$$A_I = A_o = \frac{1}{2} F(t,u) - \frac{3}{2} [F(s,t) + F(s,u)] \quad , \qquad \text{(D.11a)}$$

$$A_1 = F(s,u) - F(s,t) \quad , \qquad \text{(D.11b)}$$

$$A_2 = -F(t,u) \quad , \qquad \text{(D.11c)}$$

where

$$F(x,y) = \beta \frac{\Gamma(1 - \alpha(x)) \cdot \Gamma(1 - \alpha(y))}{\Gamma(1 - \alpha(x) - \alpha(y))}$$

$$+ \gamma \frac{\Gamma(1 - \alpha(x)) \cdot \Gamma(1 - \alpha(y))}{\Gamma(2 - \alpha(x) - \alpha(y))} + \ldots \qquad (D.12)$$

and

$$\alpha(x) = a + bx \quad . \qquad (D.13)$$

In general, the weakness of the Veneziano partial wave analysis is the failure of $V_I(v)$--the partial wave projections-- to satisfy unitarity. Tryon[86] has recently proposed a modification of $V_I(v)$ such that the new $V_I(v)$ satisfy unitarity. Using the modified Veneziano partial wave projections and keeping only the first term of the Veneziano series (D.12) phase shifts have been computed by Tryon. The quantities a and b of expression (D.13) are the Regge parameters determined by Lovelace[85] to be a = 0.483 and b = 0.017. Tryon has found two different solutions corresponding to the two indicated possible values for m_σ. In the last section a current algebra analysis showed m_σ = 730 MeV. Using this value the Veneziano model predicts a phase shift difference $\delta_o^2 - \delta_o^o =$ (59 ±10)°. Another value of m_σ equally probable in the analysis has m_σ = 900 MeV which yields a difference in phase shifts of $\delta_o^2 - \delta_2^o$ = (61 ±4)°. Thus, independent of the final

value for m_σ the value of $\delta_o^2 - \delta_o^o$ from Veneziano techniques lies in the range $(59 \pm 10)°$. Figure 25 compares δ_o^o as a function of s as predicted by Arnowitt (current algebra) and Tryon (Veneziano).

2. EXPERIMENTAL TECHNIQUES

There have been literally dozens of experiments carried out to measure, either directly or indirectly, the $\pi\pi$ phase shifts. Even though each experiment may have some small difference to separate its method from other experiments it would be unnecessary to describe all experiments since there are only a few basic types of experiments. Also, with the exception of Malamud and Schlein all experimental values of δ_2^2 have fallen in the range of -5 to -10 degrees while (preferred) values of δ_o^o have ranged all the way from[42] $(23 \pm 10)°$ to slightly over $50°$. Thus, as representative of the whole class of experiments we will describe the experimental determination of both δ_o^o and δ_o^2 by Malamud and Schlein, the experimental determination of δ_o^o by Hagopian et al. and Scharenguivel et al., anf finally the values of δ_o^2 as determined by Morese et al. and Baton and Laurens. Though in some cases the determination of the phase shifts was only a small part of the total experiment, we will concentrate only on that part of the analysis necessary for obtaining δ_o^o and/or δ_o^2.

2.1 δ_o^o and δ_o^2 - E. Malamud and P. Schlein
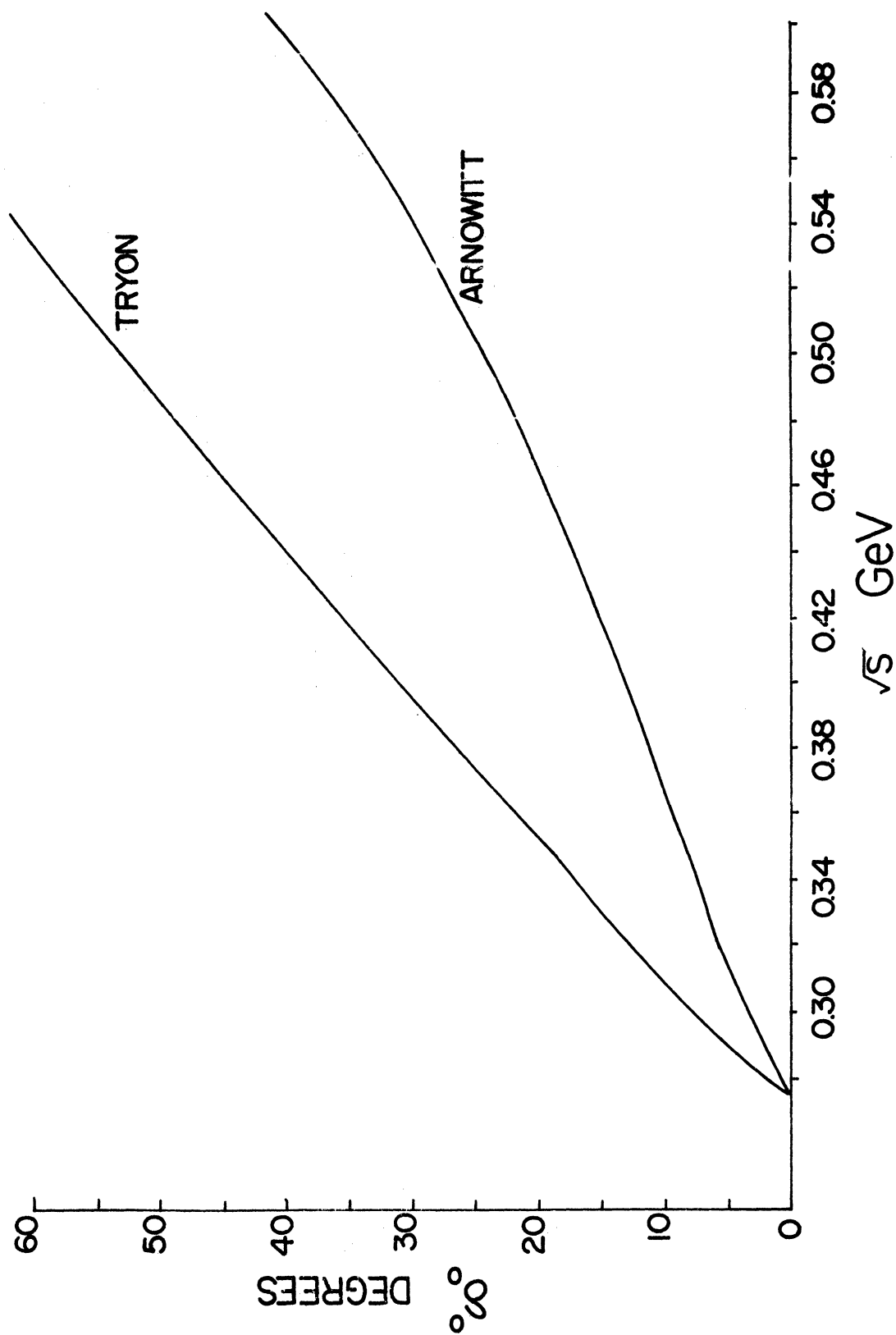
This analysis used a mass compilation of 12 previous

Figure 25. S-wave, isoscalar phase shift δ_0^0 as predicted by
current algebra (Arnowitt) and Veneziano (Tryon) techniques.
$\sqrt{S} \equiv \pi\pi$ effective mass.

experiments containing a sum total of 68,356 events distributed as follows:

$$\pi^- p \rightarrow \pi^- \pi^+ n \qquad\qquad 20{,}555 \text{ events} \qquad\qquad \text{(D.14a)}$$

$$\pi^- p \rightarrow \pi^- \pi^\circ p \qquad\qquad 14{,}536 \text{ events} \qquad\qquad \text{(D.14b)}$$

$$\pi^- p \rightarrow \pi^- \pi^- \pi^+ p \qquad\qquad 14{,}638 \text{ events} \qquad\qquad \text{(D.14c)}$$

$$\pi^+ p \rightarrow \pi^- \pi^+ \pi^+ p \qquad\qquad 18{,}627 \text{ events} \qquad\qquad \text{(D.14d)}$$

Malamud and Schlein determined δ°_o from reaction (D.14a), but before they could attempt this they had to determine a value for δ^2_o to use as input for the δ°_o determination. There are two ways to determine δ^2_o; either by examining s- and p-wave interference in the $\pi^- \pi^\circ p$ reaction or by extrapolation techniques in $\pi^- \pi^- \Delta^{++}$ or $\pi^+ \pi^+ n$. Malamud and Schlein argued against using the $\pi^- \pi^\circ p$ reaction for $m_{\pi\pi}$ less than m_ρ since there is increasing evidence for the dominance of ω exchange at these low energies which, of course, invalidates the one-pion exchange hypothesis. This increasing importance of ω exchange is particularly disastrous to interference analysis since it is suspected* that the $\pi\pi$ s-wave system results from π exchange while the $\pi\pi$ p-wave system is dominated by ω exchange. Thus, without knowledge of the phases of the ω- and

*The evidence supporting this suspicion is, however, by no means conclusive (Frank Heney, private communication). Thus the Baton et al. value of δ_0^2 can not be disregarded simply on the basis of this argument.

π-exchange components s- and p-wave interference can yield no information. In light of this Malamud and Schlein used a Durr-Pilkuhn modified one-pion exchange model in the pole extrapolation to obtain the value of δ_o^2 over the mass region considered.

In the vicinity of the K-mass the pole extrapolation of $\pi^- p \rightarrow \pi^- \pi^- \Delta^{++}$ yielded a value $\delta_o^2 = -(17 \pm 3)°$. Using this as input for the master fit described earlier it was found $\delta_o^o(m_K) = (41 \pm 5)°$. Hence $(\delta_o^o - \delta_o^2) = (58 \pm 6)°$.

2.2 δ_o^o - V. Hagopian, E. Bogart, S. Marateck, W. Selove

This experiment, as in the Malamud and Schlein analysis, used a compilation of data. From 11 previous experiments they obtained 26,872 $\pi^- p \rightarrow \pi^- \pi^+ n$ and 17,440 $\pi^- p \rightarrow \pi^- \pi^° p$ events. From analysis of these two reactions Hagopian et al. hoped to determine δ_o^o and δ_1^1.

Upon assuming that only s- and p-wave scattering contribute below 900 MeV they fit each angular distribution to

$$a_o + a_1 \cos \theta + a_2 \cos^2 \theta \qquad (D.15)$$

where θ is the angle between outgoing and incoming π^- in the dipion c.m. A new variable was defined, A_ℓ, such that extrapolation of this function would yield $\sigma_{\pi\pi}$. The function determined was

$$A_\ell = a_\ell \frac{(\Delta^2 + m_\pi^2)^2}{\Delta^2} \quad , \tag{D.16}$$

the a coming from (D.15). The extrapolated values found were

labeled B_ℓ, and they determined that the product $B_\ell u$, where

$$u = (\frac{\omega^2}{4} - m_\pi^2)^{1/2} (\frac{1}{\omega^2}) \quad , \tag{D.17}$$

is directly proportional to the phase shifts as follows (see

equation (D.10)).

$$B_0 u = \left[\frac{4}{9} \sin^2 \delta_0^0 + \frac{1}{9} \sin^2 \delta_0^2 \right.$$

$$\left. + \frac{4}{9} \cos (\delta_0^0 - \delta_0^2) \sin \delta_0^0 \sin \delta_0^2 \right] N \quad , \tag{D.18}$$

$$B_1 u = \left[4 \cos (\delta_0^0 - \delta_1) \sin \delta_0^0 \sin \delta_1 \right.$$

$$\left. + 2 \cos (\delta_0^2 - \delta_1) \sin \delta_0^2 \sin \delta_1 \right] N \quad , \tag{D.19}$$

$$B_2 u = \left[9 \sin^2 \delta_1 \right] N \quad , \tag{D.20}$$

where N is a normalization constant. δ_1 was determined

directly from $B_2 u$ and δ_0^0 was determined from the ratio of

$B_1 u$ to $B_2 u$ using as input the Baton and Laurens value of δ_0^2.

The resulting equation for δ_0^2 is quadratic so there are two

solutions for each $m_{\pi\pi}$. At the K° mass, using the Baton and Laurens value, $\delta_o^2 = -5^\circ$ they obtain $\delta_o^\circ = (23 \pm 10)^\circ$ and $(75 \pm 10)^\circ$ with the first quantity being preferred.

2.3 δ_o° - J. Scharenguivel, L. Gutay, D. Miller, F. Meiere, S. Marateck

This experiment differs from most others in that they investigate the forward-backward asymmetry in the dipion rest frame of the reaction $\pi^- p \to \pi^+ \pi^- n$ where the asymmetry is defined as

$$\alpha(S, \Delta^2) = \frac{\text{Forward} - \text{Backward}}{\text{Forward} + \text{Backward}} \qquad (D.21)$$

and then extrapolate (D.21) to obtain $\alpha(S, -m_\pi^2)$. In order to extrapolate, $\alpha(S, \Delta^2)$ was plotted at given S values and a moderate Δ^2 dependence was noted. It was found that a linear fit

$$\alpha(S, \Delta^2) = \beta(S) + \gamma(S)(\Delta^2 + m_\pi^2) \qquad (D.22)$$

was sufficiently accurate. To obtain $\alpha(S, -m_\pi^2)$, $\beta(S)$ and $\gamma(S)$ had to be determined. This was done using threshold arguments to determine $\beta(S)$ and current algebra constraints to fix $\gamma(S)$. Then using δ_o^2 as determined by Baton and Laurens and a previous determination of δ^1 by essentially the same group the value of δ_o° was determined for $M_{\pi\pi} \cong .26$ to $M_{\pi\pi} = .6$ GeV. It was found at the K mass that $\delta_o^\circ = (42 \, ^{+9}_{-11})^\circ$. Figure 26 shows

experimental values of δ_o^o.

2.4 δ_o^2 - Morse et al.[87]

This Wisconsin-Toronto collaboration analyzed the three

reactions

$$\pi^- p \rightarrow \pi^- \pi^- \Delta^{++}$$

$$\pi^- p \rightarrow \pi^- \pi^- \pi^+ \pi^- \Delta^{++}$$

$$\pi^- p \rightarrow \pi^- \pi^- \Delta^{++} + MM$$
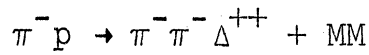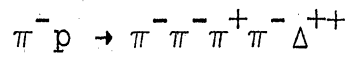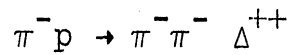
using both the standard Benecke-Durr (BD) modified Chew-Low

extrapolation and an s-wave modified Benecke-Durr calculation

as proposed by Olsson[88] (OBD). Whereas the BD model gives

$$q \, \sigma_\pi (m, \Delta^2) = \frac{u \, (q, \ldots)}{u \, (q_o, \ldots)} \, q_o \, \sigma_{\pi\pi}(m_{\pi\pi}) \qquad (D.23)$$

where q and q_o are the "off-shell" and "on-shell" momentum

and the u are modified Legendre functions of the second kind,

the OBD model gives

$$q \, \sigma_{\pi\pi}(m, \Delta^2) = \left(\frac{m_{\pi\pi}^2 + \Delta^2 - m_\pi^2}{m_{\pi\pi}^2 - 2m_\pi^2} \right) q_o \, \sigma_{\pi\pi}(m_{\pi\pi}) \, . \quad (D.24)$$

After cleaning the sample, $\sigma_{\pi\pi}$ was calculated over the mass

range 0.3-2.0 GeV, from which δ_0^2, δ_2^2, and δ_4^2 were extracted

for both the BD and OBD models. In the region of the K mass

we find their value of δ_0^2 to be $(-15.4 \pm 1.1)°$ using the BD

modification and $(-9.8 \pm .7)$ using the OBD model.

2.5 δ_0^2 - Baton and Laurens

This Saclay group used the reaction $\pi^- p \rightarrow \pi^- \pi^° p$ to

determine the I = 2 s-wave phase from $m_{\pi\pi} = .28$ to $m_{\pi\pi} = .8$

GeV. Note that this is the reaction that Malamud and Schlein

found inadequate for determining δ_0^2 (see Section 2.1). Fol-

lowing the standard extrapolation techniques they found that

in the region of the K-mass $\delta_0^2 = (-5 \pm 2)°$. Figure 27 compares

experimental values of δ_0^2.
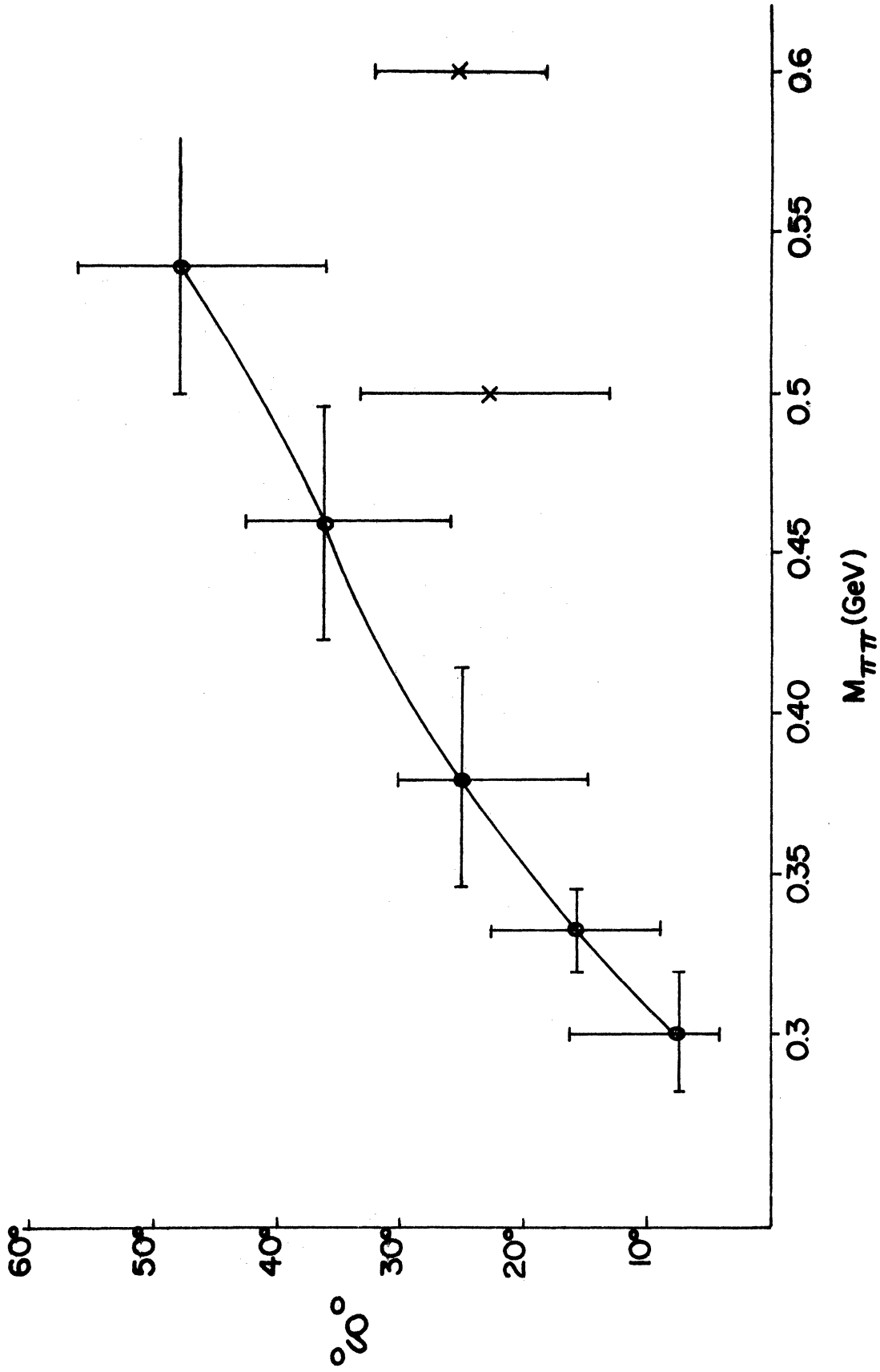
Figure 26. Experimental determination of δ° as a function of $M_{\pi\pi}$ by Scharenguivel et al. ($\vdash\!\!\!\circ\!\!\!\dashv$) and by Hagopian $^\circ$ et al. ($\mathbf{\bar{x}}$).
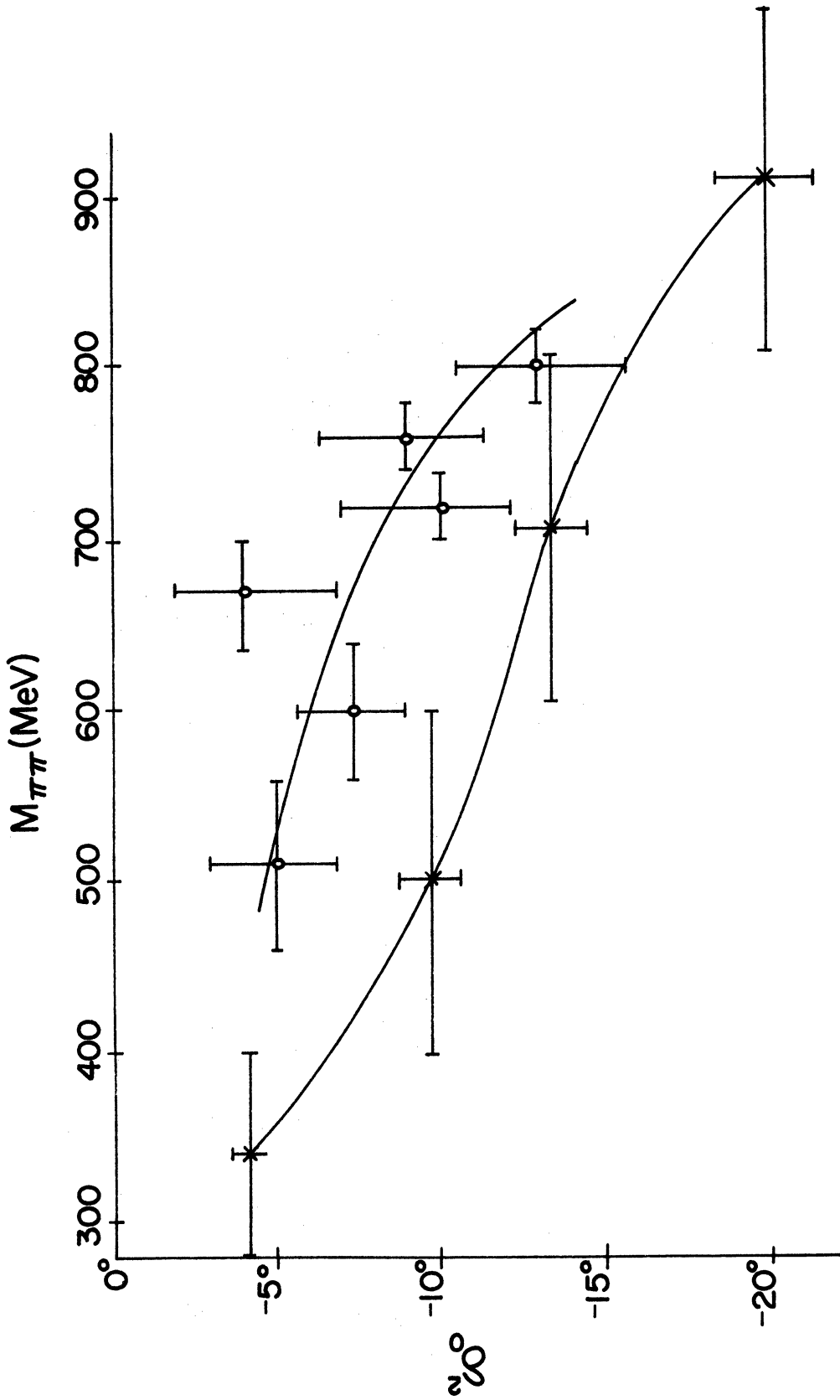
Figure 27. Experimental value of the I = 2 s-wave phase shift δ_2^0 as a function of $M_{\pi\pi}$ by Baton and Laurens ($\circ$) and Morse et al. ($*$). Curve fit to Baton and Laurens is our own approximation.

REFERENCES

1. M. Gell-Mann and A. Pais, Proceedings of the Glasgow Conference (Pergamon Press, London, 1954).

2. R. E. Marshak, Riazuddin, and Ryan, Theory of Weak Interactions in Particle Physics (John Wiley and Sons, Inc., New York, 1969).

3. E. F. Beall, B. Cork, D. Keefe, W. C. Murphy, and W. A. Wenzel, Phys. Rev. Letters 8, 75 (1962).

4. R. O. Bangerter, A. Barbaro-Galtieri, J. P. Berge, J. J. Murray, F. T. Solmitz, M. L. Stevenson, and R. D. Tripp, Phys. Rev. Letters 17, 495 (1966).

5. F. Harris, O. E. Overseth, E. Dettman, and L. G. Pondrom, Bull. of Am. Phys. Soc. 14, 519 (1969).

6. O. E. Overseth, Nonleptonic Weak Decay Processes, p. 12. Paper presented at International Conference on Symmetry and Quark Models at Wayne State University, Detroit, Michigan, 1969. (To be published by Gordon and Breach.)

7. N. Barash-Schmidt, A. Barbaro-Galtieri, L. R. Price, A. Rosenfeld, P. Soding, C. G. Wohl, M. Roos, and G. Conforto, Rev. Mod. Phys. 41, 109 (1969).

8. B. Aubert, Proceedings of the Topical Conference on Weak Interactions, p. 205 (CERN Report 69-7, 1969).

9. O. E. Overseth, pp. 3-5.

10. G. H. Trilling, Proceedings of International Conference of Weak Interactions, Argonne (ANL-7130, 1965).

11. T. J. Devlin, Phys. Rev. Letters 20, 683 (1968).

REFERENCES (Continued)

12. W. Heisenberg, Zeit. Physik $\underline{77}$, 1 (1932).

13. R. Hagedorn, <u>Relativistic Kinematics</u> (W. A. Benjamin, Inc., New York, 1963), p. 80.

14. F. Abbud, B. W. Lee, and C. N. Yang, Phys. Rev. Letters $\underline{18}$, 980 (1967).

15. G. Field and P. K. Kabir, <u>The Parameters of $K^\circ \to 2\pi$ Decay and the Magnitude of $Re(A_2/A_o)$</u>. Preprint (Rutherford High Energy Lab No. RL/K/10, n.d.). (To be published in Zeit. Physik.)

16. T. T. Wu and C. N. Yang, Phys. Rev. Letters $\underline{13}$, 180 (1964).

17. A. A. Belavin and I. M. Narodetsky, Phys. Letters $\underline{26B}$, 668 (1968).

18. P. Franzini, L. Kirsch, P. Schmidt, J. Steinberger, and R. J. Plano, Phys. Rev. $\underline{140}$, B127 (1965).

19. T. D. Lee and C. S. Wu, Ann. Rev. Nucl. Sci. $\underline{16}$, 528 (1966).

20. O. Nachtmen and E. de Rafael, <u>On Radiative Corrections to the $\Delta I = 1/2$ Rule in $K_S \to \pi^+\pi^-$ and $K_S \to \pi^\circ\pi^\circ$ Decays</u>. Preprint (CERN TH.1031, Geneva, 1969).

21. G. D. Rochester and C. C. Bulter, Nature Lond. $\underline{160}$, 855 (1947).

22. F. Eisler, R. Plano, N. Samios, M. Schwartz, and J. Steinberger, Nuovo Cimento $\underline{5}$, 1700 (1957).

23. B. Gobbi, D. Green, W. Hakel, R. Moffett, and J. Rosen,

REFERENCES (Continued)

Phys. Rev. Letters 22, 682 (1969).

24. F. S. Crawford, M. Cresti, Jr., A. L. Douglass, M. L.
     Good, G. R. Kalbfleisch, M. L. Stevenson, and H. K.
     Ticho, Phys. Rev. Letters 2, 266 (1959).

25. C. Baglin, M. Block, V. Bresson, J. Hennessy, A. Lagarrigue,
     P. Mittner, P. Musset, A. Orkin-Lecourtois, P. Rancon,
     A. Rousset, A. M. Sarius, X. Sauteron, and J. Six,
     Proceedings of the 1960 Annual Internation Conference on
     High Energy Physics at Rochester (Interscience Publishers,
     Inc., New York, 1960), p. 594.

26. J. L. Brown, H. C. Bryant, R. A. Burnstein, D. A. Glaser,
     R. Hartung, J. A. Kadyk, J. D. Van Putten, D. Sinclair,
     G. H. Trilling, and J. C. Vander Velde, Nuovo Cimento 19,
     1155 (1961).

27. J. Anderson, F. Crawford, B. Crawford, R. Golden, L.
     Lloyd, G. Meisner, and L. Price, Proceedings of the 1962
     International Conference on High Energy Physics at CERN
     (CERN, Geneva, 1962), p. 836.

28. J. L. Brown, J. A. Kadyk, G. H. Trilling, B. P. Roe,
     D. Sinclair, and J. C. Vander Velde, Phys. Rev. 130,
     769 (1963).

29. M. Chretien, V. Fischer, H. Cronch, R. Lanon, J. Massimo,
     A. Shapiro, J. Averell, A. Brenner, D. Firth, L. Hyman,
     M. Law, R. Milburn, E. Ronat-Pless, L. Rosenson, and
     G. Salandin, Phys. Rev. 131, 2208 (1963).

REFERENCES (Continued)

30. R. Green, University of Michigan Bubble Chamber Group Research Note No. 84/68, April 1968 (unpublished).

31. D. G. Falconer, Large-Angle Antiproton-Proton Elastic Scattering. Dissertation (University of Michigan Technical Report No. COO-1112-6, 1969), p. 298.

32. C. T. Murphy, University of Michigan Bubble Chamber Group Research Note No. 65/67, 1967 (unpublished).

33. The Complete SHAPE Manual, University of Michigan Bubble Chamber Group, Section VIII (unpublished).

34. E. Lee, University of Michigan Bubble Chamber Group Research Notes No. 54/66 and No. 55/66, 1966 (unpublished).

35. A. Bohm, P. Dariulat, C. Grosso, V. Kaftanov, K. Kleinknecht, H. L. Lynch, C. Rubbia, H. Ticho, K. Tittel, The Phase Difference Between $K_L \to \pi^+\pi^-$ and $K_S \to \pi^+\pi^-$ Decay Amplitudes. Preprint (CERN, Geneva, 1969). (To be published in Nulcear Physics.)

36. H. Faissner, Neutral Kaons and CP (PITHA-26, Aachen, 1968), p. 12.

37. G. Bozoki, E. Fenyves, E. Gombosi, E. Nagy, G. Suranyi, F. Telbisz, and T. Vesztergombi, Determination of the K_S Decay Branching Ratio. Preprint (Hungarian Academy of Sciences, Budapest, 1969).

38. L. J. Gutay, Proceedings of the Conference on $\pi\pi$ and $K\pi$ Interactions, F. Loeffler and E. Malamud, Editors (Argonne National Laboratory, Argonne, Illinois, 1969),

REFERENCES (Continued)

pp. 241-277.

39. D. D. Carmony, Proceedings of the Conference on $\pi\pi$ and $K\pi$ Interactions, F. Loeffler and E. Malamud, Editors (Argonne National Laboratory, Argonne, Illinois, 1969), pp. 27-54.

40. N. N. Biswas, Proceedings of the Conference on $\pi\pi$ and $K\pi$ Interactions, F. Loeffler and E. Malamud, Editors (Argonne National Laboratory, Argonne, Illinois, 1969), pp. 55-74.

41. E. Malamud and P. Schlein, Proceedings of the Conference on $\pi\pi$ and $K\pi$ Interactions, F. Loeffler and E. Malamud, Editors (Argonne National Laboratory, Argonne, Illinois, 1969), pp. 93-130.

42. V. Hagopian, E. Bogart, S. Marateck, and W. Selove, Proceedings of the Conference on $\pi\pi$ and $K\pi$ Interactions, F. Loeffler and E. Malamud, Editors (Argonne National Laboratory, Argonne, Illinois, 1969), pp. 149-178.

43. D. Cline, K. J. Braun, and V. R. Scherer, Proceedings of the Conference on $\pi\pi$ and $K\pi$ Interactions, F. Loeffler and E. Malamud, Editors (Argonne National Laboratory, Argonne, Illinois, 1969), pp. 179-216.

44. J. H. Scharenguivel, L. J. Gutay, D. H. Miller, F. T. Meiere, and S. Marateck, Experimental Low Mass S-Wave $\pi\pi$ Phase Shifts Consistent with the Off-Mass-Shell Dependence of Current Algebra. Preprint (Purdue University, No. COO-1428-154, Lafayette, Indiana, 1969).

REFERENCES (Continued)

45. D. H. Saxon, J. H. Mulvey, and W. Chinowsky, Proceedings of the Conference on $\pi\pi$ and Kπ Interactions, F. Loeffler and E. Malmud, Editors (Argonne National Laboratory, Argonne, Illinois, 1969), pp. 316-325.

46. J. P. Baton and G. Laurens, Proceedings of the Conference on $\pi\pi$ and Kπ Interactions, F. Loeffler and E. Malamud, Editors (Argonne National Laboratory, Argonne, Illinois, 1969), pp. 131-148.

47. W. M. Katz, T. Ferbel, P. F. Slattery, and H. Yuta, Proceedings of the Conference on $\pi\pi$ and Kπ Interactions, F. Loeffler and E. Malamud, Editors (Argonne National Laboratory, Argonne, Illinois, 1969), pp. 300-305.

48. G. A. Smith and R. J. Manning, $\pi^\circ\pi^\circ$ Mass Spectrum and δ_0° Below One GeV. Preprint (Michigan State University, East Lansing, Michigan, 1969).

49. R. Arnowitt, Proceedings of the Conference on $\pi\pi$ and Kπ Interactions, F. Loeffler and E. Malamud, Editors (Argonne National Laboratory, Argonne, Illinois, 1969), pp. 619-647.

50. E. P. Tryon, Veneziano Versus Partial Wave Dispersion Relations: A Unitary, Crossing Symmetric Synthesis and the $\pi\pi$ Phase Shifts. Preprint (Columbia University No. NYO-1932(2)-153).

51. J. H. Christenson, J. W. Cronin, V. L. Fitch, and R. Turlay, Phys. Rev. Letters 13, 138 (1964).

REFERENCES (Continued)

52. G. Luders, Ann. Phys. $\underline{2}$, 1 (1957).

53. R. C. Casella, Phys. Rev. Letters $\underline{21}$, 1128 (1968).

54. R. C. Casella, Phys. Rev. Letters $\underline{22}$, 554 (1969).

55. R. C. Casella, Direct Tests of Time Reversal Invariance in the Decays K° to Two Pions. Paper presented at the Third Hawaii Topical Conference in Particle Physics, Honolulu, Hawaii, 1969.

56. J. S. Bell and J. Steinberger, Proceedings of Oxford International Conference on Elementary Particles (Oxford, Chilton, England, 1966).

57. P. K. Kabir, The CP Puzzle (Academic Press, London, 1968), p. 49.

58. D. Sinclair, University of Michigan Bubble Chamber Group Research Notes No. 79/68 and No. 80/68, 1968 (unpublished).

59. V. F. Weisskopf and E. P. Wigner, Zeit. Physik $\underline{63}$, 54 (1930) and Zeit. Physik $\underline{65}$, 18 (1932).

60. G. Breit and I. S. Lowen, Phys. Rev. $\underline{46}$, 590 (1934).

61. G. Kallen, Handbuch der Physik (Springer Verlag, Berlin, 1958), Vol. I, p. 274.

62. P. K. Kabir, pp. 99-105.

63. T. D. Lee, R. Oehme, and C. N. Yang, Phys. Rev. $\underline{106}$, 340 (1957).

64. A. Pais and O. Piccioni, Phys. Rev. $\underline{100}$, 1487 (1955).

65. J. H. Christenson, J. W. Cronin, V. L. Fitch, and R. Turlay, Phys. Rev. $\underline{140}$, B74 (1965).

REFERENCES (Continued)

66. D. Sinclair, University of Michigan Bubble Chamber Group
    Research Note No. 1/69, 1969 (unpublished).

67. H. Faissner, p. 48.

68. L. J. Gutay, pp. 241-242.

69. H. Muirhead, The Physics of Elementary Particles (Pergamon
    Press, New York, 1965), pp. 234-246.

70. J. P. Baton and J. Regnier, Nuovo Cimento $\underline{36}$, 1149
    (1965); P. E. Schlein, Phys. Rev. Letters $\underline{19}$, 1052
    (1967); E. Malamud and P. E. Schlein, Phys. Rev. Letters
    $\underline{19}$, 1056 (1967).

71. M. Jacob and G. C. Wick, Ann. Phys. $\underline{7}$, 404 (1959).

72. P. L. Csonka and L. J. Gutay, UCRL-50101 (1966).

73. C. Goebel, Phys. Rev. Letters $\underline{1}$, 337 (1958).

74. G. F. Chew and F. E. Low, Phys. Rev. $\underline{113}$, 1640 (1959).

75. G. Wolf, Proceedings of the Conference on $\pi\pi$ and $K\pi$
    Interactions, F. Loeffler and E. Malamud, Editors
    (Argonne National Laboratory, Argonne, Illinois, 1969),
    p. 690.

76. J. Naisse and J. Reignier, Fortschritte der Physik $\underline{12}$,
    523 (1964).

77. J. P. Baton, G. Laurens, and J. Reignier, Phys. Letters
    $\underline{25B}$, 419 (1967); Z. Ming Ma, G. A. Smith, R. J. Sprafka,
    E. Colton, and P. E. Schlein, preprint (University of
    California No. UCLA-1030, 1968).

78. P. E. Schlein, Report UCLA-1029 (1968).

REFERENCES (Concluded)

79. H. P. Durr and H. Pilkuhn, Nuovo Cimento 40, 899 (1965).

80. J. Benecke and H. P. Durr, Nuovo Cimento 56, 269 (1968).

81. S. Weinberg, Phy. Rev. Letters 17, 616 (1966).

82. M. Gell-Mann and F. Zachariasen, Phy. Rev. 124, 953 (1961).

83. R. Arnowitt, M. H. Friedman, P. Nath, and R. Suitor, Phys. Rev. Letters 20, 475 (1968); Phys. Rev. 175, 1820 (1968).

84. C. Lovelace, Proceedings of the Conference on $\pi\pi$ and Kπ Interactions, F. Loeffler and E. Malamud, Editors (Argonne National Laboratory, Argonne, Illinois, 1969), pp. 562-618.

85. C. Lovelace, Phys. Letters 28B, 264 (1968).

86. E. P. Tryon, p. 2.

87. R. Morse, A. Garfinkel, B. Y. Oh, W. Walker, P. Berenyi, J. Prentice, and N. R. Steenberg, I = 2 $\pi\pi$ Phase Shifts. Preprint (University of Wisconsin, Madison, Wiscons, n.d.).

88. Private communciation between M. Olsson and R. Morse et al., reference 87.